

1/385

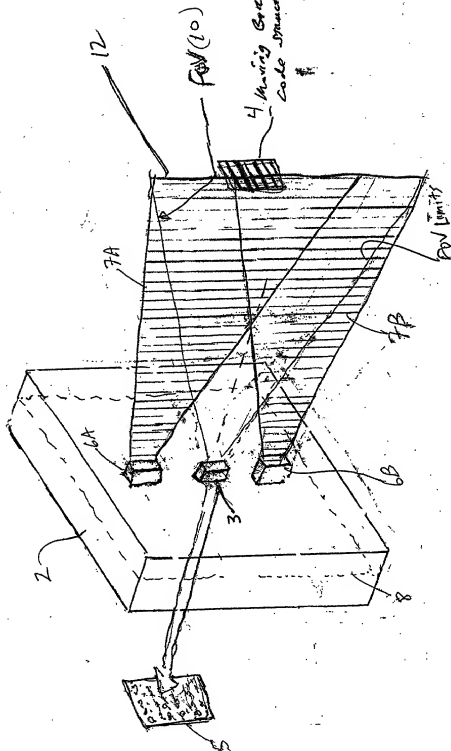
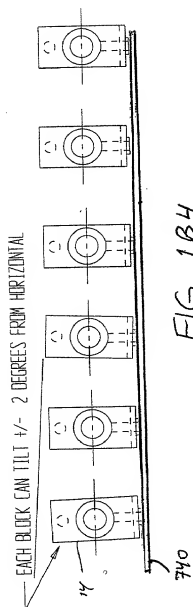


FIG 1A

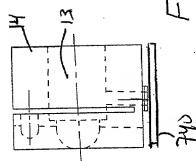


FIG. 1B1

FIG 1B3



VLD BLOCK CAN PITCH FORWARD FOR ALIGNMENT WITH OTHER VLD BEAMS



0

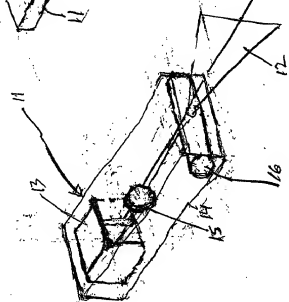


FIG. 1C

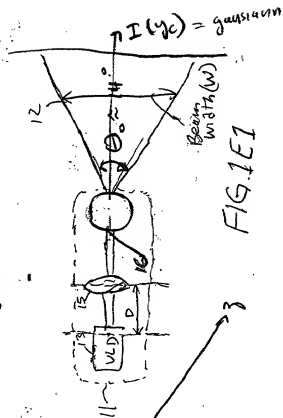


FIG. 1E1

FIG. 1D

5/385

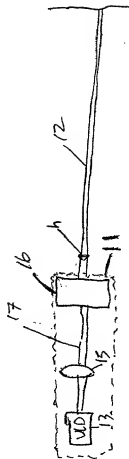


FIG. 1E2

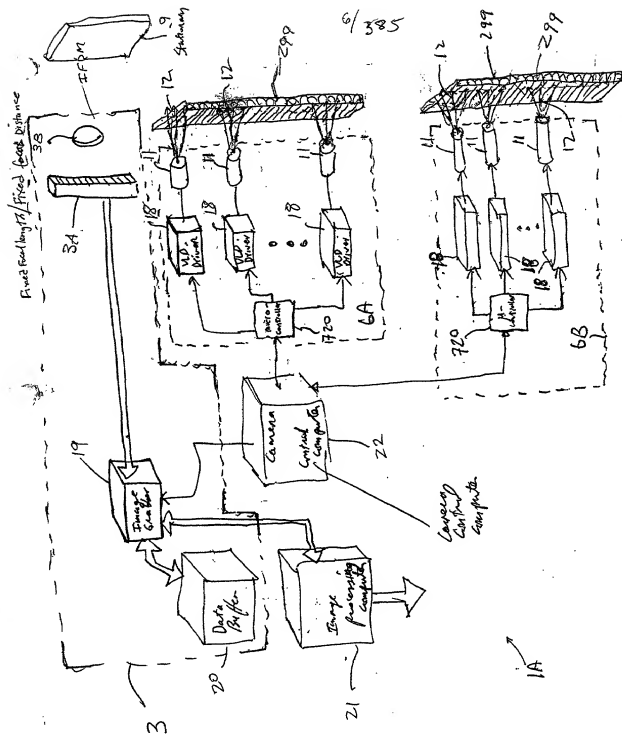
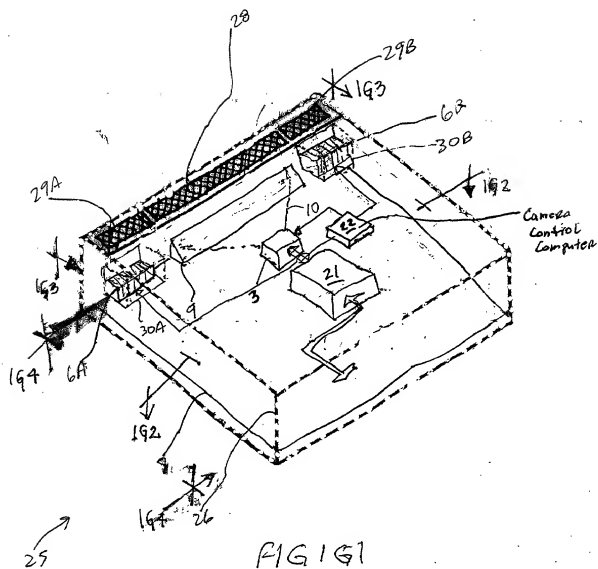


FIG. 1F

7/385



8/ 385

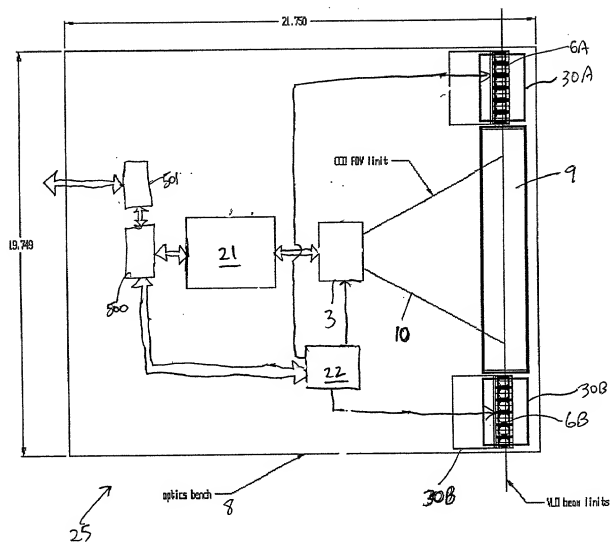
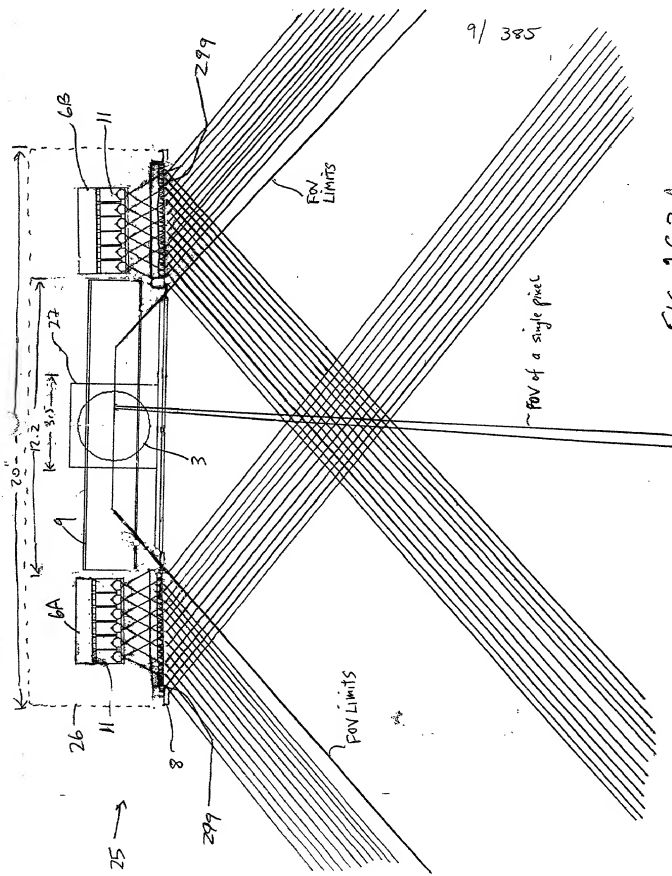


FIG. 152



9/ 385

FIG. 193

10/385

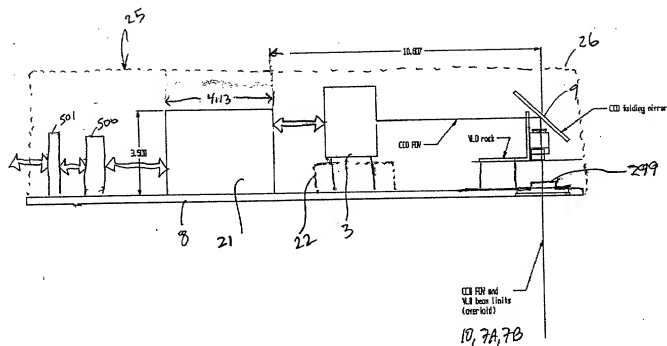


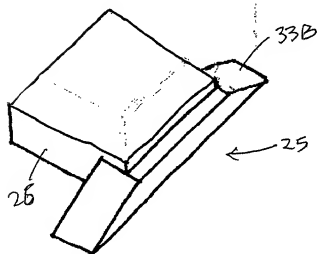
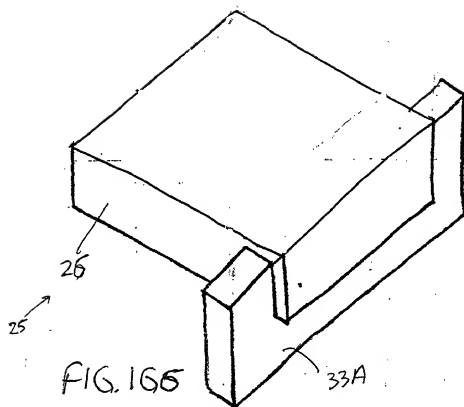
FIG. 164.

00000000000000000000

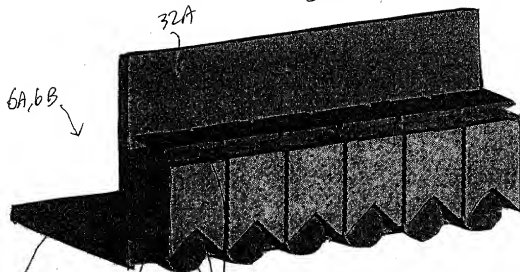


FIG. 1G5

12/385



13/385



32B

32A

16

13

FIG. 1G8

14

L bracket

14B

VLD sticking out of block

13

32A

32B

2.000"

14 block

cylindrical lens

16

2.000"

FIG. 1G9

16

14B

14

13

32B

32A

3.500"

3.250"

2.675"

2.075"

1.475"

.875"

.275"

.000"

FIG. 1G10

14/
385

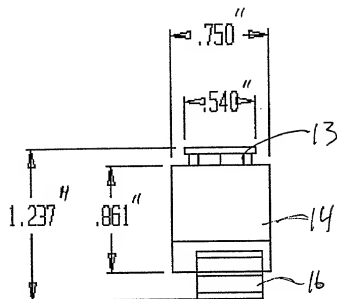


FIG. 1G11

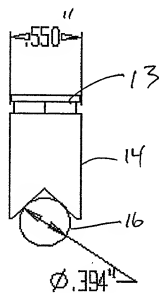


FIG. 1G12

15/
385

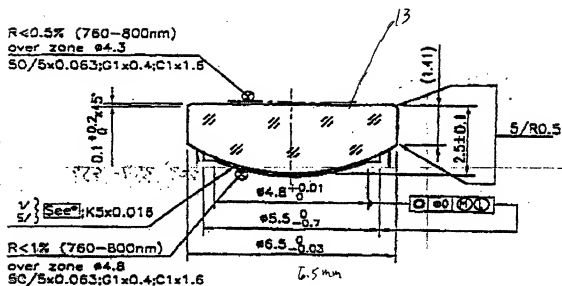


FIG. 1G13

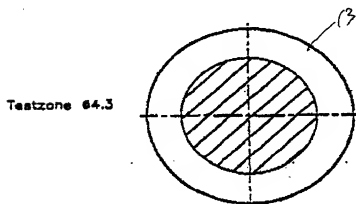


FIG. 1G14

16/385

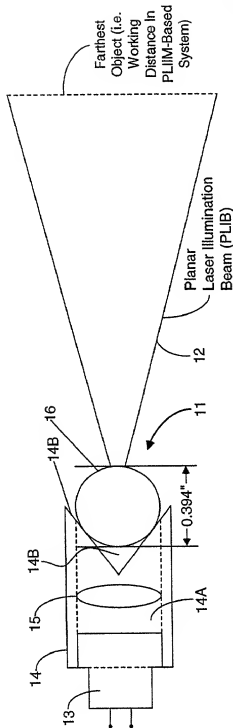


FIG. 1G15A

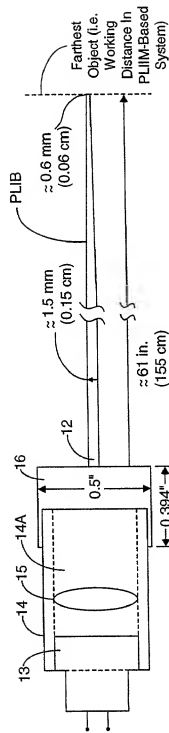


FIG. 1G15B

17/385

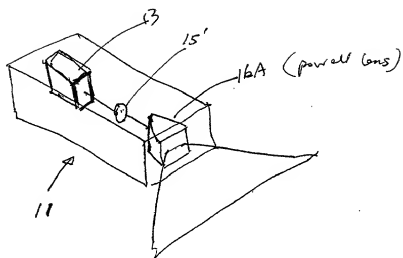


FIG. 1G.16A

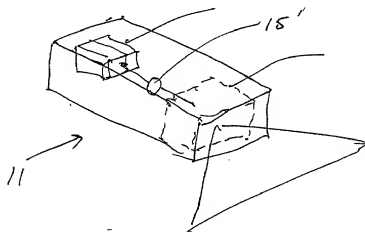


FIG. 1G.16B

• PLIM of
parallel lens

10/385

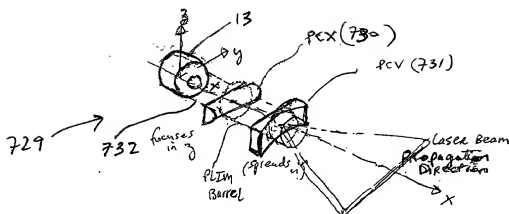


FIG. 16.17A

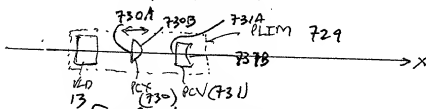


FIG. 16.17B

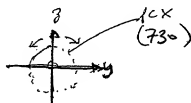


FIG. 16.17C

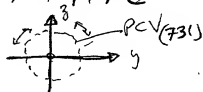


FIG. 16.17D



FIG. 16.17E

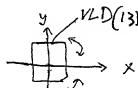


FIG. 16.17F

19/385

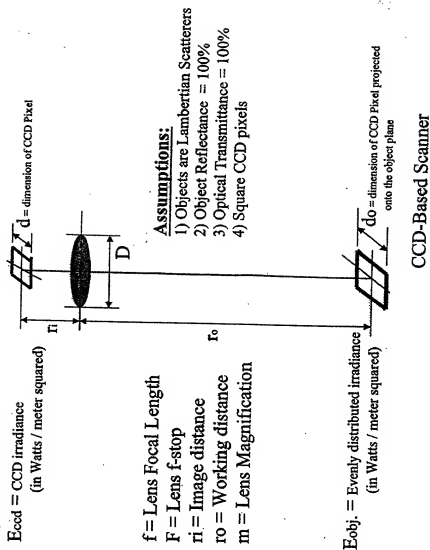


FIG. 1H6

FIRST GENERALIZED METHOD
OF REDUCING SPECKLE-NOISE
PATTERNS AT RANGE
DETECTION ARRAY OF THE
SPD SUBSYSTEM (3)
 (SPMF)

20/ 385

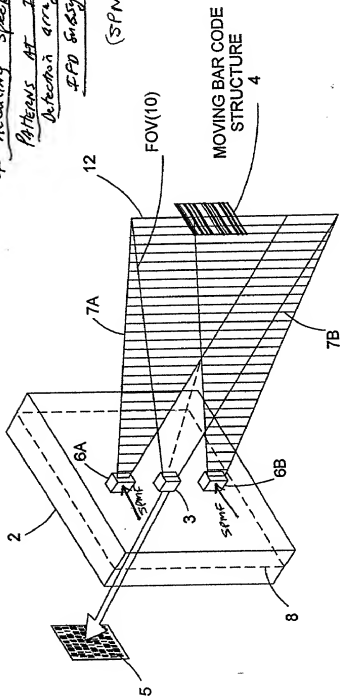
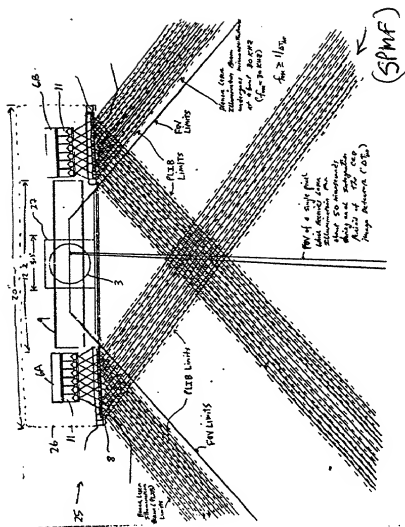


FIG. 1I1



Prior to object illumination

FIG. 1I2A

The First Generalized Speckle-Noise Pattern Reduction Method
Of The Present Invention

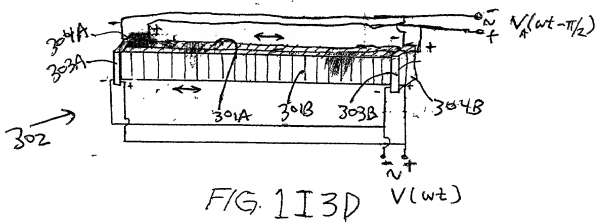
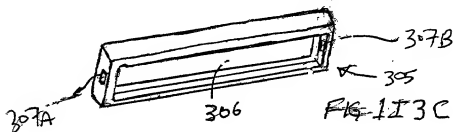
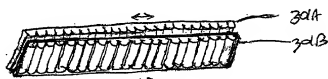
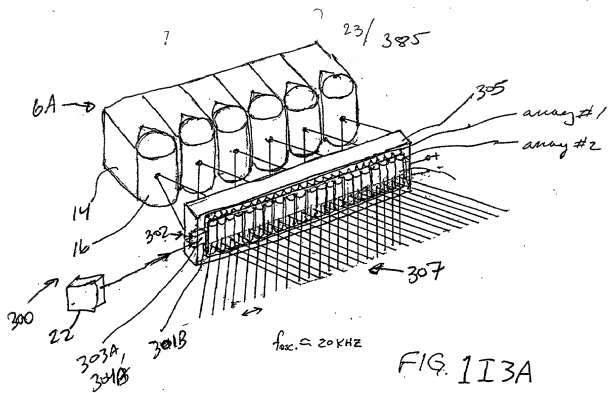
Prior to illumination of the target with the planar laser illumination beam (PLIB), modulate the spatial phase of the transmitted PLIB along the planar extent thereof according to a spatial phase modulation function (SPMF) so as to

produce numerous substantially different time-varying speckle-noise patterns at the image detection array of the IFD Subsystem during the photo-integration time period thereof.



Temporally average the numerous substantially different time-varying speckle-noise patterns produced at the image detection array in the IFD Subsystem during the photo-integration time period thereof, so as to thereby reduce the power of the speckle-noise pattern observed at the image detection array.

FIG. 1I2B



24/385

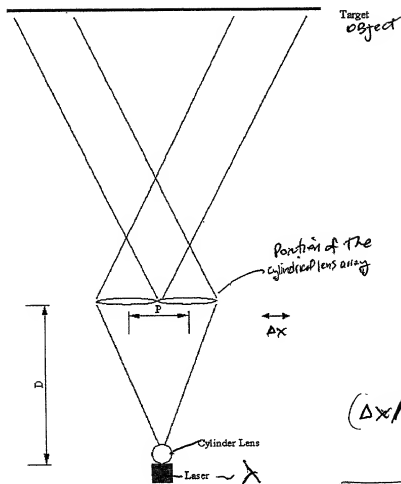
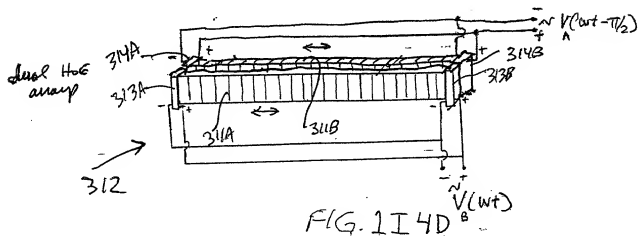
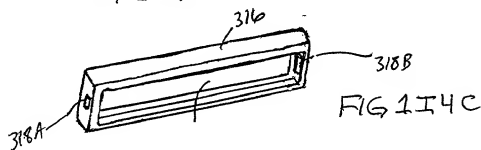
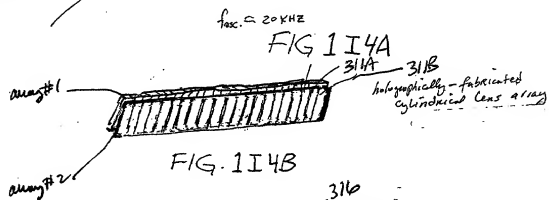
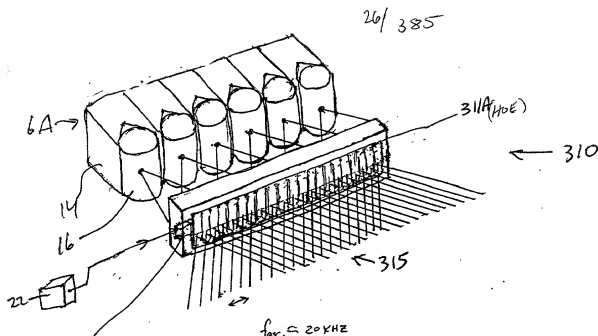


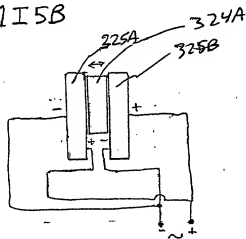
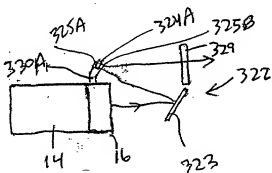
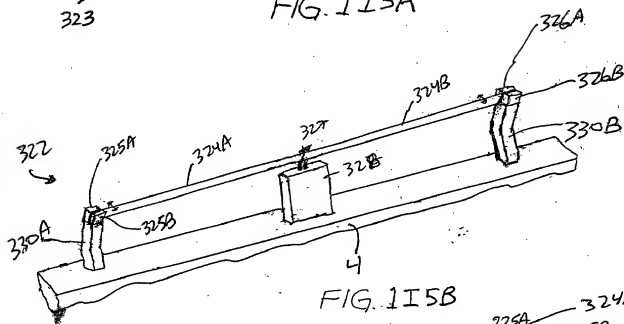
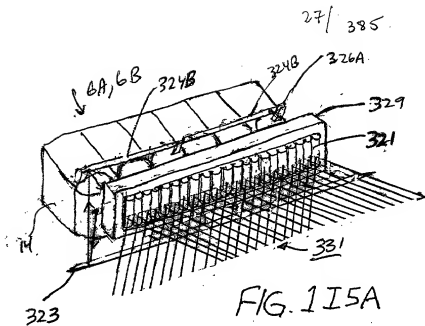
Figure 1

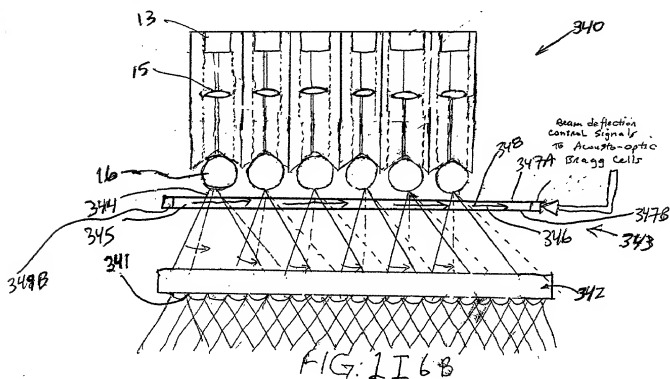
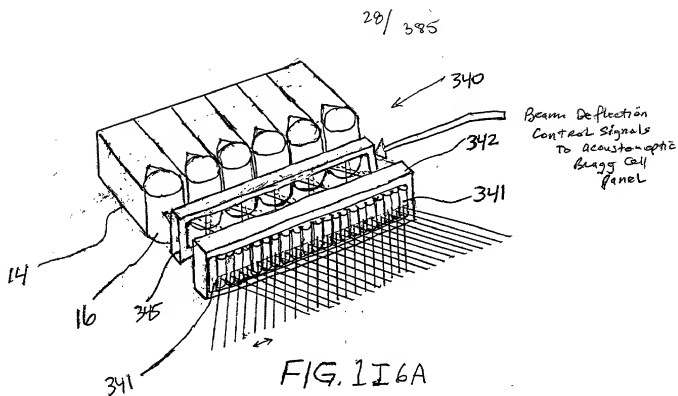
$$(\Delta x / D) P = \lambda$$

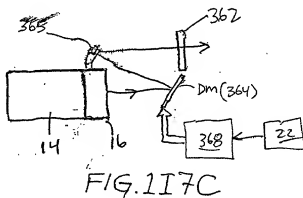
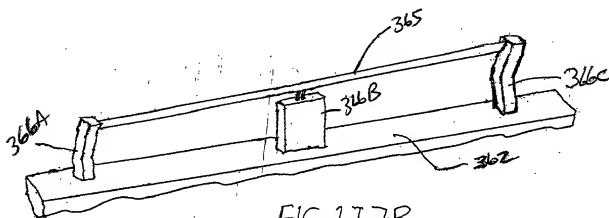
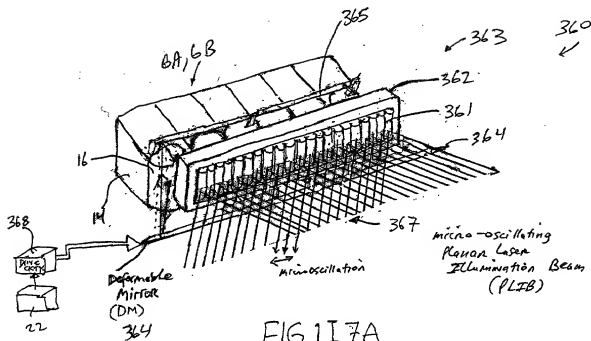
$$\Delta x \geq \frac{\lambda}{P} \cdot D$$

FIG. 1I3E









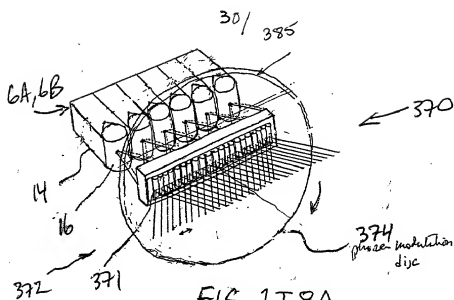


FIG. 1I8A

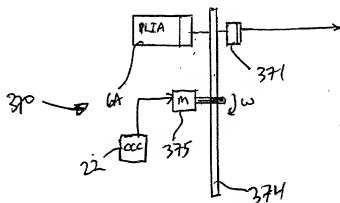


FIG. 118B

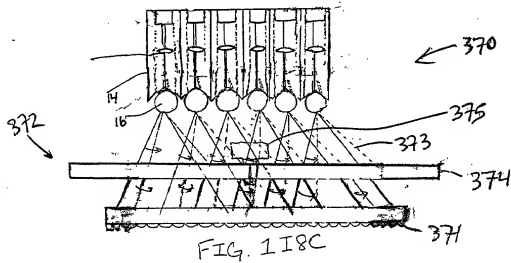


FIG. 1I8C

10:21:58.060 11:24:1

31 / 285

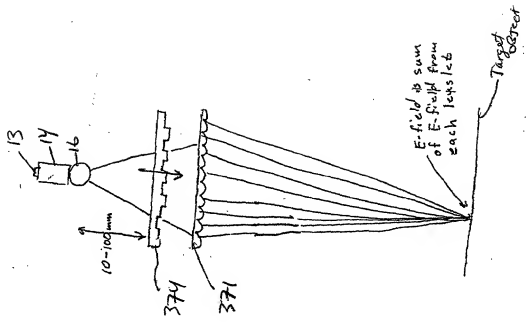


FIG 118E

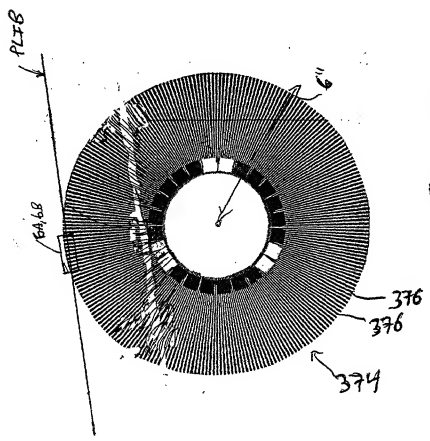
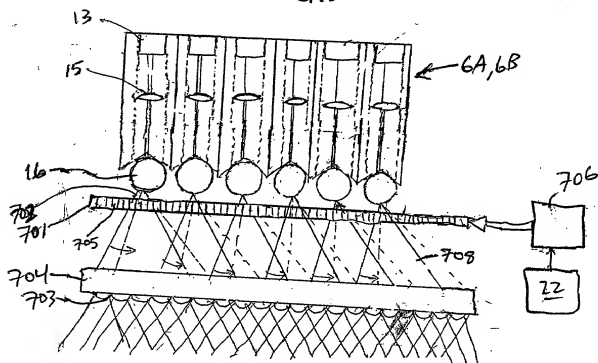
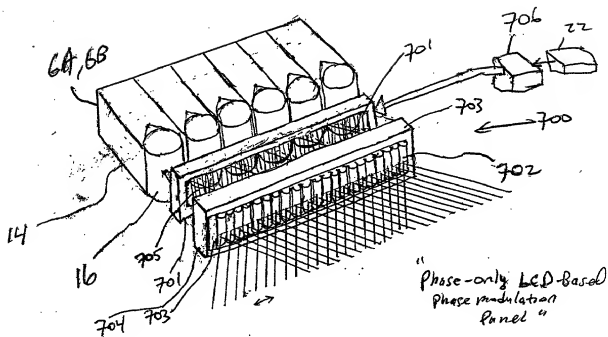


FIG 118D



33/ 385

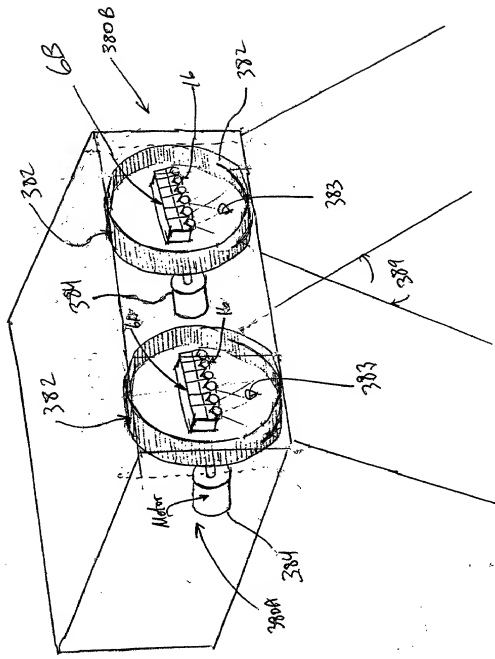
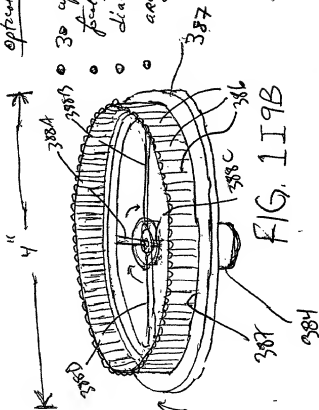


FIG. 1I 9A

3A/ 385

Optical specifications:

- 30 cylindrical lens (lenses) per linear inch
- lens length: 2.0 millimeters
- diameter of lenslets covered ≈ 4 inches
- acrylic material



TOTAL 5850660

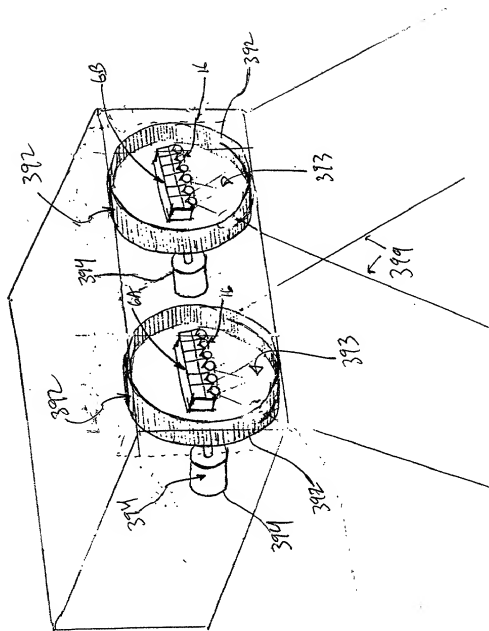
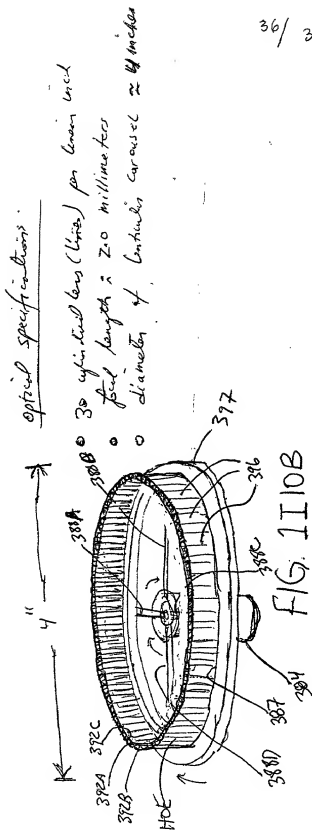


FIG. 1I 10A



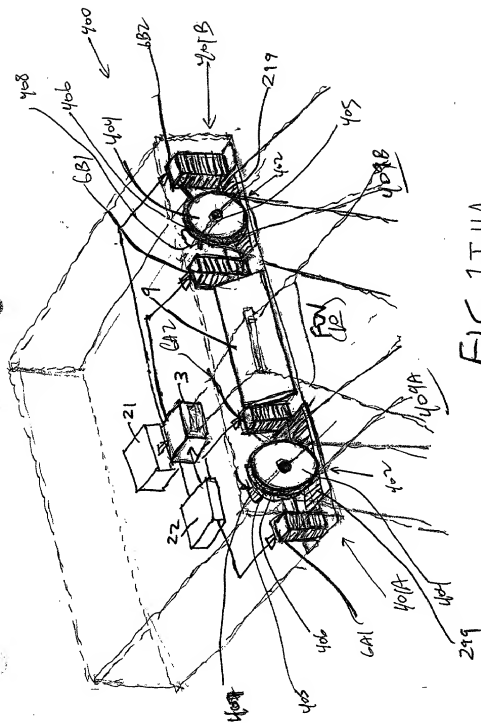


FIG. 11A

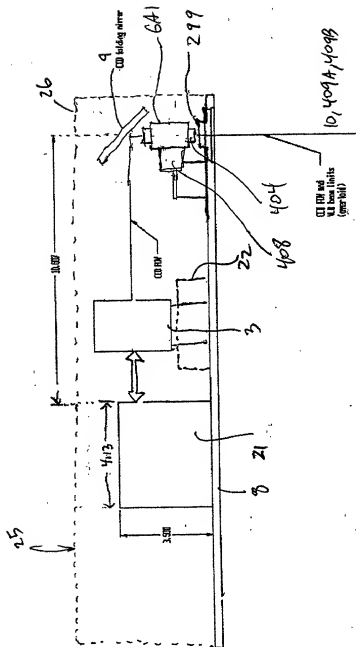


FIG 1I1/B

39/ 385

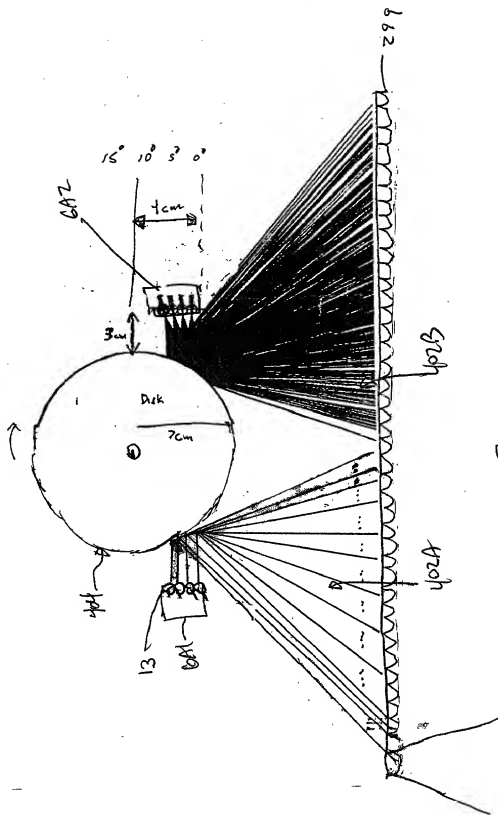


FIG. 111C

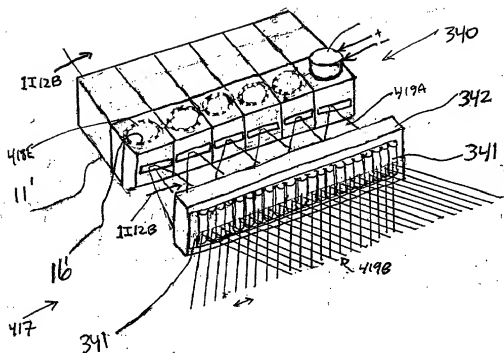


FIG. 1I12A

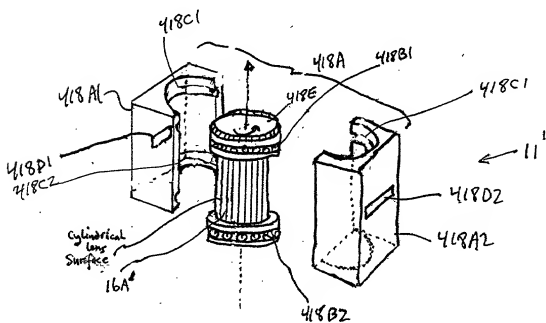


FIG. 1I12B

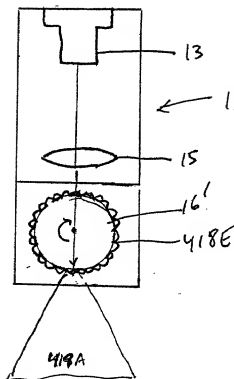


FIG. 1I12C

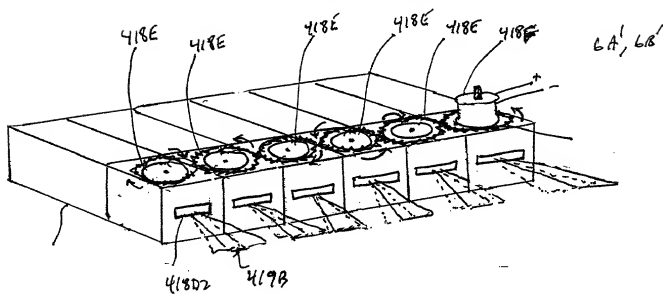


FIG. 1112D

Second Generalized Method of
Reducing Spoke-Nose Patterns
at Image Detection Array
of the FPD Integrator (3)

(T_{PMF})

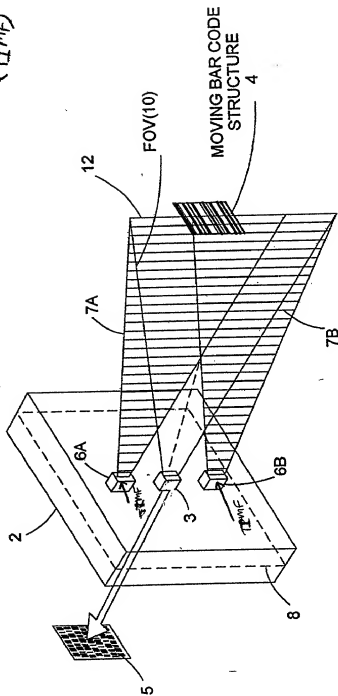


FIG. 1113

43/ 385

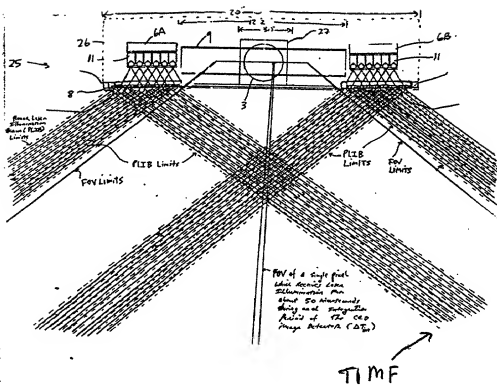


FIG. 1 I 13A

44/385

The Second Generalized Speckle-Noise Pattern Reduction Method
Of The Present Invention

Prior to illumination of the target with the planar laser illumination beam (PLIB), modulate the temporal intensity of the transmitted PLIB along the planar extent thereof according to a temporal intensity modulation function (TIME) so as to

produce numerous substantially different time-varying speckle-noise patterns at the image detection array of the IFD Subsystem during the photo-integration time period thereof.

A



Temporally average the numerous substantially different time-varying speckle-noise patterns produced at the image detection array in the IFD Subsystem during the photo-integration time period thereof, so as to thereby reduce power of the speckle-noise pattern observed at the image detection array.

B

FIG. 1I/3B

45/ 385

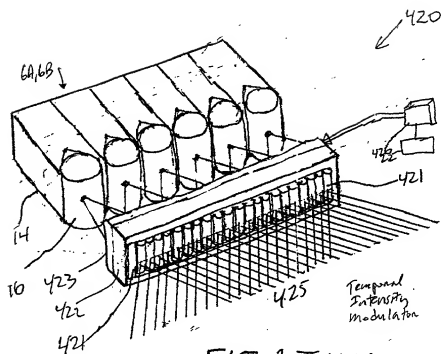


FIG. 1I14A

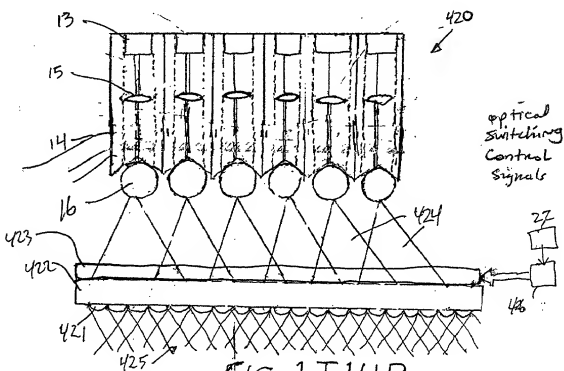


FIG. 1I14B

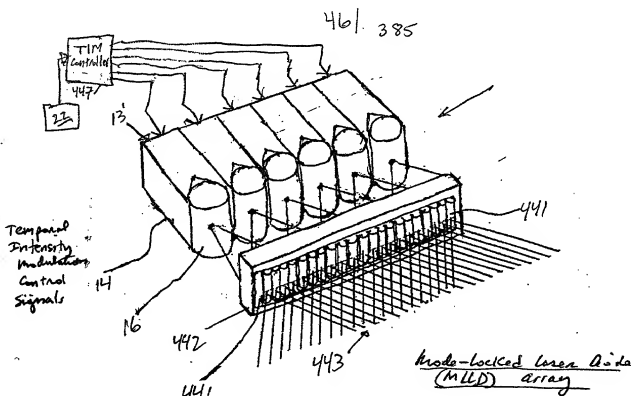


FIG. 1I15A

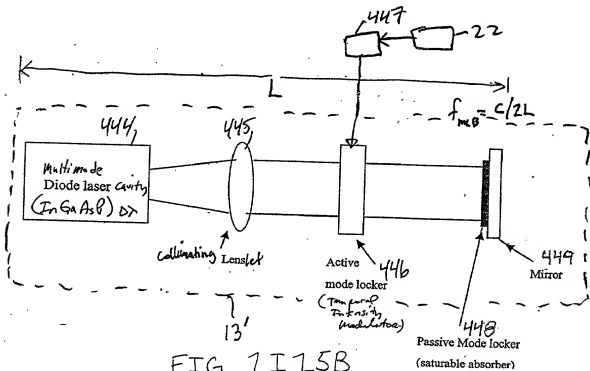


FIG. 1I15B

47 | 385

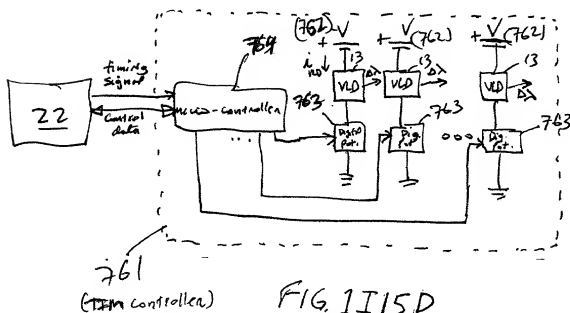
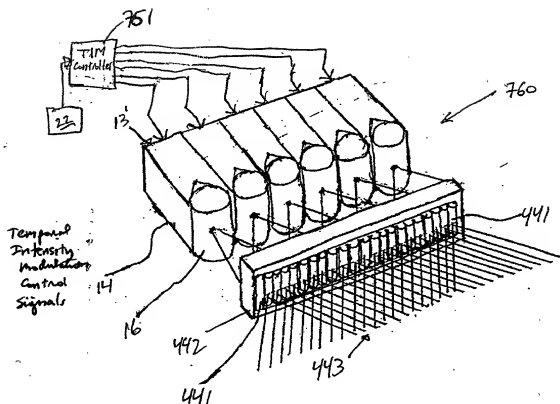
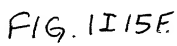
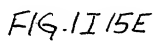


Figure 1



Third Generalized Method of
Reducing Spacker Noise Patterns
at Image Detection Array
of the FPD Subsystem (3)

49/
 385

(TIME)

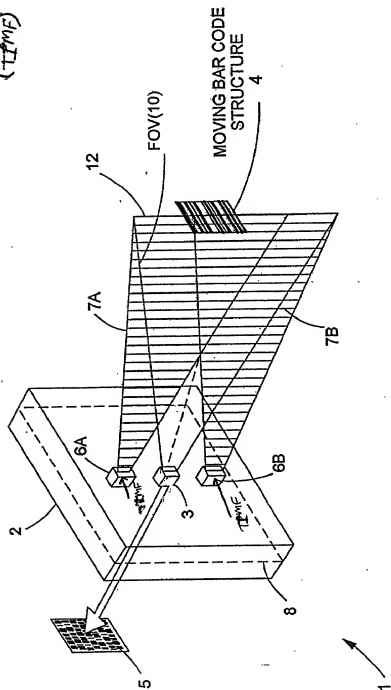
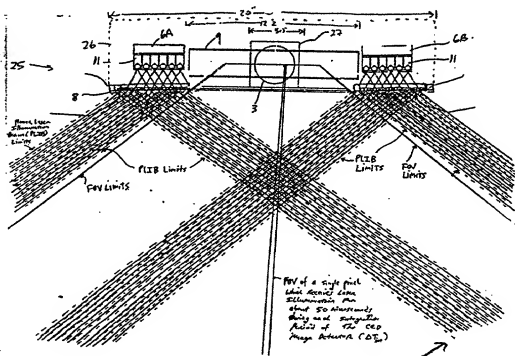


FIG. 11/16

50/ 385



TPMF

FIG. 1 I 16A

Third Generalized Speckle-Noise Pattern Reduction Method
Of The Present Invention

Prior to illumination of the target with the planar laser illumination beam (PLIB), modulate the temporal *phase* of the transmitted PLIB ~~along the planar extent thereof~~ according to a *Temporal phase* modulation function (TPMF) so as to:

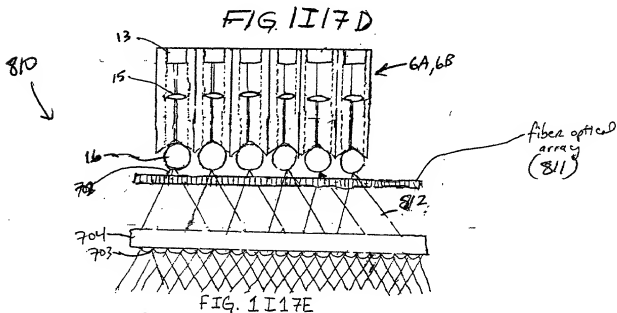
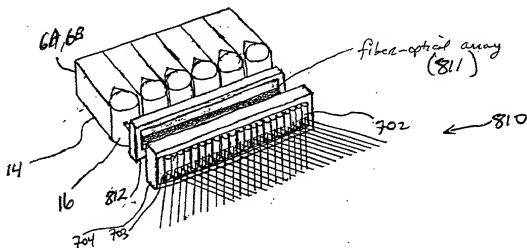
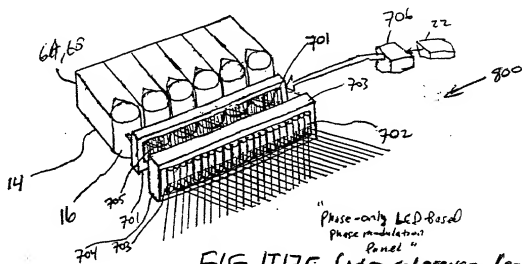
produce numerous substantially different time-varying speckle-noise patterns at the image detection array of the IFD Subsystem during the photo-integration time period thereof.

↓

Temporally average the numerous substantially different time-varying speckle-noise patterns produced at the image detection array in the IFD Subsystem during the photo-integration time period thereof, so as to thereby reduce power of the speckle-noise pattern observed at the image detection array.

FIG. 1I/6B

53/ 385



Fourth Generalized Method of
Reducing Speckle-Noise Patterns
at Range Detection Array
of the FFD Subsystem (3)

(TFmp)

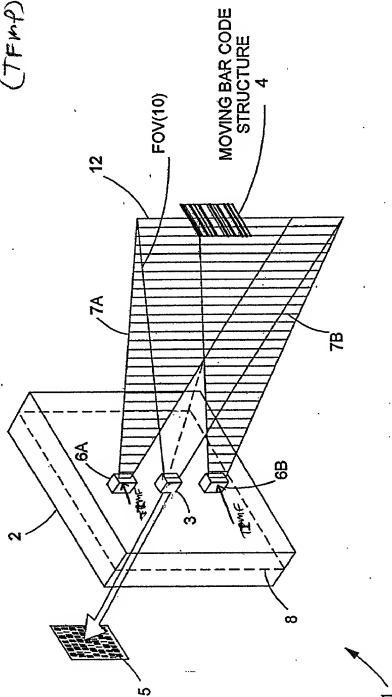


FIG. 1118



FIG. 1I 18A

Fourth Generalized Speckle-Noise Pattern Reduction Method
Of The Present Invention

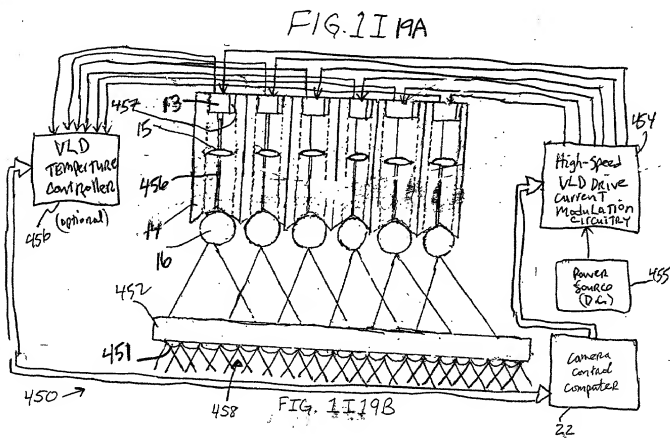
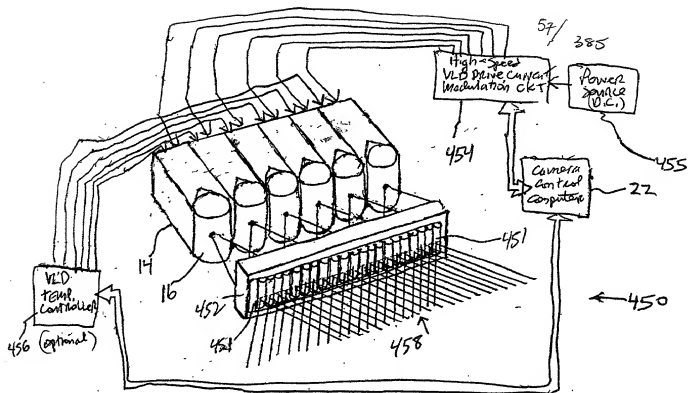
Prior to illumination of the target with the planar laser illumination beam (PLIB), modulate the temporal frequency of the transmitted PLIB according to a temporal intensity modulation function (TIMF) so as to:

produce numerous substantially different time-varying speckle-noise patterns at the image detection array of the IFD Subsystem during the photo-integration time period thereof.

Temporally average the numerous substantially different time-varying speckle-noise patterns produced at the image detection array in the IFD Subsystem during the photo-integration time period thereof, so as to thereby reduce power of the speckle-noise pattern observed at the image detection array.

FIG 1I 18B

0000055-112101



58/385

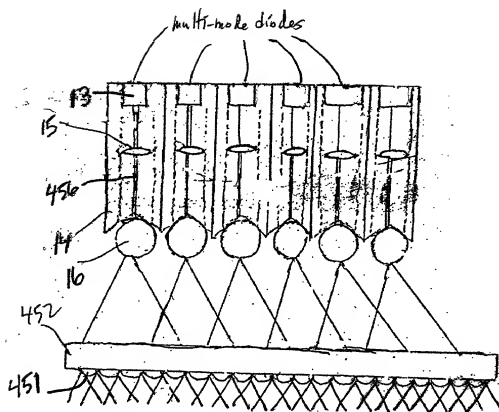


FIG 1I19C

FIG. 1 GENERALIZED METHOD
OF Reducing Speckle-Noise
PATTERNS AT Image
Detection array OF
FPD Subsystem (3)

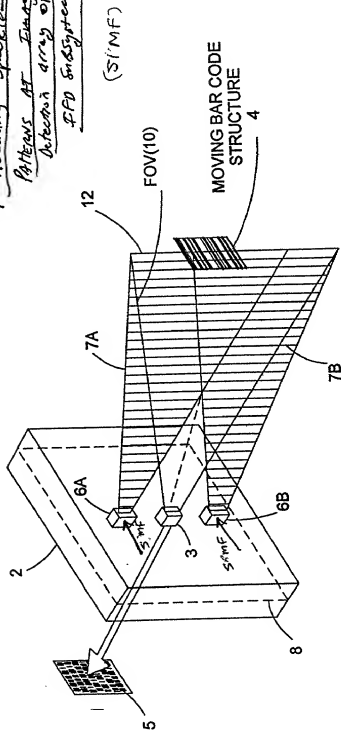


FIG. 1F 20

61/ 395

Fifth Generalized Speckle-Noise Pattern Reduction Method
Of The Present Invention

Prior to illumination of the target with the planar laser illumination beam (PLIB), modulate the spatial intensity of the transmitted PLIB along the planar extent thereof according to a spatial intensity modulation function (SIMF) so as to

produce numerous substantially different time-varying speckle-noise patterns at the image detection array of the IFD Subsystem during the photo-integration time period thereof.

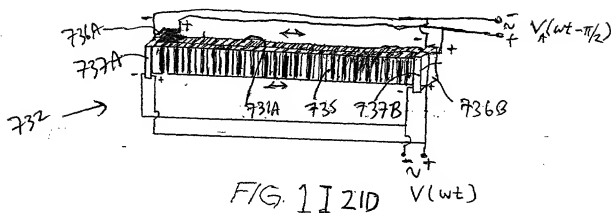
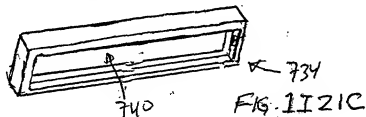
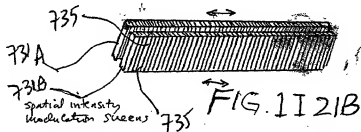
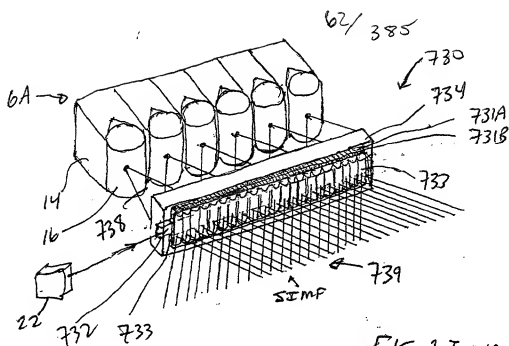
A

↓

Temporally average the numerous substantially different time-varying speckle-noise patterns produced at the image detection array in the IFD Subsystem during the photo-integration time period thereof, so as to thereby reduce power of the speckle-noise pattern observed at the image detection array.

B

FIG. 1I20B



Generalized Method of
Reducing Speckle-Noise Patterns
at Image Detection Array
of the IFD Subsystem
 (SIMF)

63/ 385

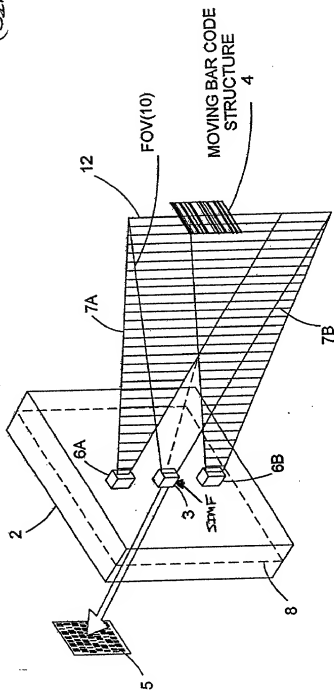


FIG. 11 22

64/385

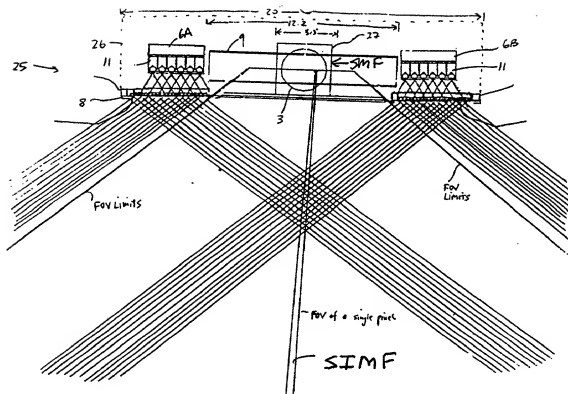


FIG. 1122A

65/ 385

Sixth Generalized Speckle-Noise Pattern Reduction Method
Of The Present Invention

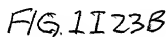
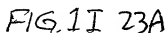
After illumination of the target with the planar laser illumination beam (PLIB), modulate the spatial intensity of the reflected/scattered (i.e. received) PLIB along the planar extent thereof according to a spatial intensity modulation function (SIMF) so as to :

produce numerous substantially different time-varying speckle-noise patterns at the image detection array of the IFD Subsystem during the photo-integration time period thereof.

Temporally average the many substantially different time-varying speckle-noise patterns produced at the image detection array in the IFD Subsystem during the photo-integration time period thereof, so as to thereby reduce the speckle-noise pattern observed at the image detection array.

FIG. 1I 22B

 UNIVERSITY OF MICHIGAN PRESS



Seventh Generalized Method of
Reducing Specle-Noise Patterns
at Image Detection Array
of IR IFD Subsystem

(TIME)

67/ 385

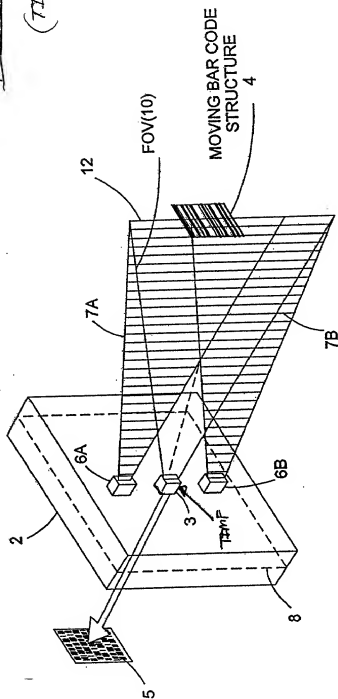


FIG. 124

680/385

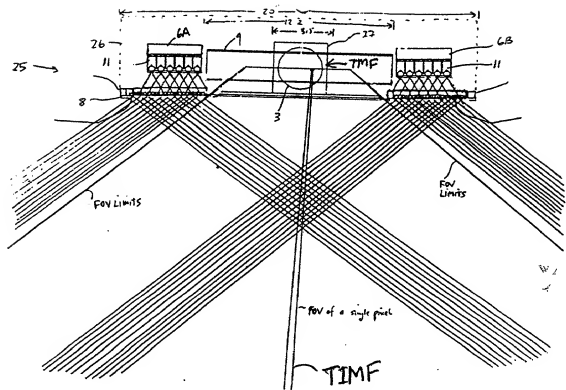


FIG. 1I24A

69/ 395

Seventh Generalized Speckle-Noise Pattern Reduction Method
Of The Present Invention

After illumination of the target with the planar laser illumination beam (PLIB), modulate the temporal intensity of the reflected/scattered (i.e. received) PLIB along the planar extent thereof according to a temporal intensity modulation function (TIMF) so as to

produce many substantially different time-varying speckle-noise patterns at the image detection array of the IFD Subsystem during the photo-integration time period thereof.

Temporally average the many substantially different time-varying speckle-noise patterns produced at the image detection array in the IFD Subsystem during the photo-integration time period thereof, so as to thereby reduce the speckle-noise pattern observed at the image detection array.

FIG. 1I 24B

71/295

EIGHT GENERALIZED METHOD OF REDUCING THE SPECKLE PATTERN
NOISE OBSERVED IN PLIIM-BASED IMAGING SYSTEMS

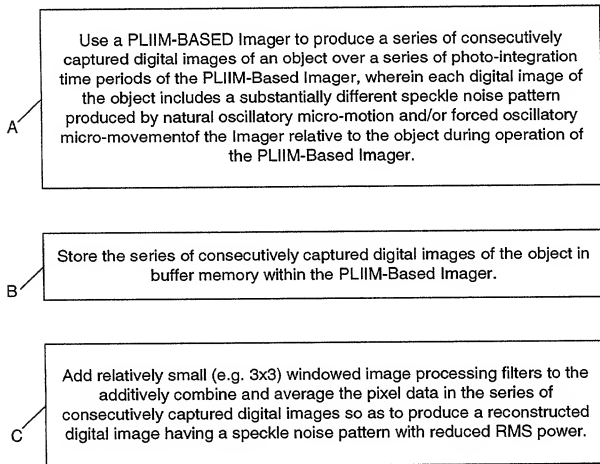
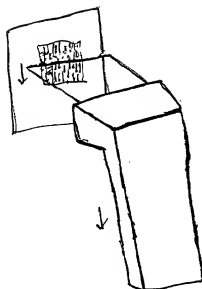


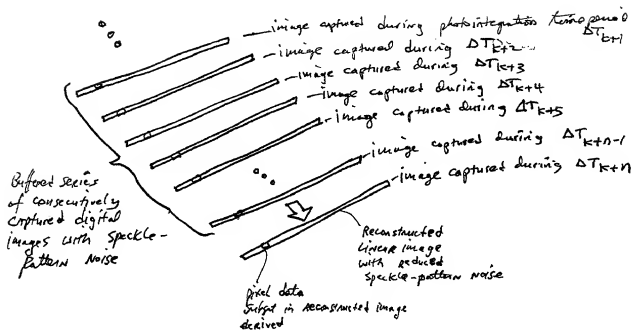
FIG. 1124D

72/385



Manual
Sweeping
Action
across Code Symbol
or
graphical indicia

FIG. 1124E



Case: Linear Image

FIG. 1124F

73/ 385

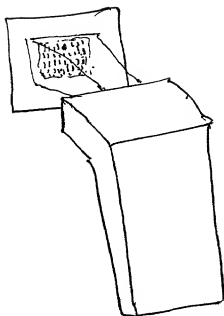


FIG. 1124G

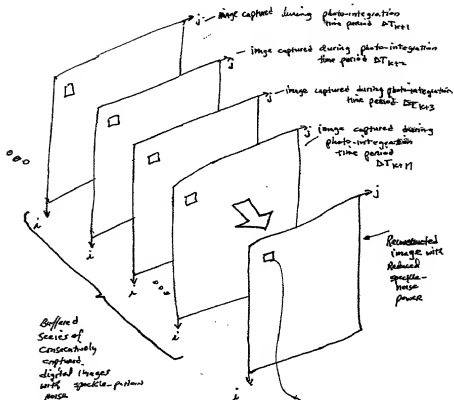


FIG. 1124H

Case: 2D Area Images

74/285

NINTH GENERALIZED METHOD OF REDUCING SPECKLE PATTERN
NOISE IN PLIM-BASED IMAGING SYSTEMS

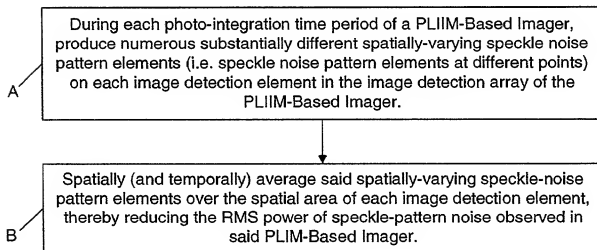
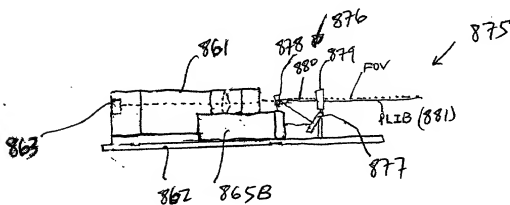
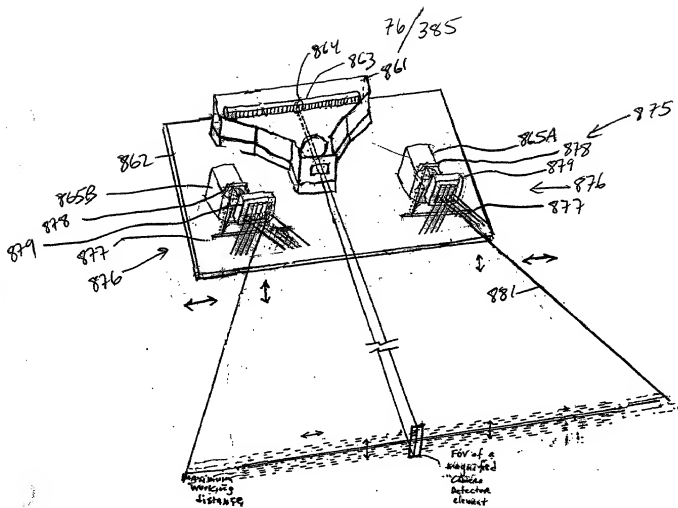
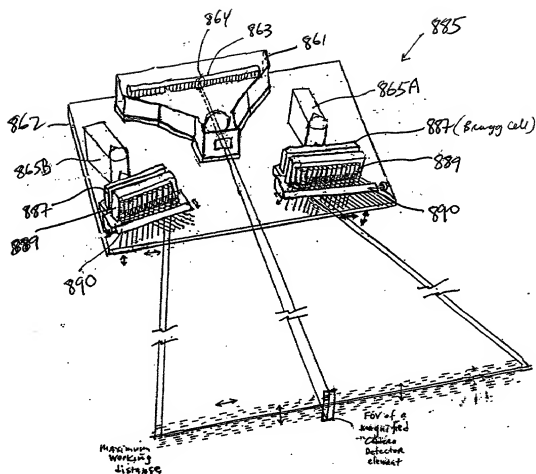


FIG. 11241



79/385



* Lateral and Transverse Misalignment of PLIB

FIG. 1I 25C1

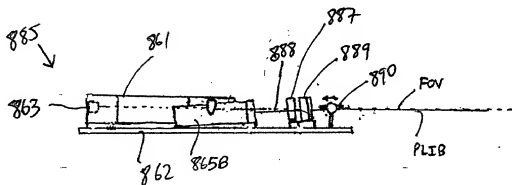


FIG. 1I 25C2

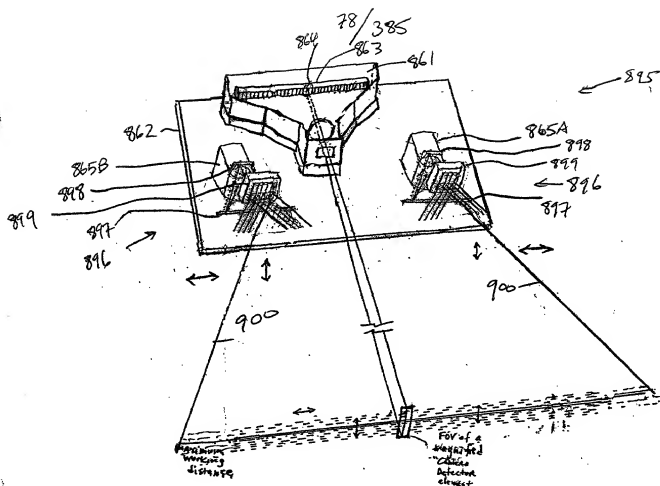


FIG. 1 I 25 D1

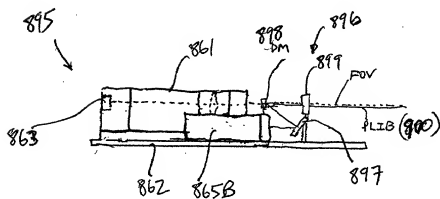
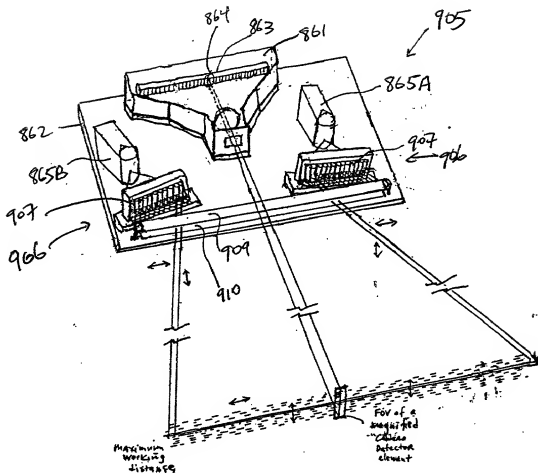


FIG. 1I 25D2

79/385



* Lateral and Transverse Misalignment of ALB

905

FIG. 1I25E1

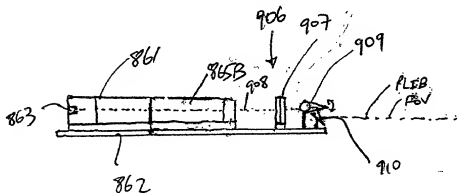
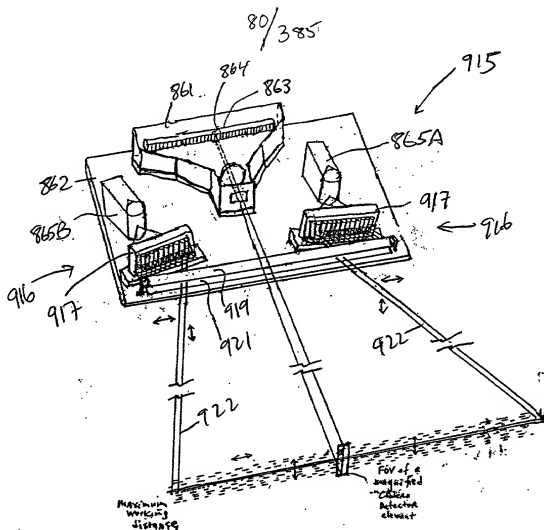


FIG. 1I25E2



* Lateral and Transverse Misalignment of PLIB

FIG. 1I25F1

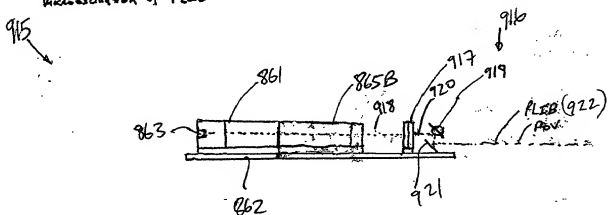


FIG. 1I25F2

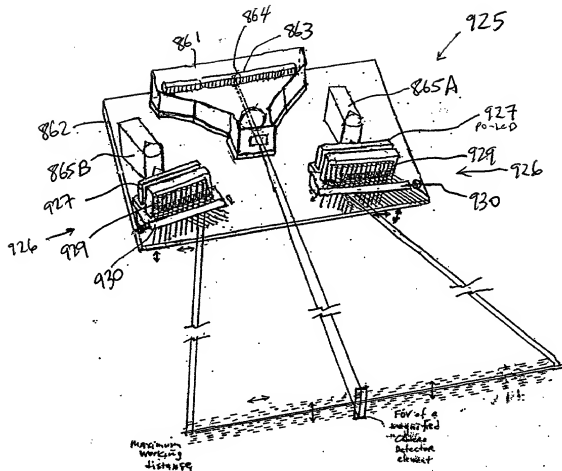


FIG. 1I25G1

- * Lateral and Transverse Microcirculation of ALIB

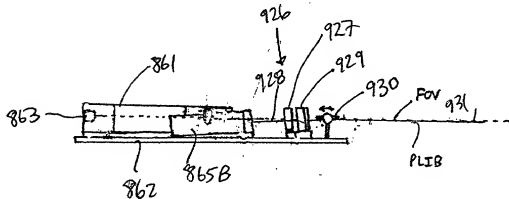
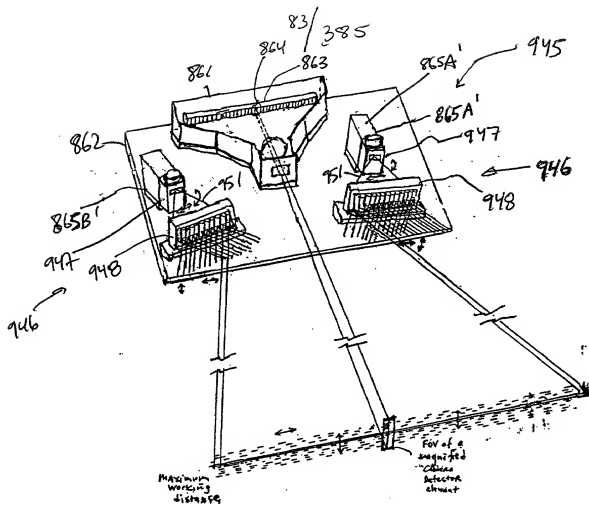
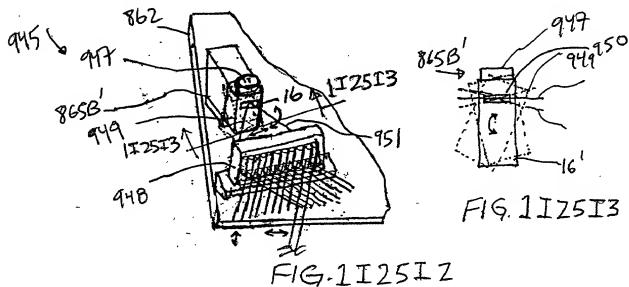


FIG. 1I25G2



Lateral and
 Transverse
 Vibration of PLB

FIG. 1 I 25 I 1



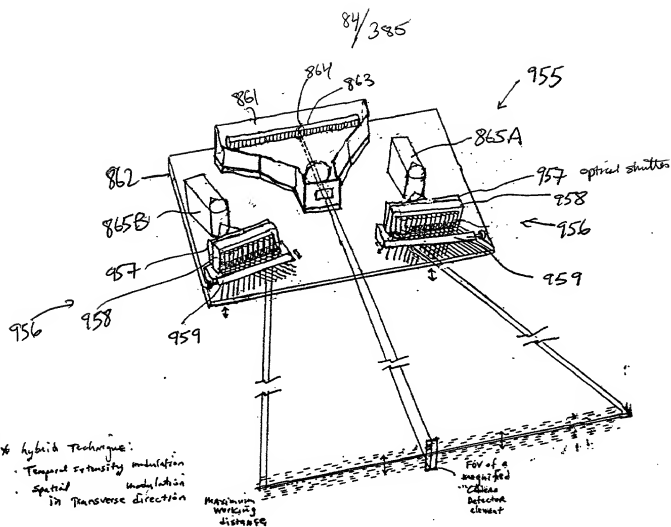


FIG. 1I25J1

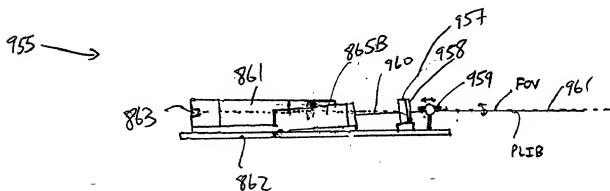
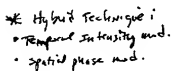


FIG. 1I25J2



965

FIG. 1 IZ5K1

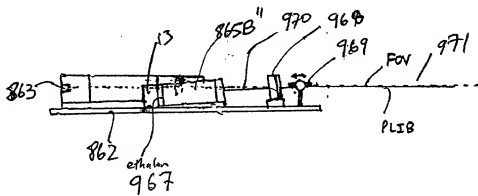


FIG. 1I 25KZ

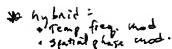
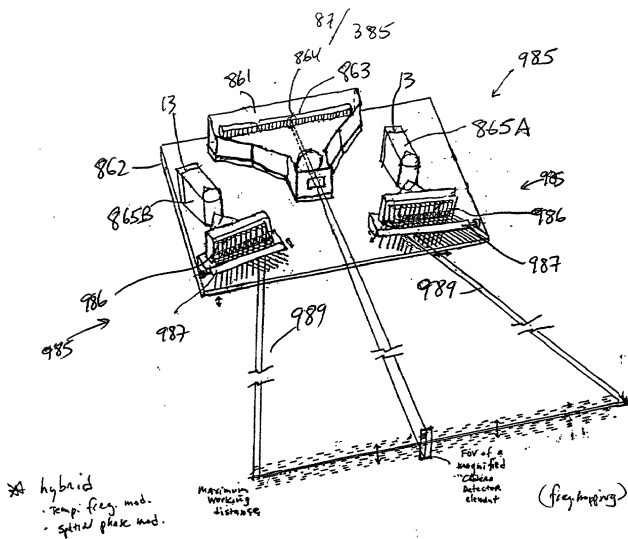


FIG. 1I 25 L1





* Transverse
 Microconstellation of PLIB

FIG. 1I25M1

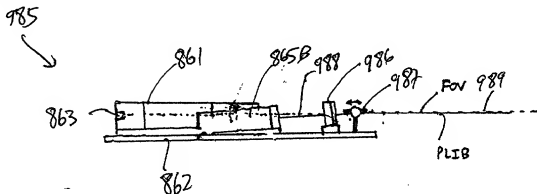
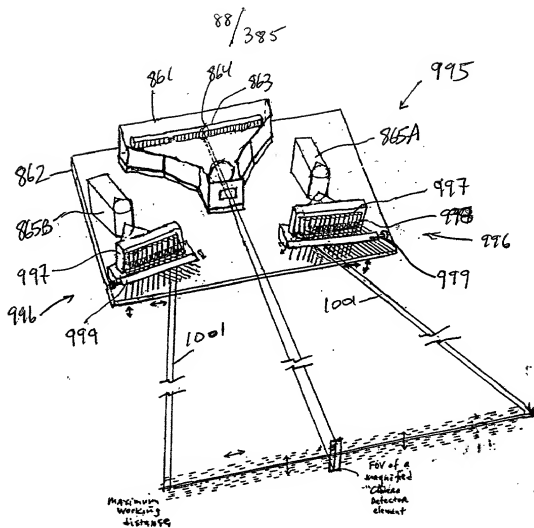


FIG. 1I25M2



- hybrid:
 - spatial intensity mod.
 - spatial phase

- * Lateral and Transverse Excitation of PLIB

FIG. 1125N1

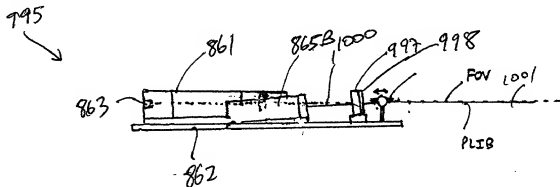


FIG. 1I25NZ

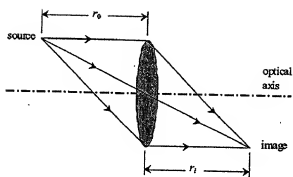
[illegible]

FIG. 141

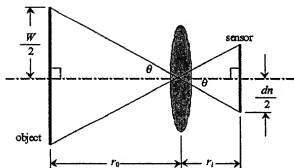


FIG. 1H2

90/385

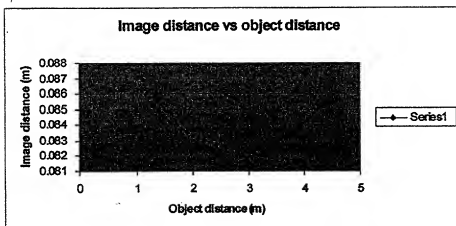


FIG. 1H3

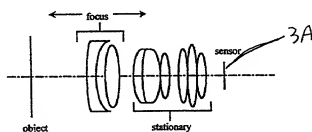


FIG. 1H4

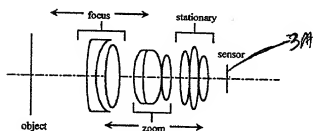


FIG. 1H5

0090085.1.12101

9/385

Fixed focal length lens cases

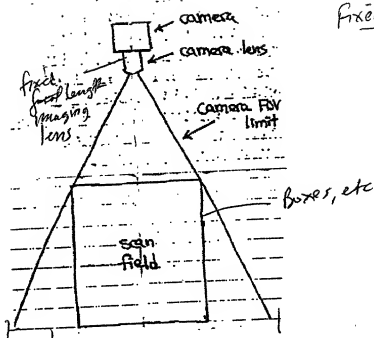


FIG. 1K1

Lawyer 34

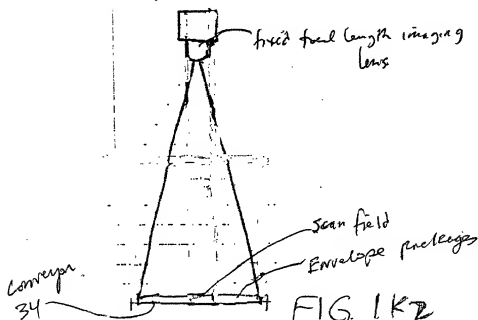


FIG. 1K2

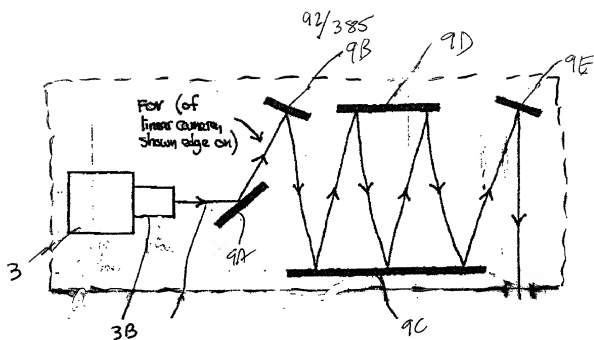


FIG. 1L1

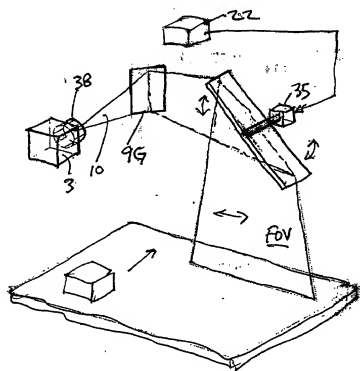


FIG. 1L2

93/385

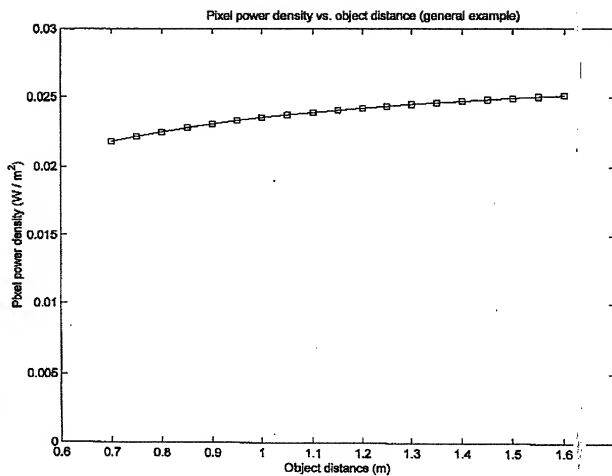


FIG-1M1

94/385

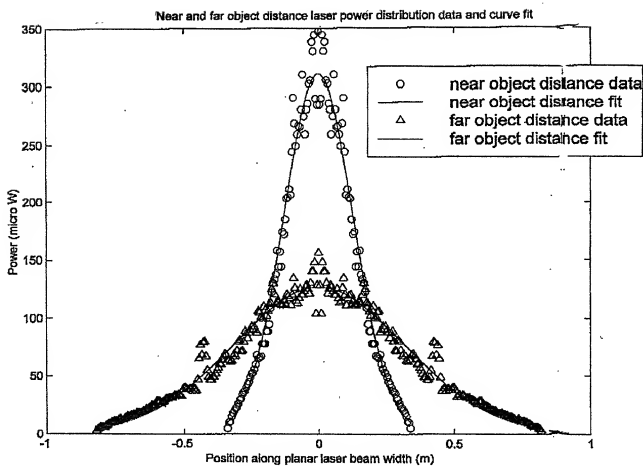


FIG. 1M2

95/
385

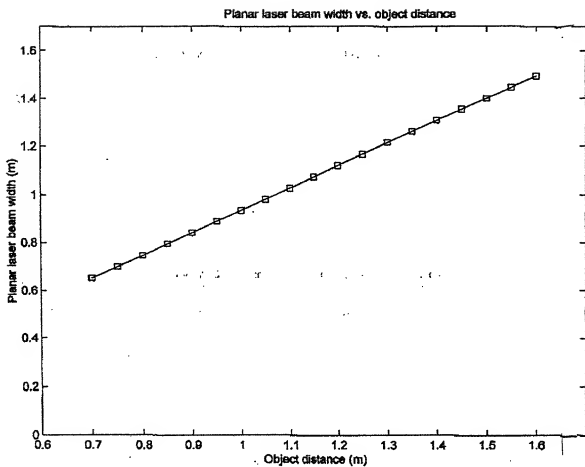
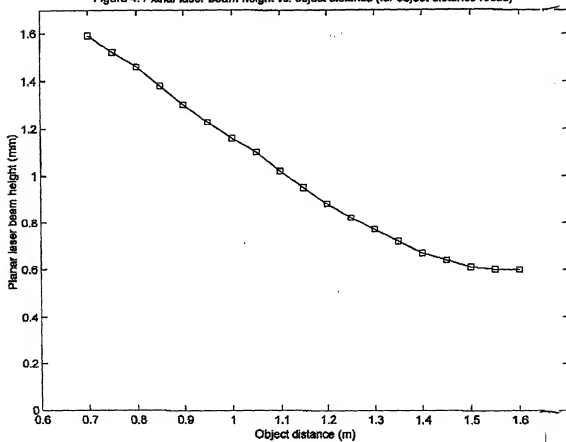


FIG. 1M3

000005.112101

96/385

Figure 4: Planar laser beam height vs. object distance (for object distance focus)



FIG/M4

97/385

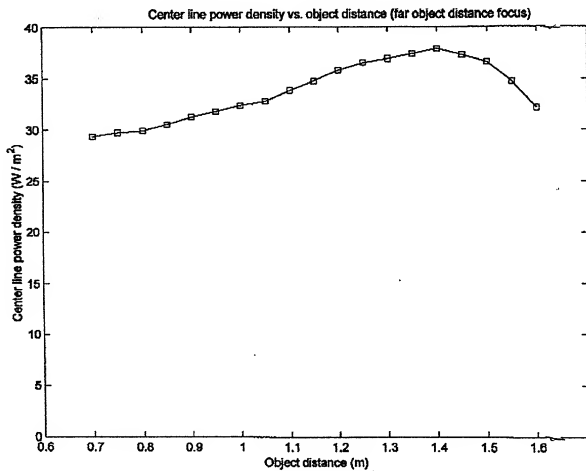


FIG. 1N

98/385

Figure 6: Pixel power densities vs. object distance

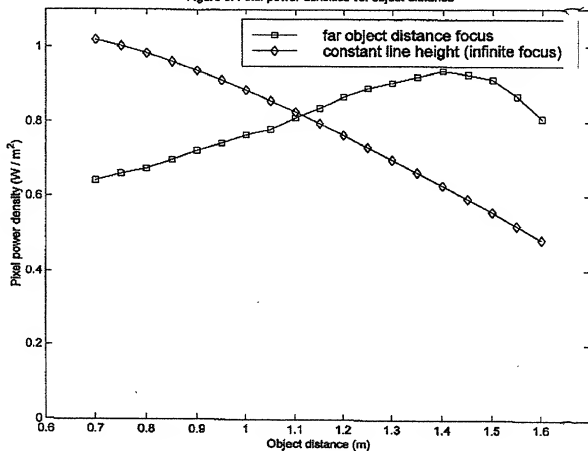
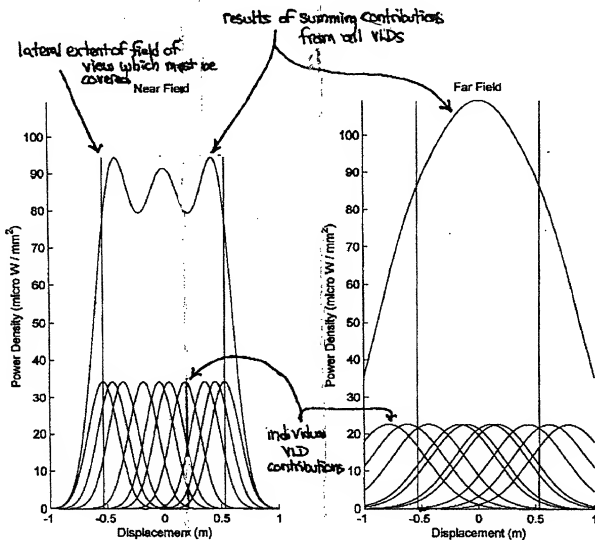


FIG. 10

99/385



100/385

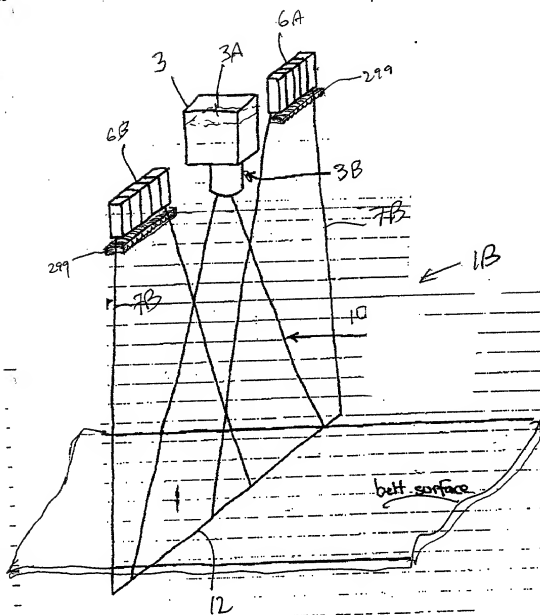
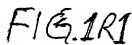


FIG. 101

[illegible]

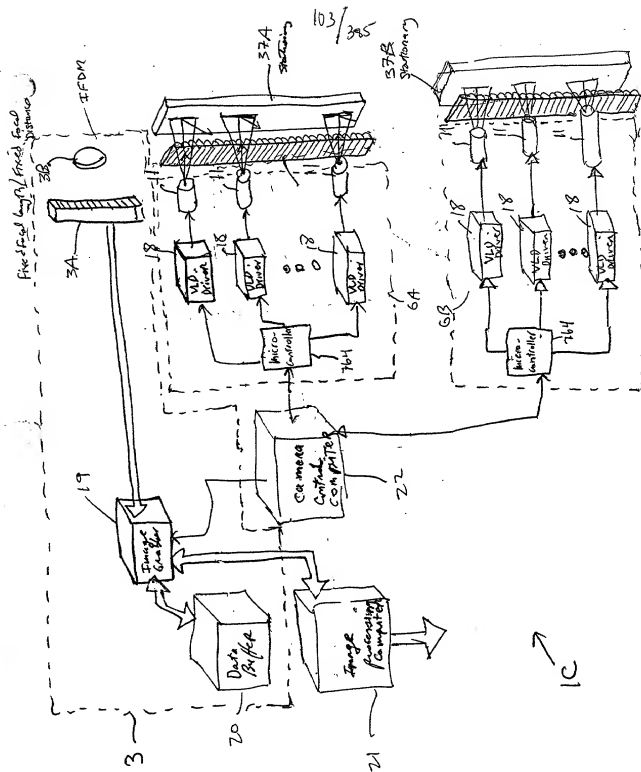
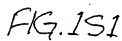


FIG. 1R2

[illegible]

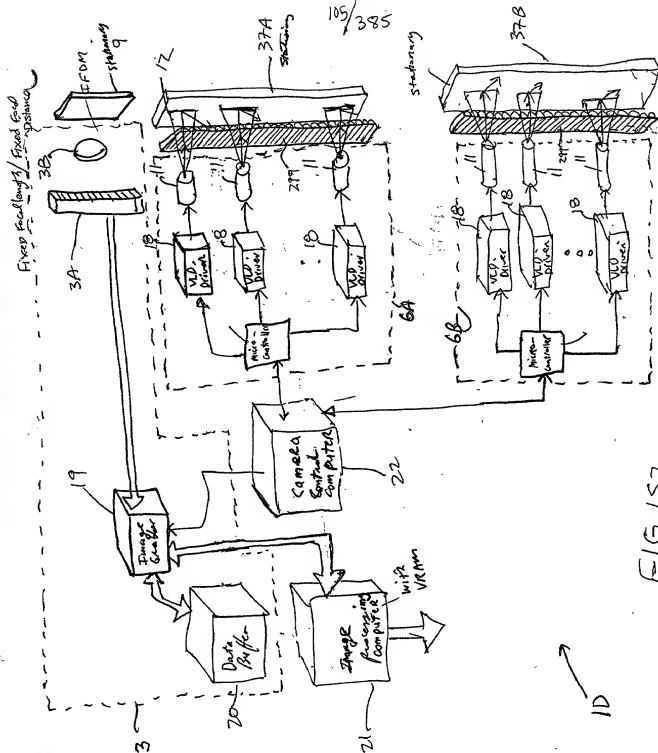
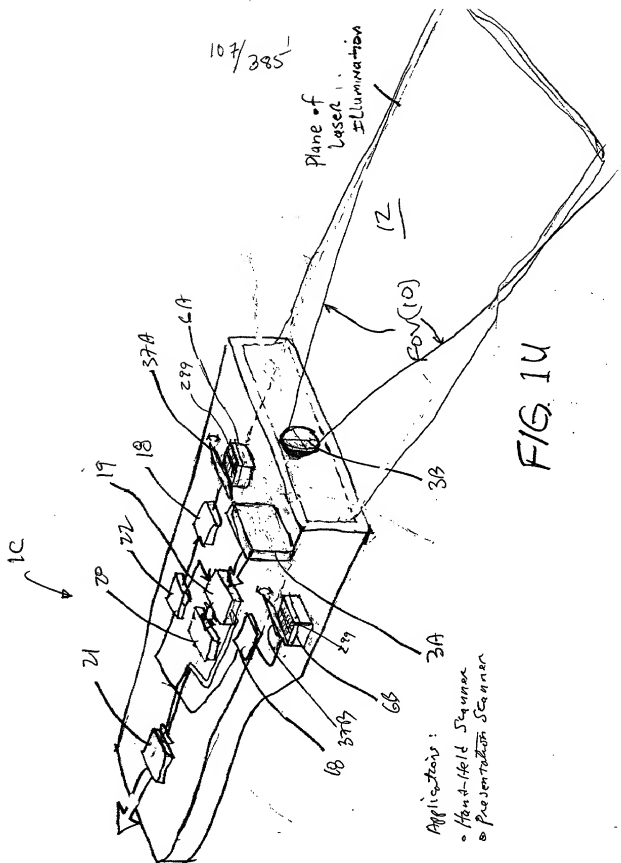


FIG. 152



109/385

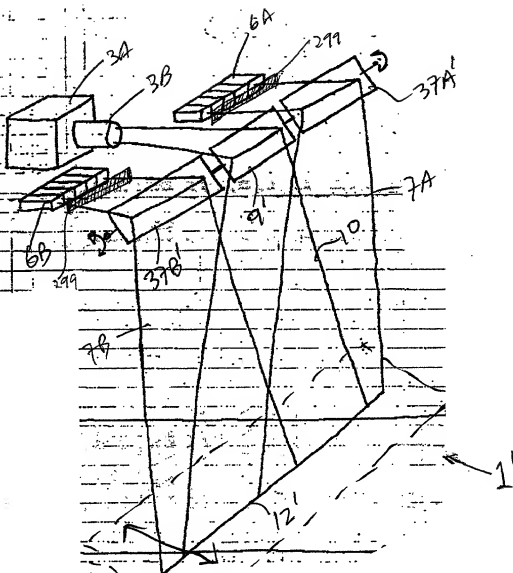


FIG. 1V2

3-D
region
space

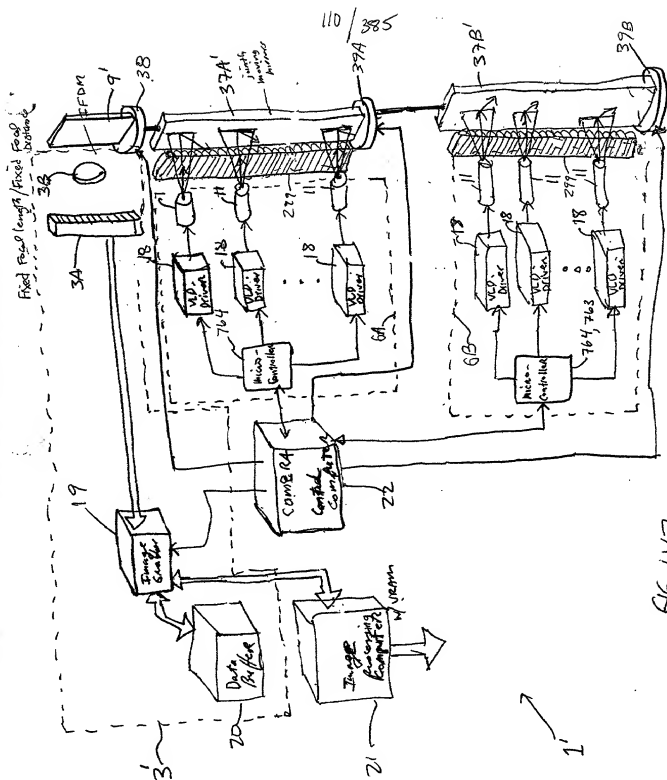
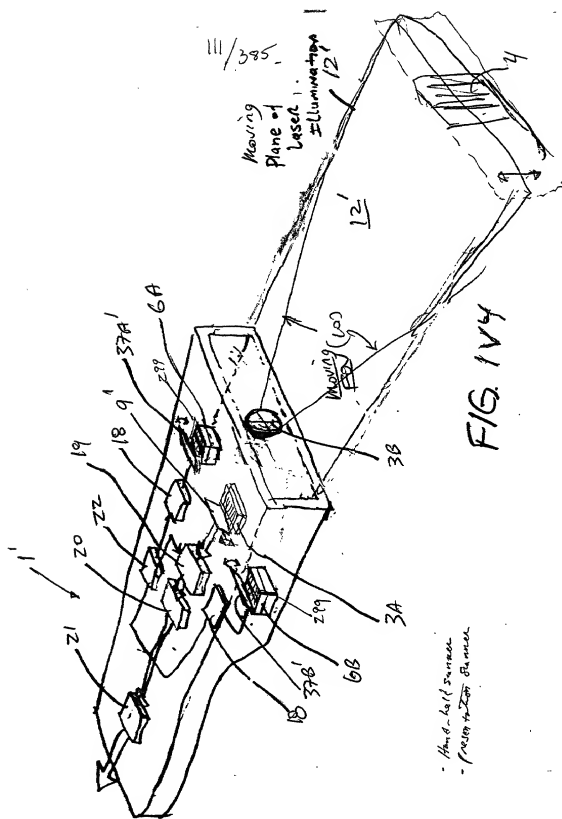


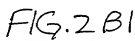
FIG. 1V3

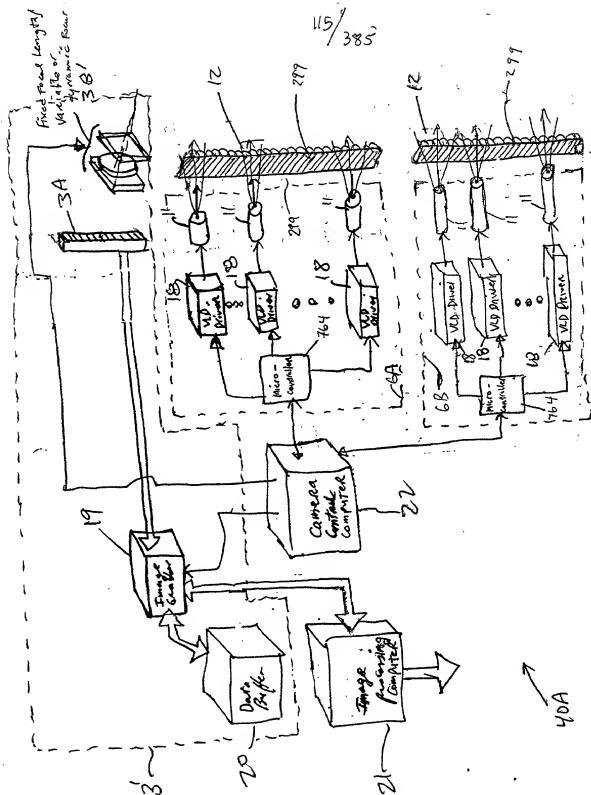
COPIES 12101



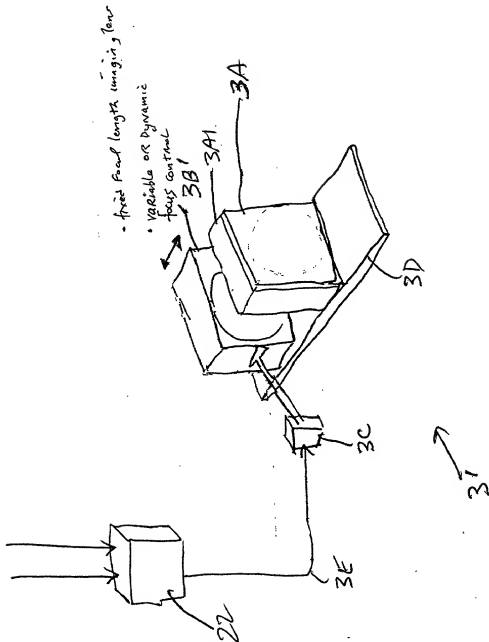
- Hand-drawn
- (Not to Scale)

Figure 1 illustrates the steps of the proposed algorithm for finding a minimum spanning tree. The process starts with a graph with 6 nodes and 7 edges. The algorithm proceeds by selecting edges in increasing order of weight, ensuring no cycles are formed. The selected edges are: (1,2) with weight 1, (2,3) with weight 1, (3,4) with weight 1, (4,5) with weight 1, (5,6) with weight 1, (1,3) with weight 2, (2,4) with weight 2, (3,5) with weight 2, (4,6) with weight 2, and (1,4) with weight 3. The final minimum spanning tree has 5 edges and a total weight of 10.




$$115 / 385$$

11/6/385



• fixed focal length imaging lens
• variable or dynamic focus control

FIG. 2C2

117/385

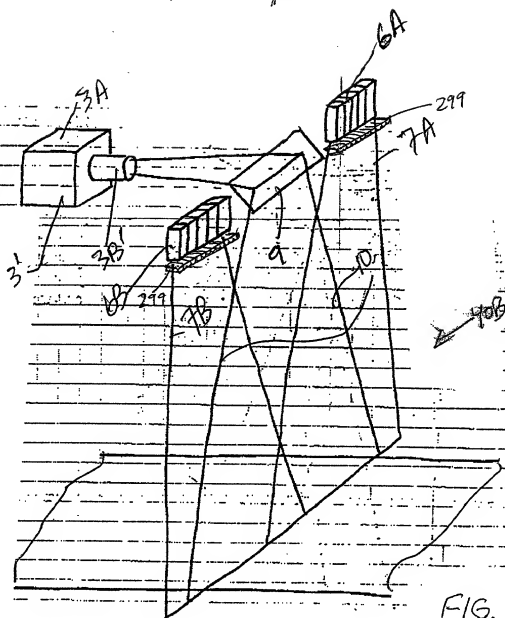
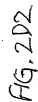


FIG. 2D1



403

119/285

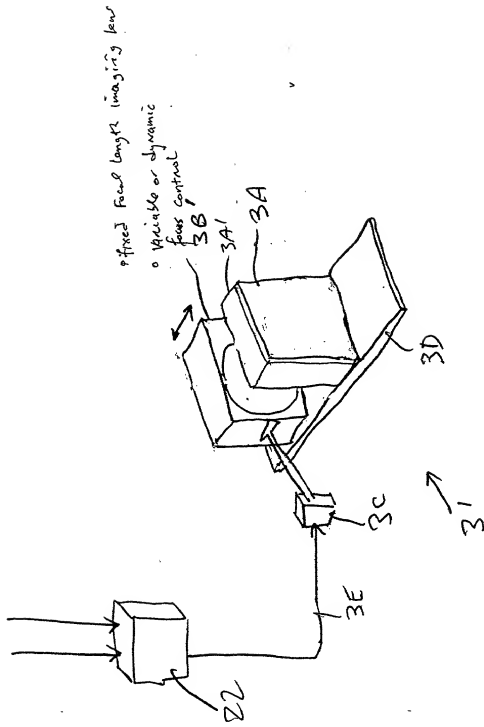
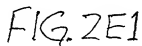


FIG. 2D3



122/385-

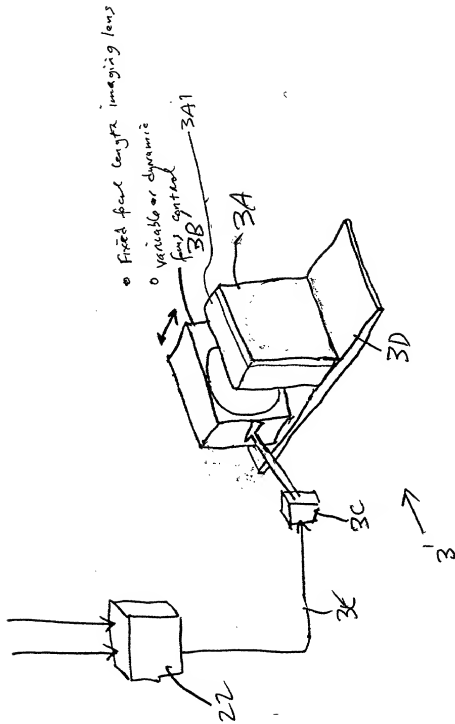


FIG. 2E3

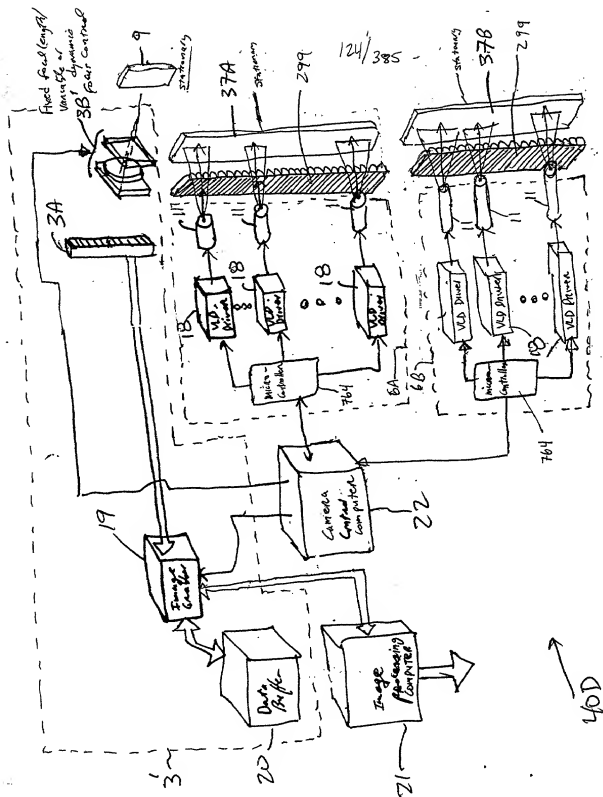


FIG. 2FZ

125/385

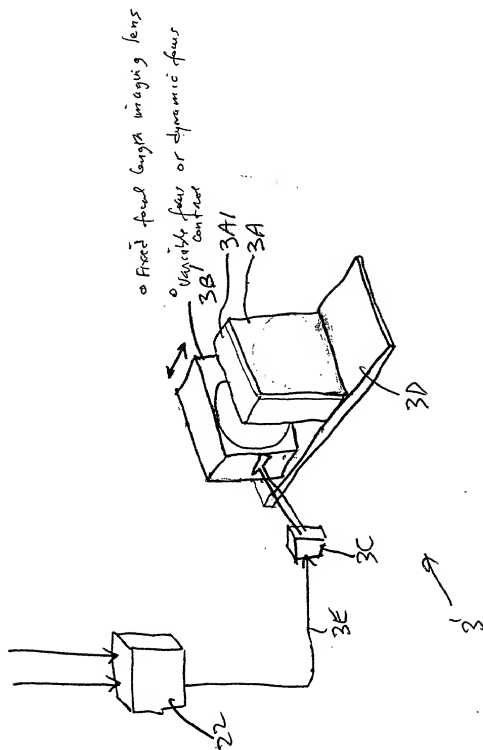


FIG. 2F3

126/385

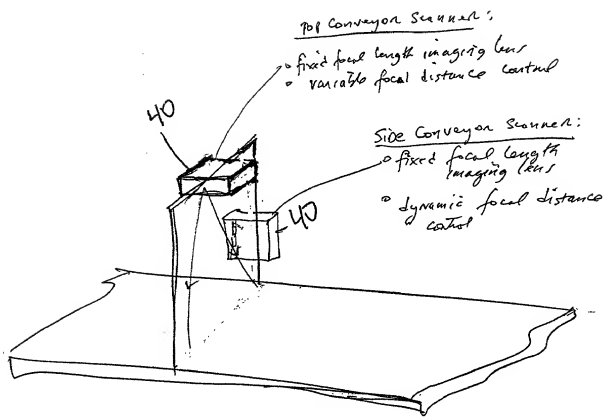
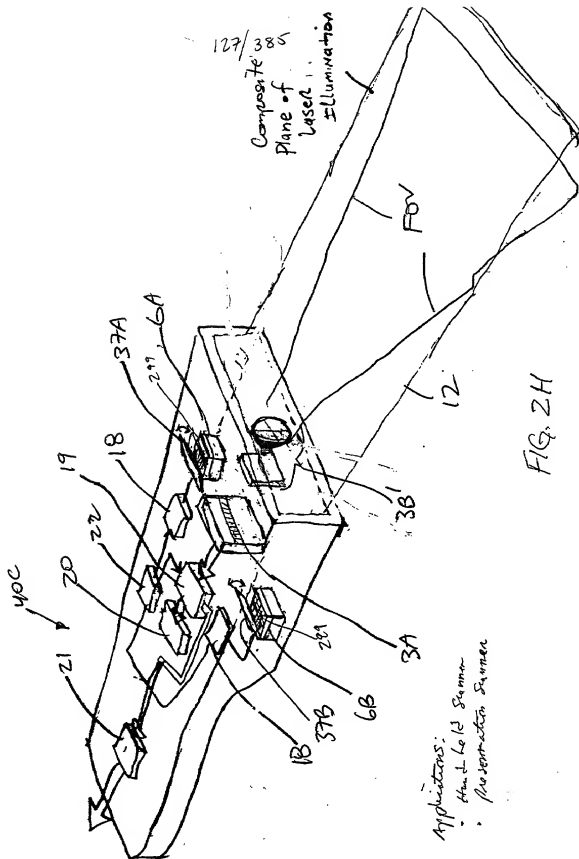


FIG. 2G



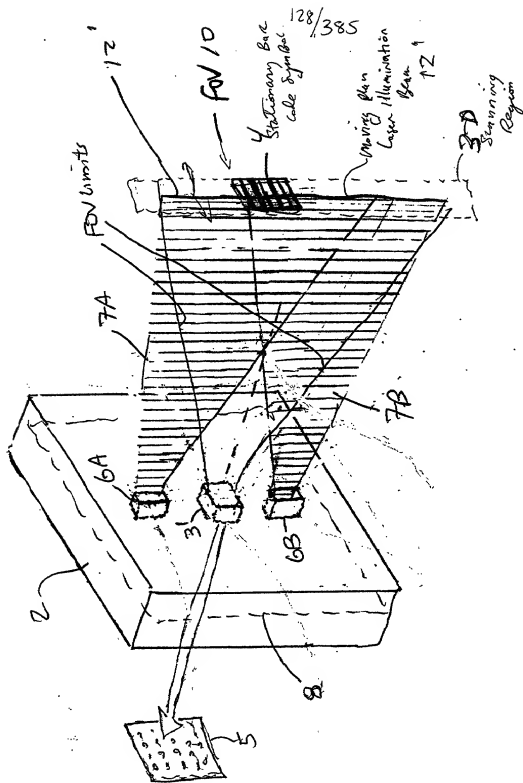


FIG. 211

अथवा

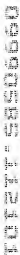


FIG 212

131/385

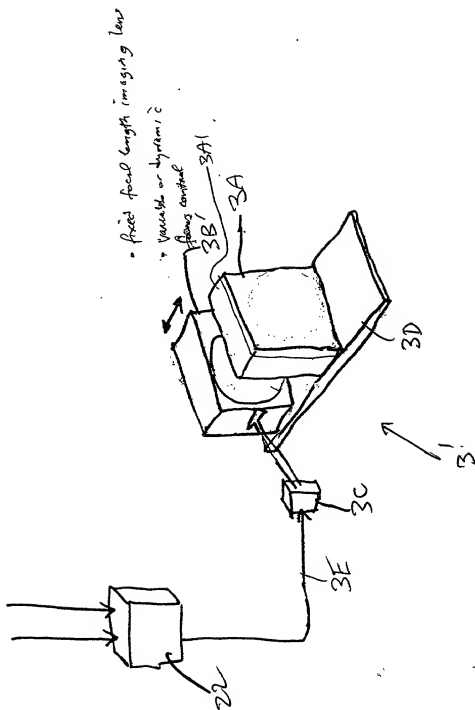
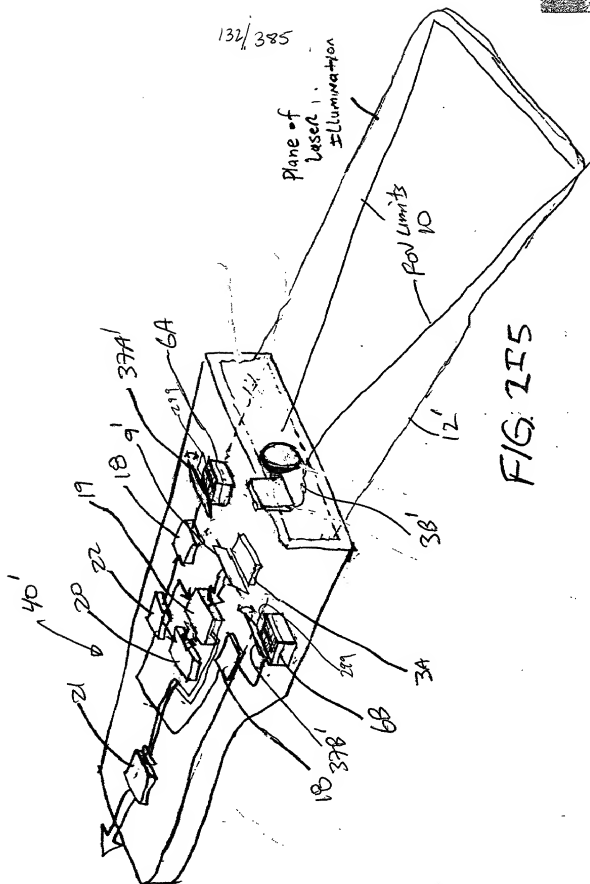


FIG. 2I4



133/385

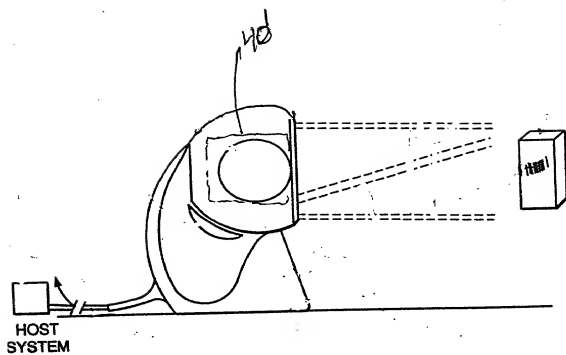
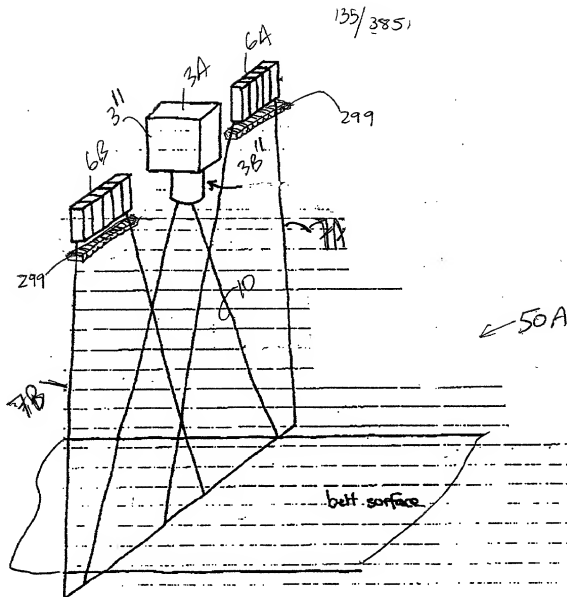


FIG. 2I6



138/395

- Variable focal length camera lens
- Variable focus distance

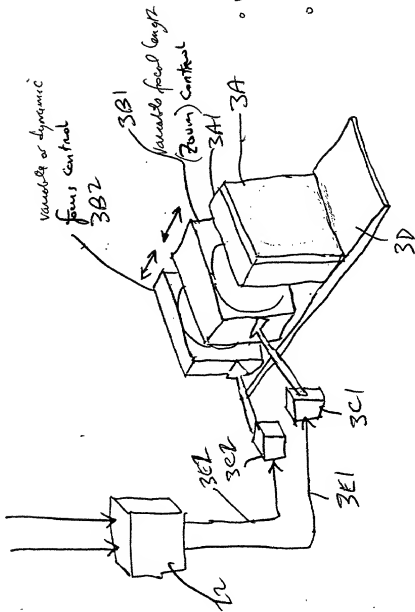
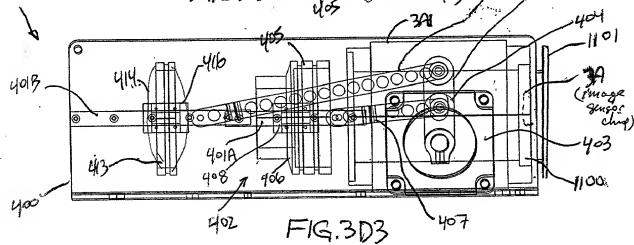
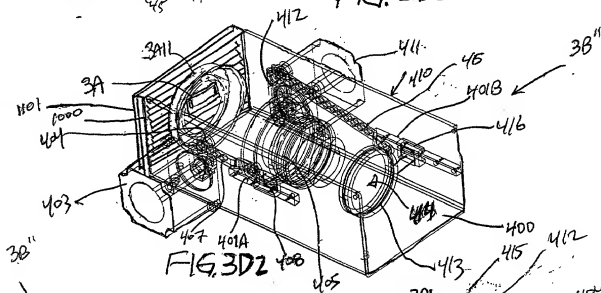
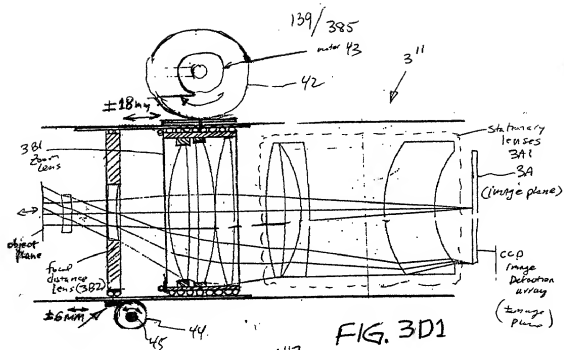


FIG. 3CZ



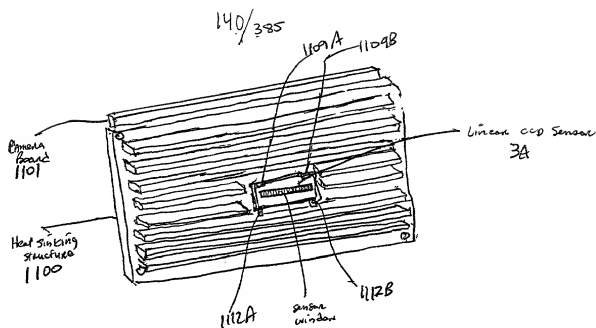


FIG. 3D4

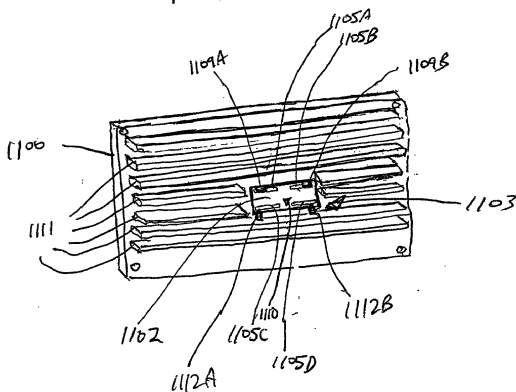


FIG. 3D5

141/385

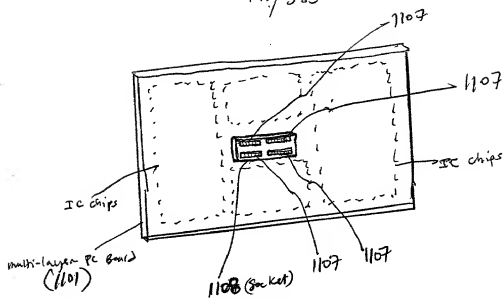


FIG. 3D6

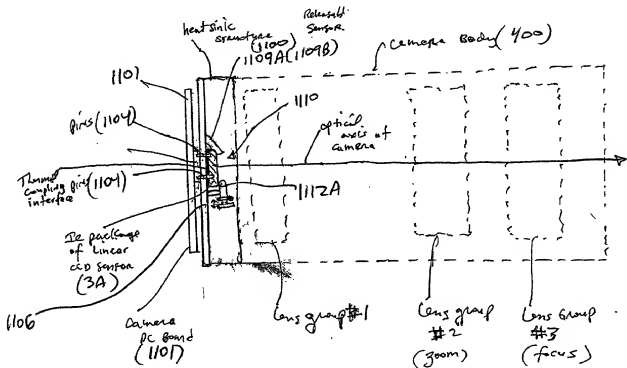


FIG. 3D7

142/385

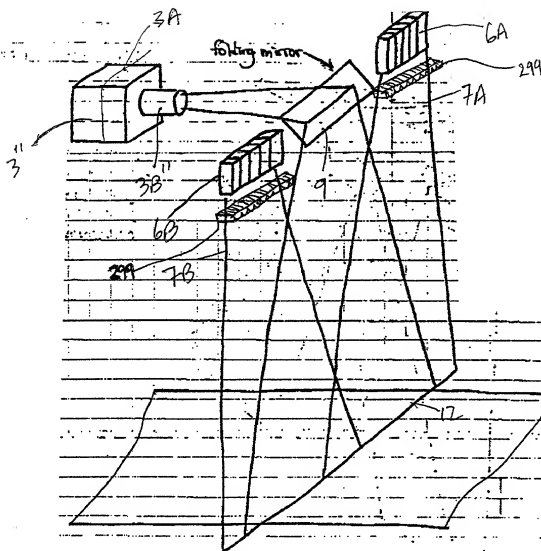


FIG 3E1

143/385

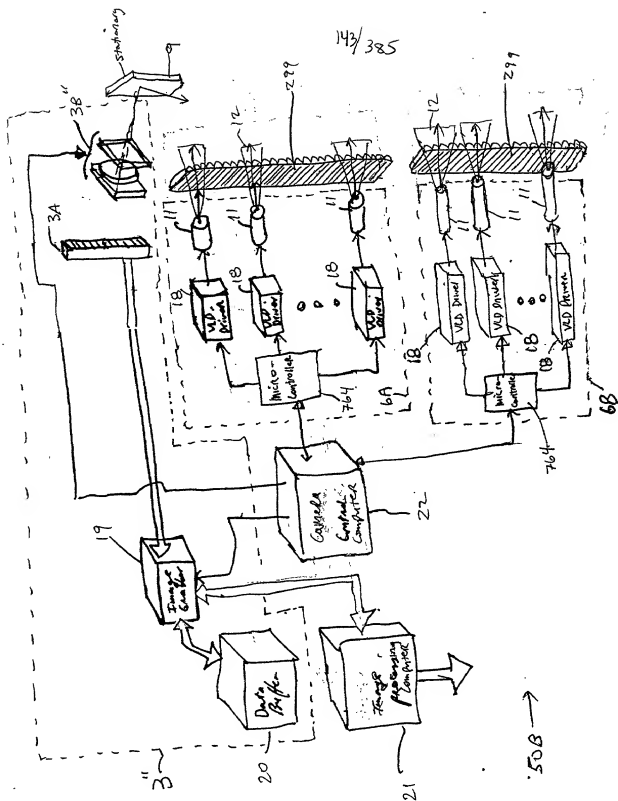


FIG. 3E2

508 →

TOTAL 3850600

144/385

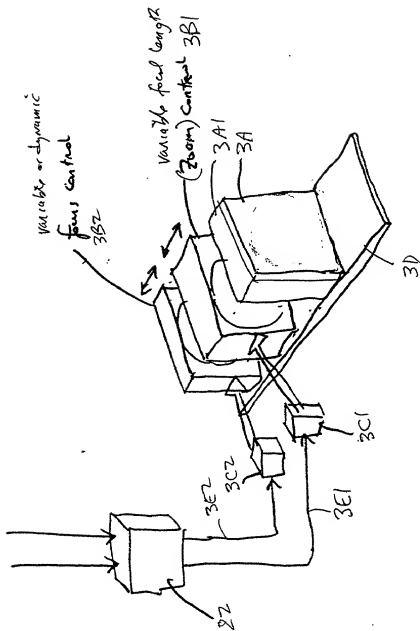
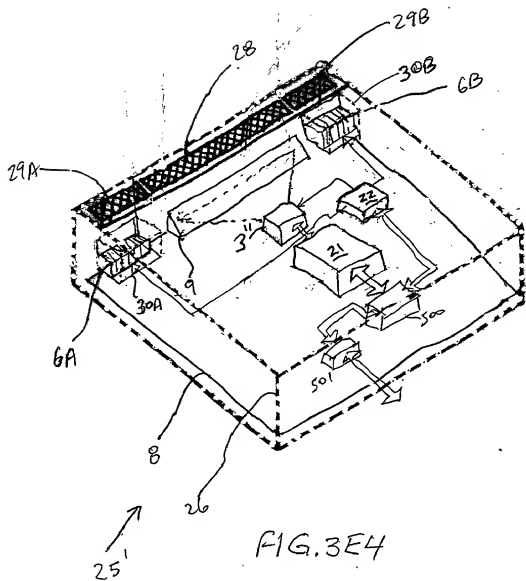


FIG. 3E3

M5/385,



146/385

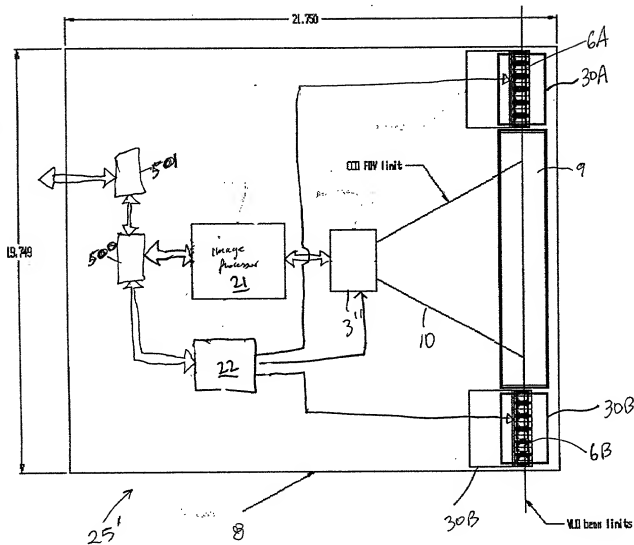


FIG. 3E5

147/385

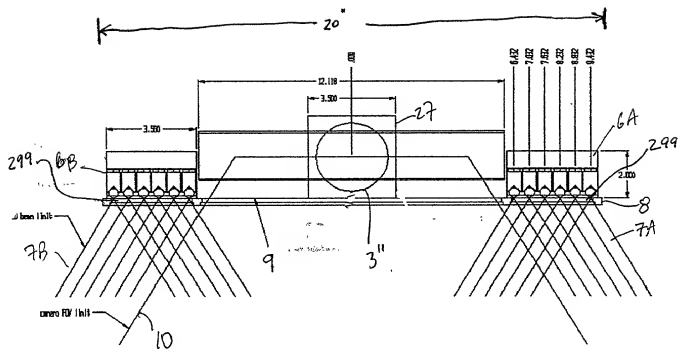


FIG. 3E6

148/385

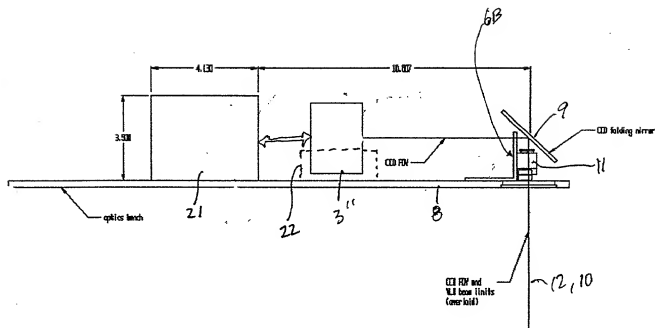


FIG. 3E7

149/385

*Variable FON

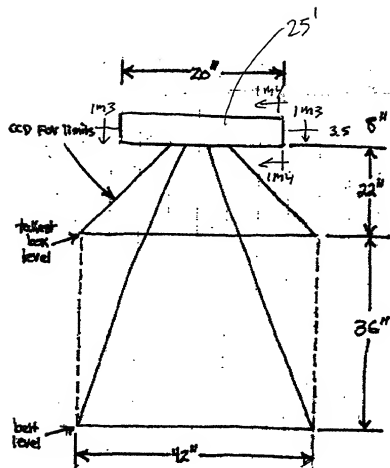


FIG. 3E8

150/385

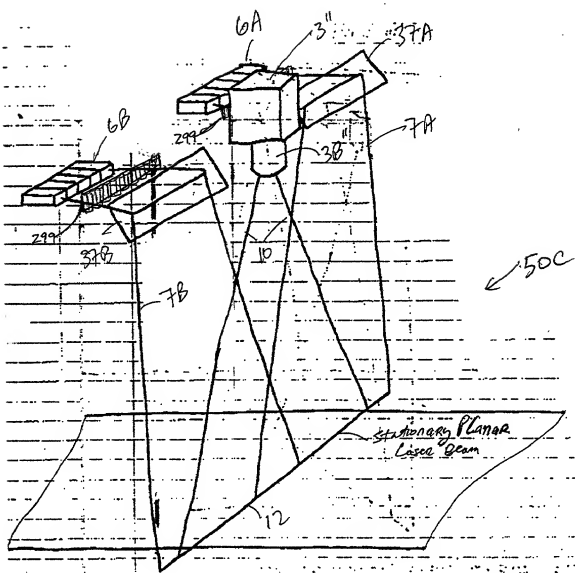
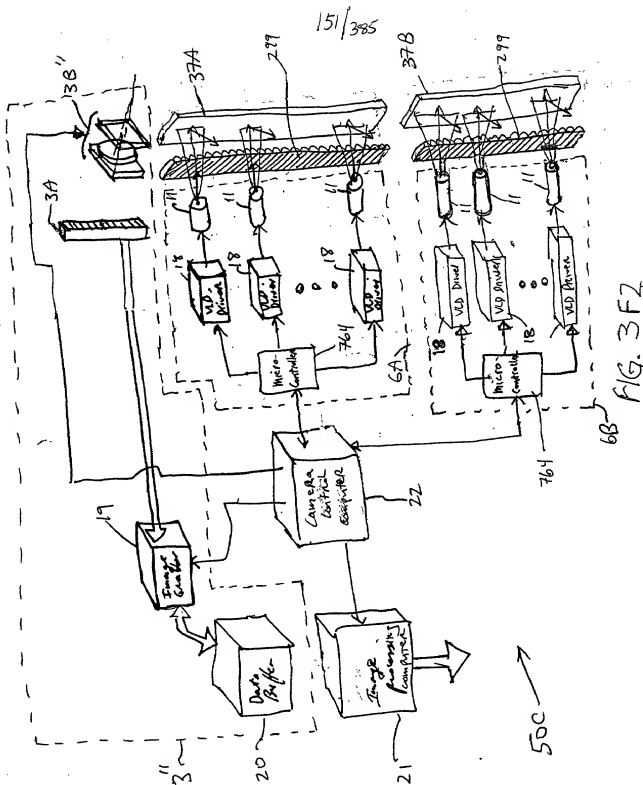


FIG. 3F1



154/385

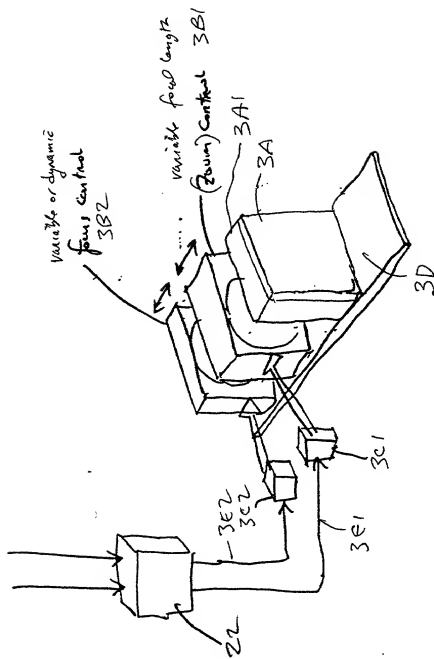


FIG. 3F3

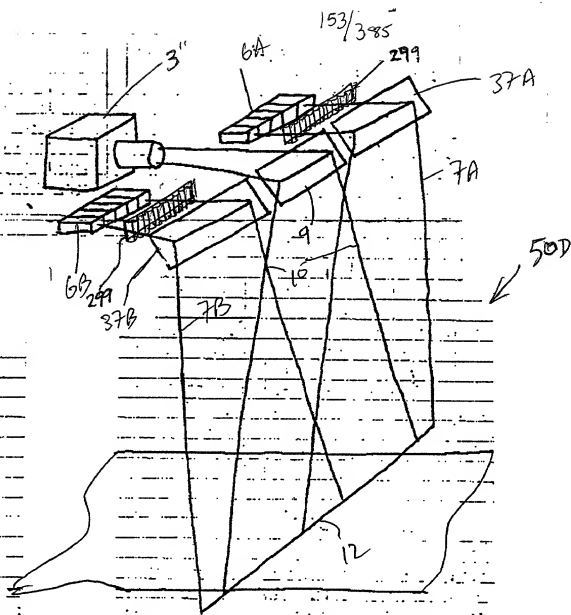


FIG. 3G1

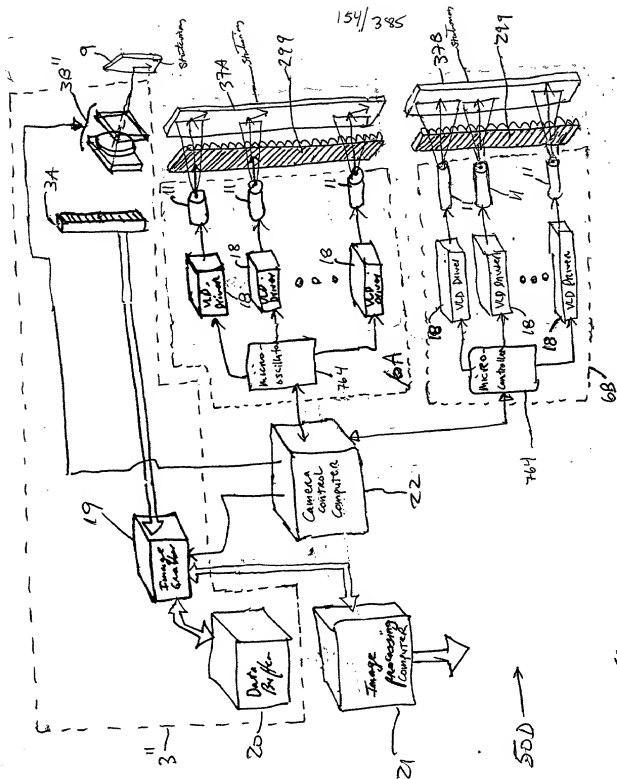
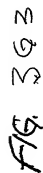
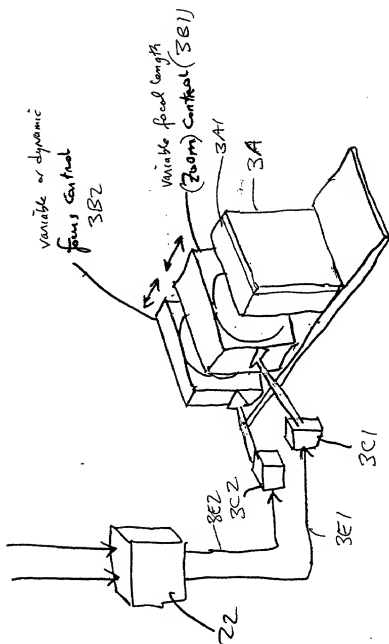


FIG. 3G2



311

156/385

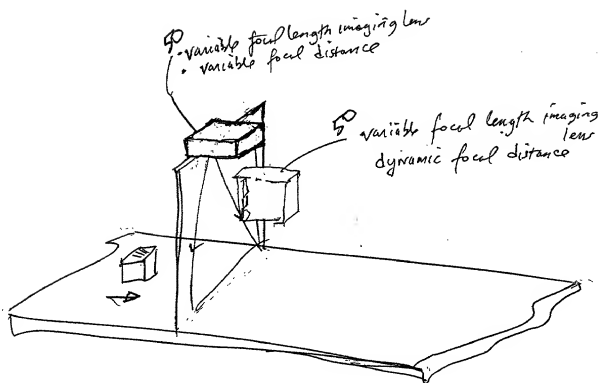
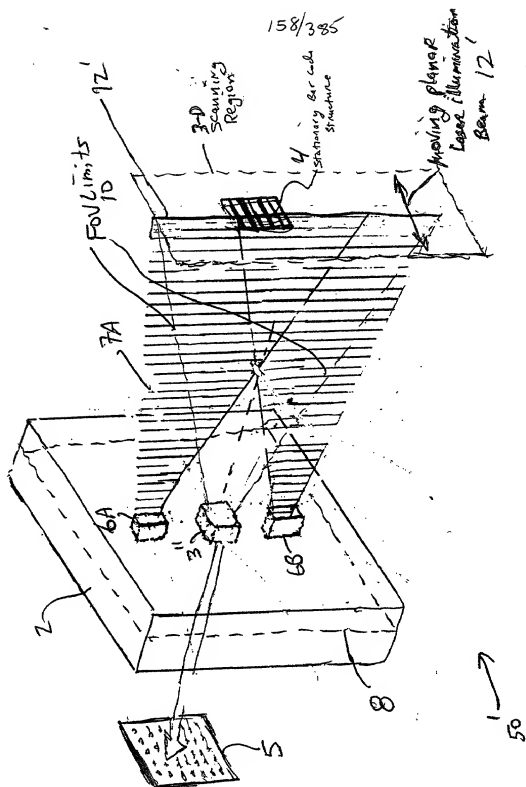


FIG. 3H



FIG. 31

FIG. 3J1



DISCLAIMER: The information on this page is not intended to be used for medical advice. It is for informational purposes only. Please consult your physician for more information.

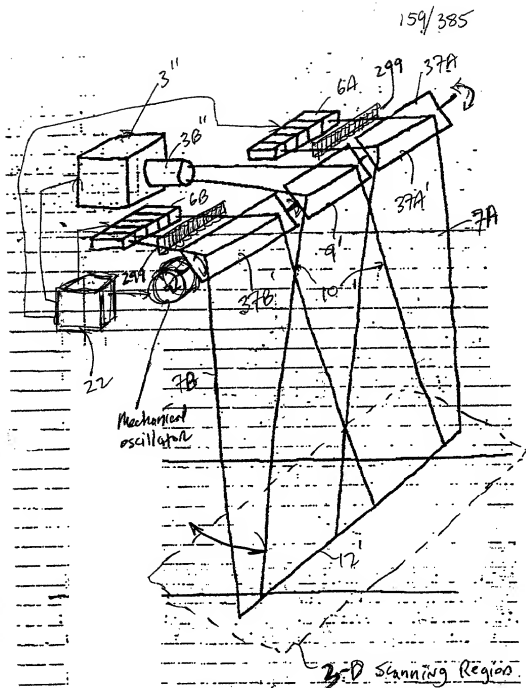


FIG. 3JZ

Category	Item	Value	Unit
Energy	Electricity	100	kWh
	Gas	100	kWh
Water	Water	100	m ³
	Wastewater	100	m ³
Waste	Waste	100	kg
	Recycling	100	kg
Transport	Transport	100	km
	Public Transport	100	km
Communication	Communication	100	min
	Internet	100	min
Health	Health	100	min
	Exercise	100	min
Education	Education	100	min
	Reading	100	min
Culture	Culture	100	min
	Art	100	min
Leisure	Leisure	100	min
	TV	100	min
Food	Food	100	min
	Drinking	100	min
Clothing	Clothing	100	min
	Shoes	100	min
Housing	Housing	100	min
	Rent	100	min
Finance	Finance	100	min
	Banking	100	min
Travel	Travel	100	min
	Car	100	min
Security	Security	100	min
	Police	100	min
Justice	Justice	100	min
	Court	100	min
Government	Government	100	min
	Parliament	100	min
Military	Military	100	min
	Army	100	min
Science	Science	100	min
	Research	100	min
Technology	Technology	100	min
	Innovation	100	min
Environment	Environment	100	min
	Nature	100	min
Society	Society	100	min
	Community	100	min
Religion	Religion	100	min
	Church	100	min
Philosophy	Philosophy	100	min
	Logic	100	min
Art	Art	100	min
	Music	100	min
Literature	Literature	100	min
	Books	100	min
History	History	100	min
	Events	100	min
Geography	Geography	100	min
	Maps	100	min
Mathematics	Mathematics	100	min
	Numbers	100	min
Physics	Physics	100	min
	Atoms	100	min
Chemistry	Chemistry	100	min
	Elements	100	min
Biology	Biology	100	min
	Cells	100	min
Medicine	Medicine	100	min
	Drugs	100	min
Law	Law	100	min
	Contracts	100	min
Economics	Economics	100	min
	Markets	100	min
Politics	Politics	100	min
	Policy	100	min
Social	Social	100	min
	Groups	100	min
Psychology	Psychology	100	min
	Mind	100	min
Philosophy	Philosophy	100	min
	Thought	100	min
Ethics	Ethics	100	min
	Morals	100	min
Aesthetics	Aesthetics	100	min
	Beauty	100	min
Logic	Logic	100	min
	Reason	100	min
Science	Science	100	min
	Discovery	100	min
Technology	Technology	100	min
	Invention	100	min
Environment	Environment	100	min
	Conservation	100	min
Society	Society	100	min
	Community	100	min
Religion	Religion	100	min
	Belief	100	min
Philosophy	Philosophy	100	min
	Wisdom	100	min
Art	Art	100	min
	Expression	100	min
Literature	Literature	100	min
	Writing	100	min
History	History	100	min
	Events	100	min
Geography	Geography	100	min
	Maps	100	min
Mathematics	Mathematics	100	min
	Numbers	100	min
Physics	Physics	100	min
	Atoms	100	min
Chemistry	Chemistry	100	min
	Elements	100	min
Biology	Biology	100	min
	Cells	100	min
Medicine	Medicine	100	min



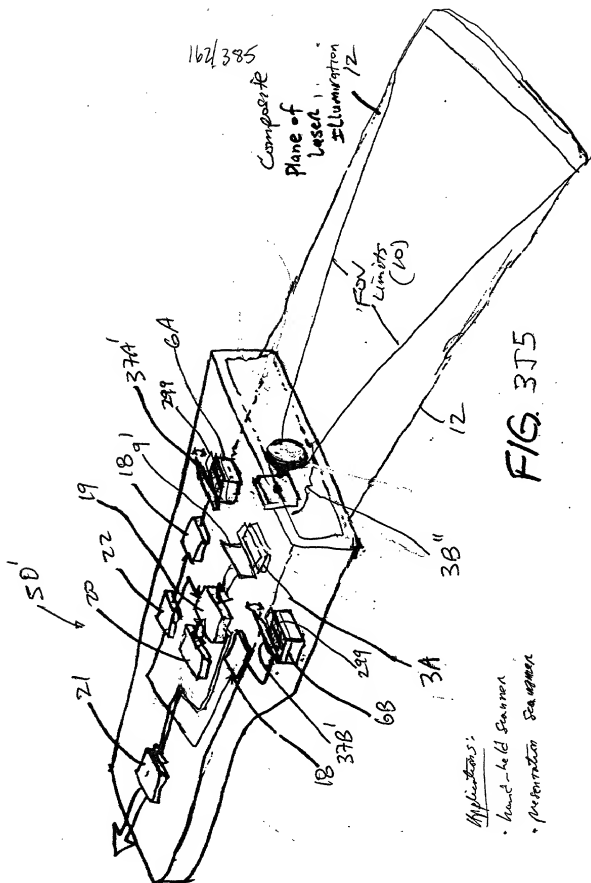


FIG. 3T5

Applications:

- hand-held scanner
- presentation scanner

163/385

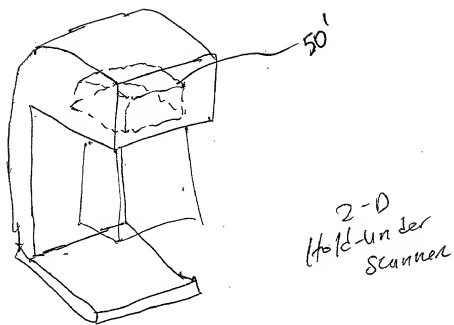


FIG-3J6

1165/385

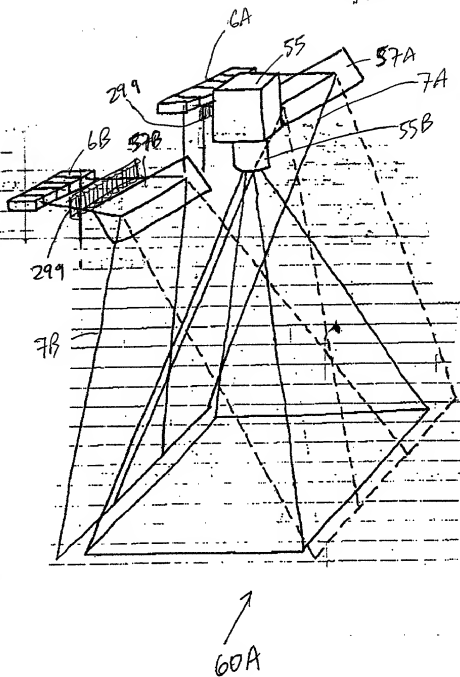


FIG. 4B1

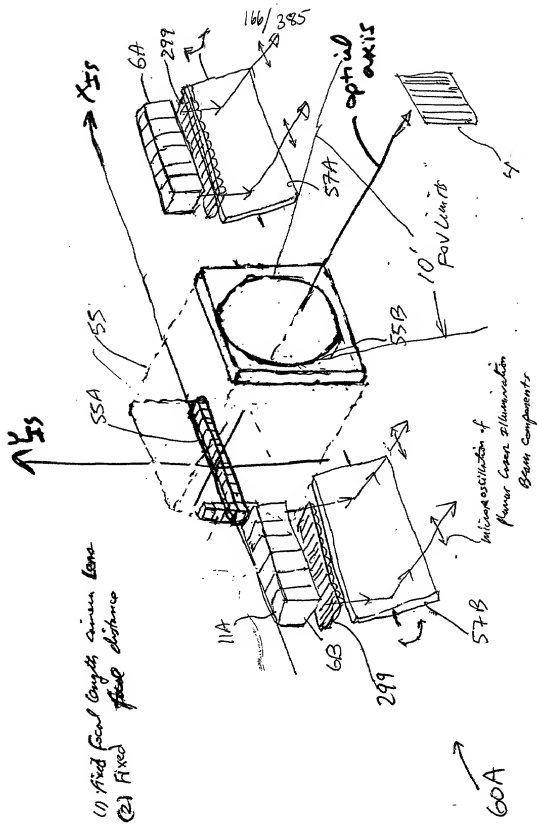
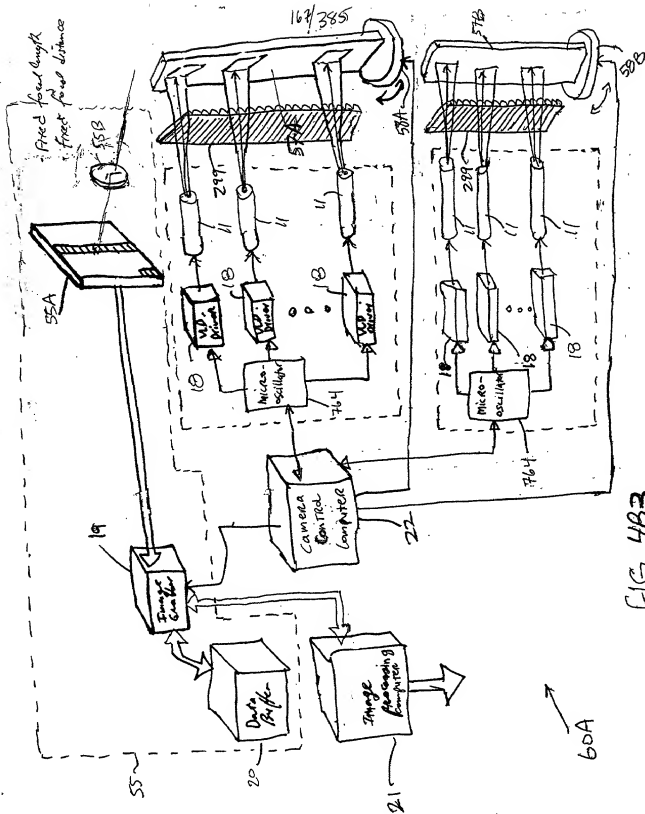


FIG. 4B.Z

- (1) First focal length minus lens
- (2) Fixed field distance



168/385

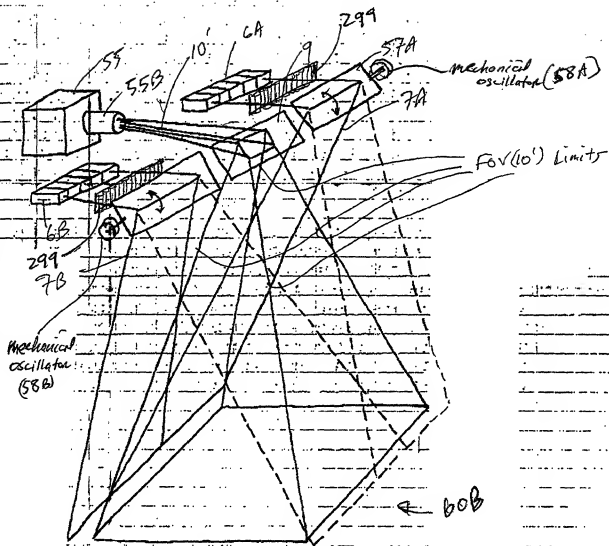
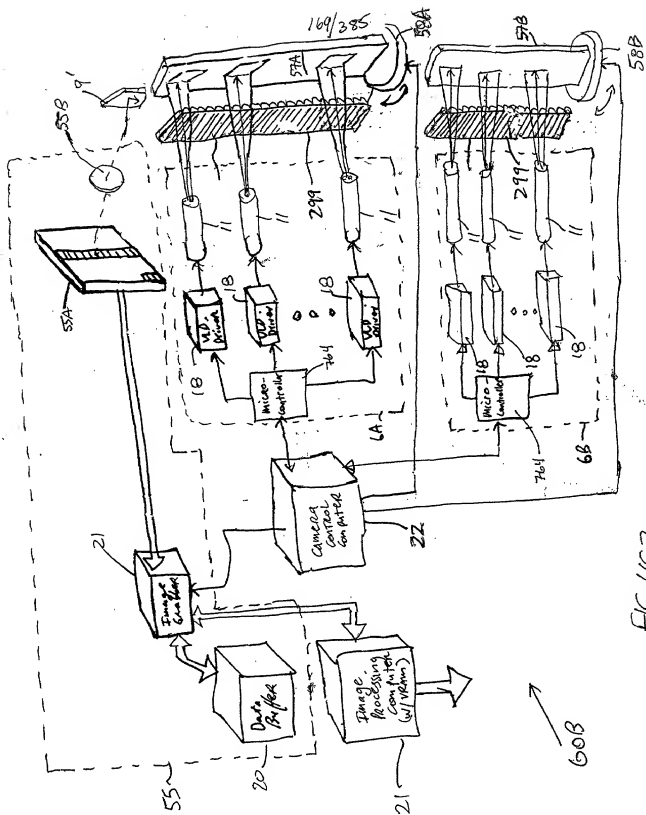


FIG. 4C-1



170/385

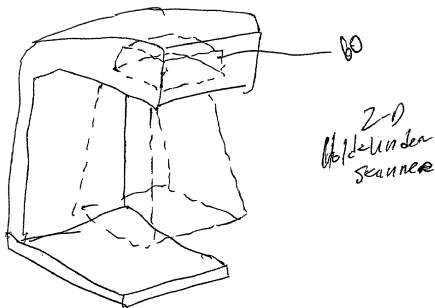


FIG. 4D

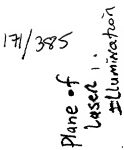


FIG. 4E

Applications:

- Hand-held Scanner
- Presentation Scanner



Fig. 5A

of

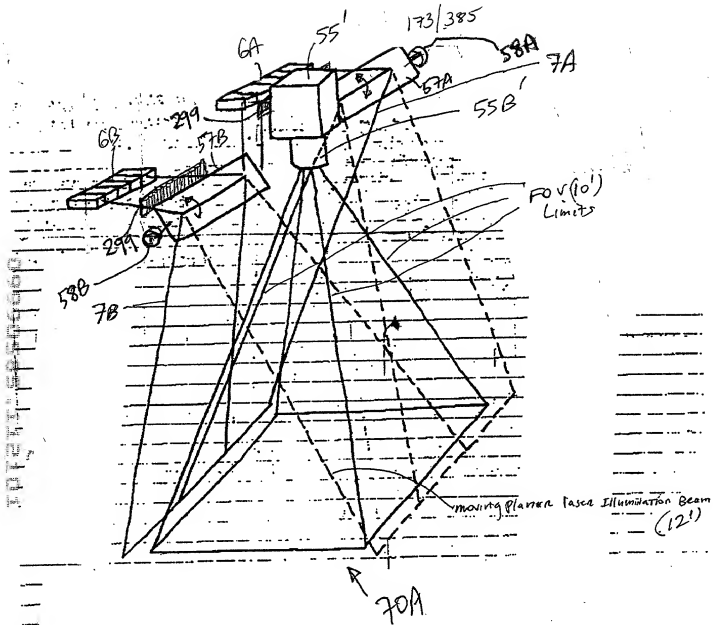
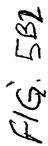


FIG 5B1



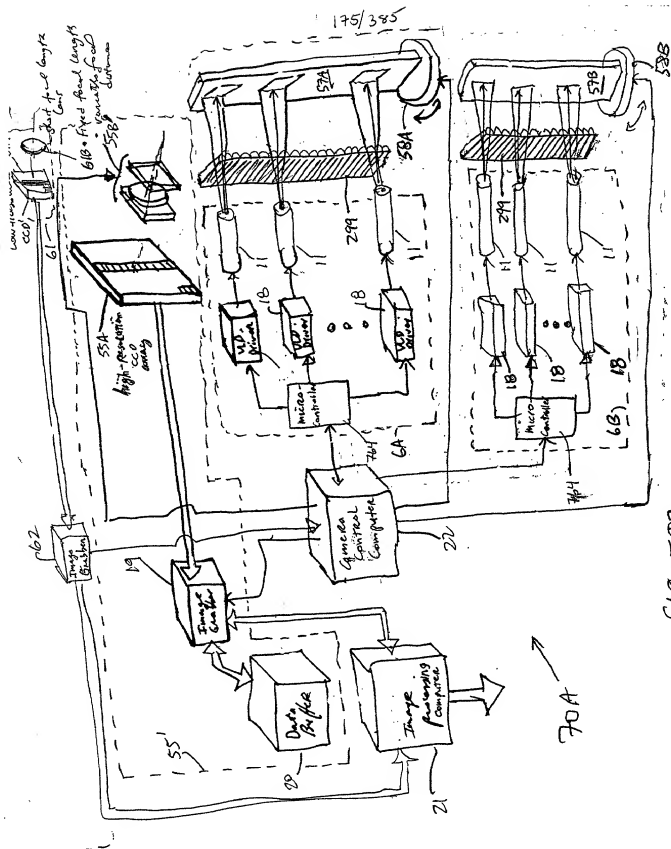


Fig. 5B3

00000585 112101

176/385

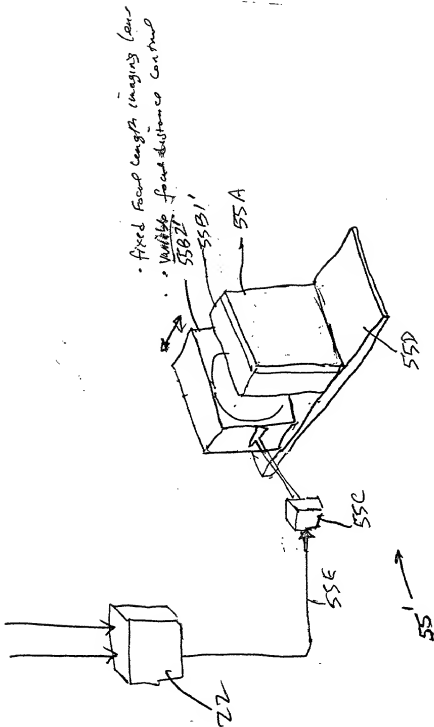


FIG. 5B4

177/385

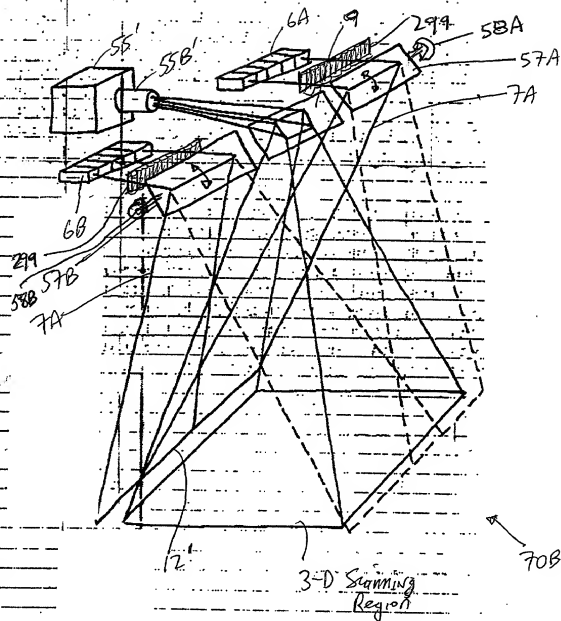


FIG. 5C1

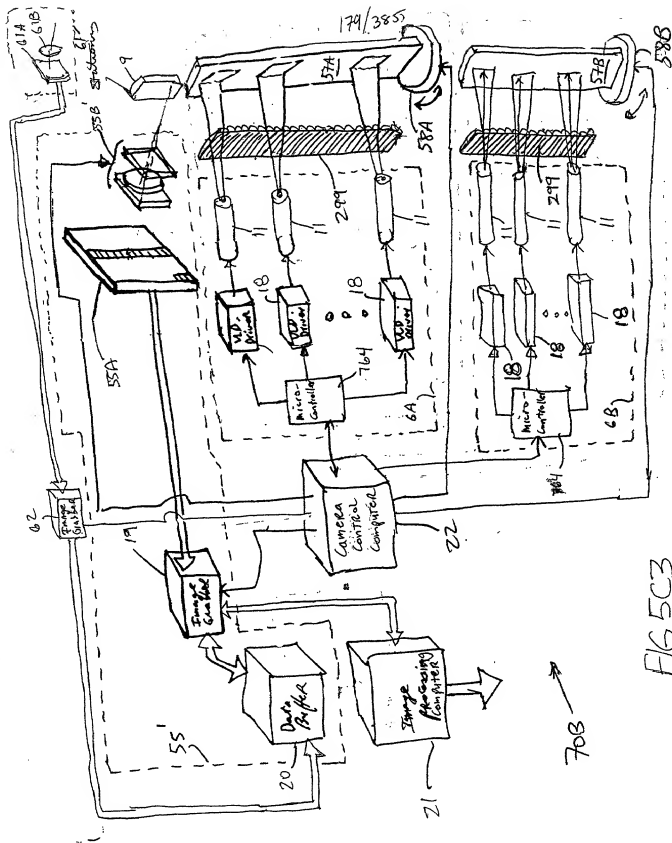


Fig. 5C

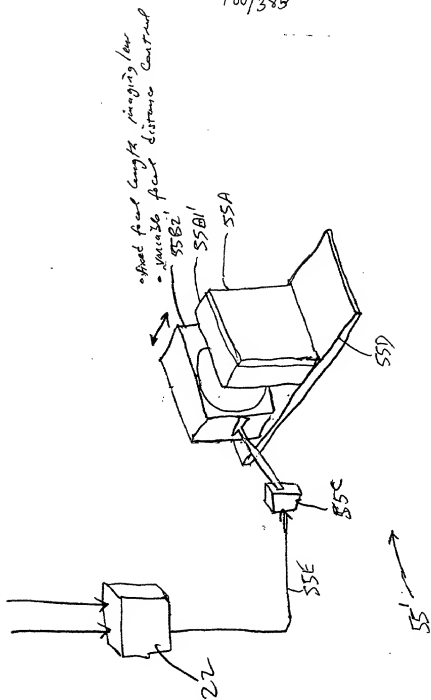


Fig. 5C4

181/385

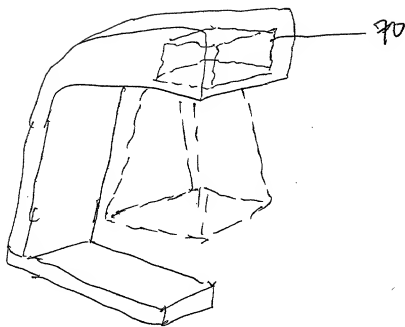


FIG. 5D

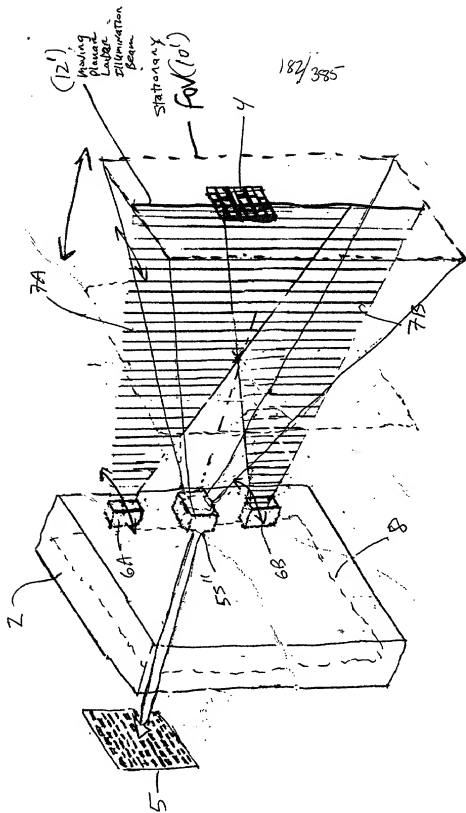
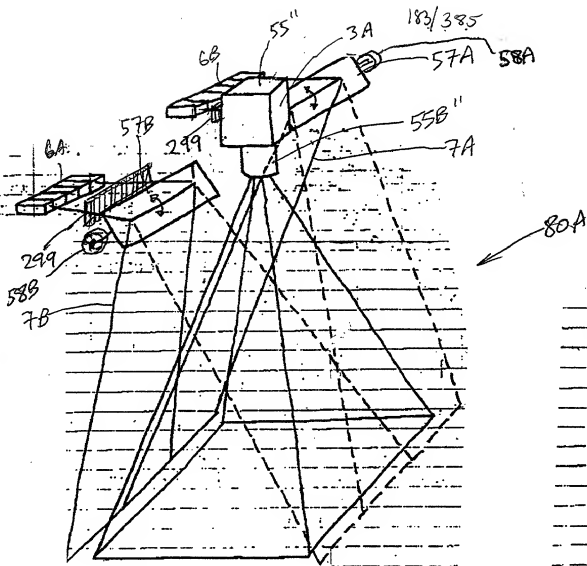


FIG. 6A



00000585.112131

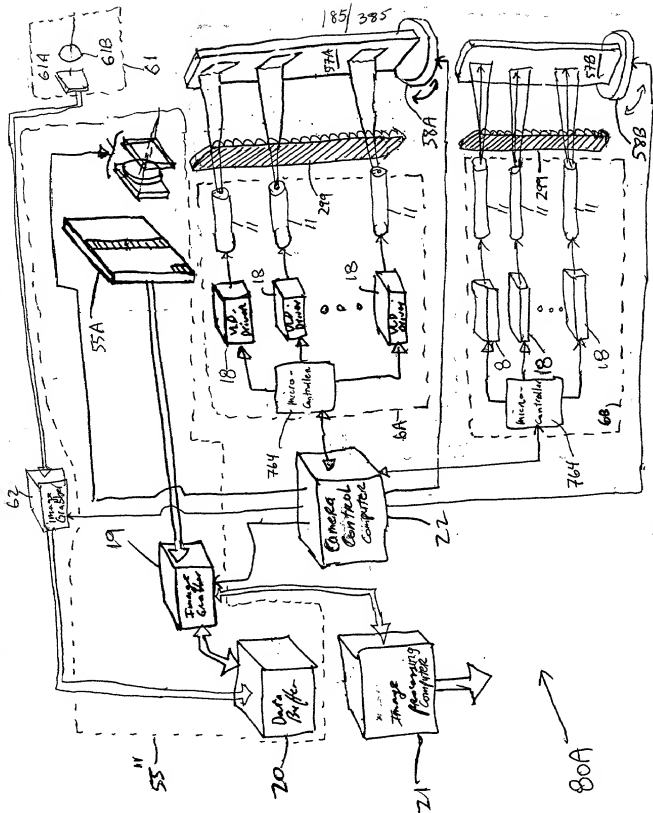


FIG. 6B3

186/385

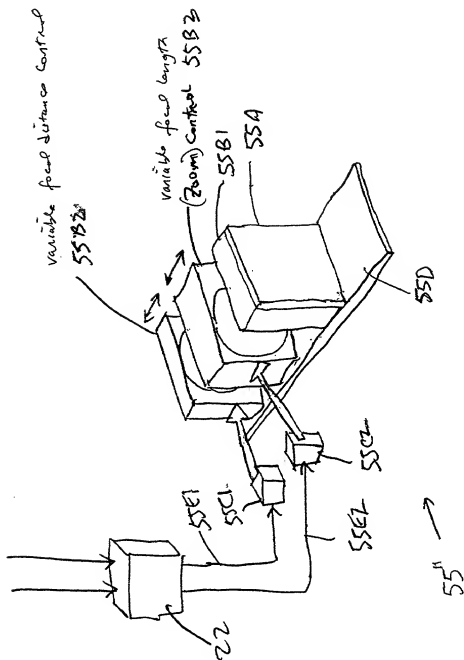


FIG. 6B4

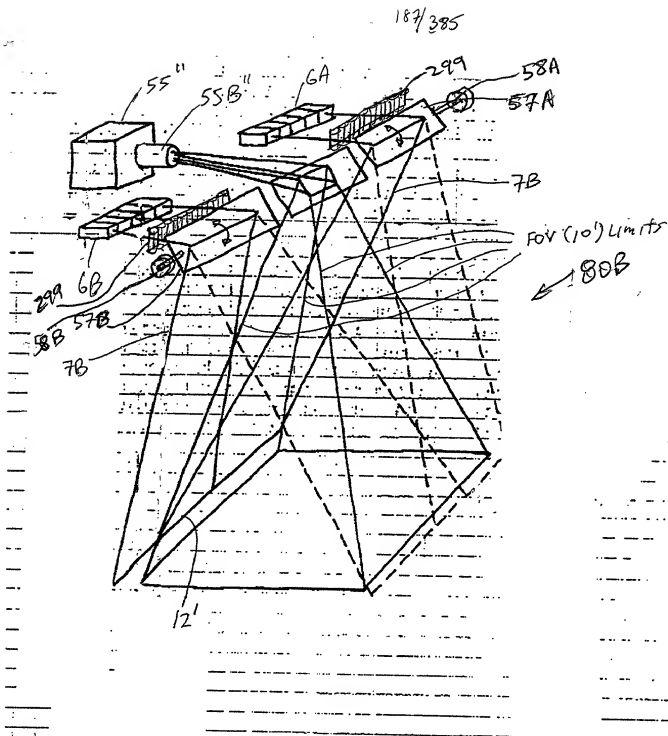


FIG. 6C1

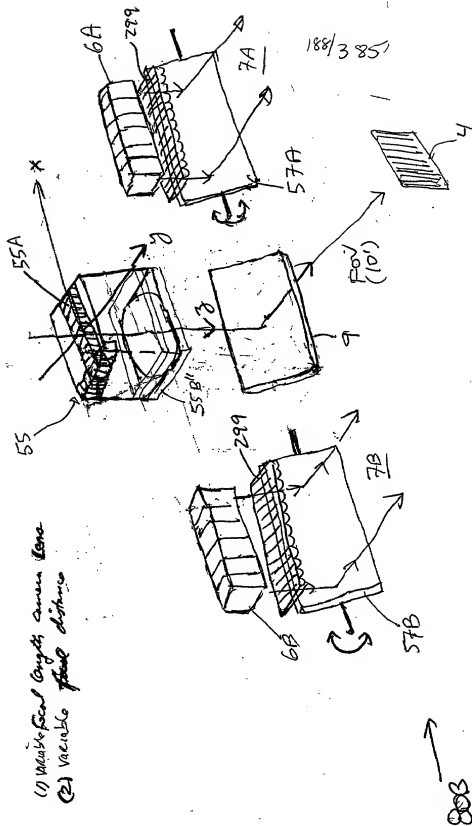


FIG. 6C2

(1) Vacuum tube
(2) Variable fluid diaphragm

800

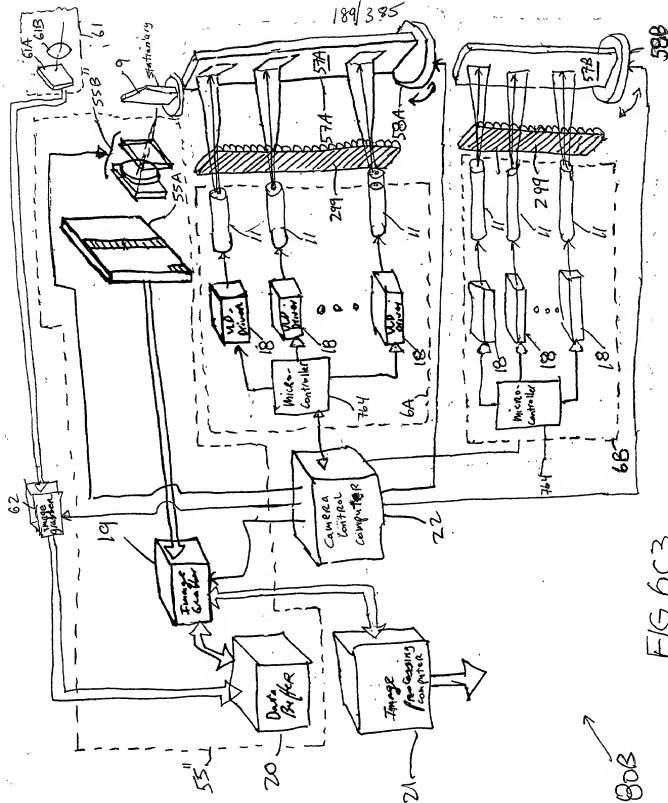


FIG. 6C3

191/385

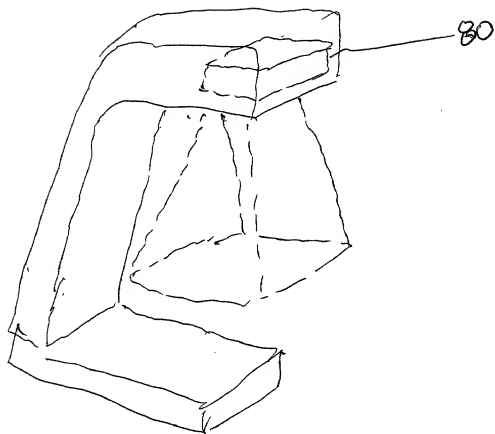
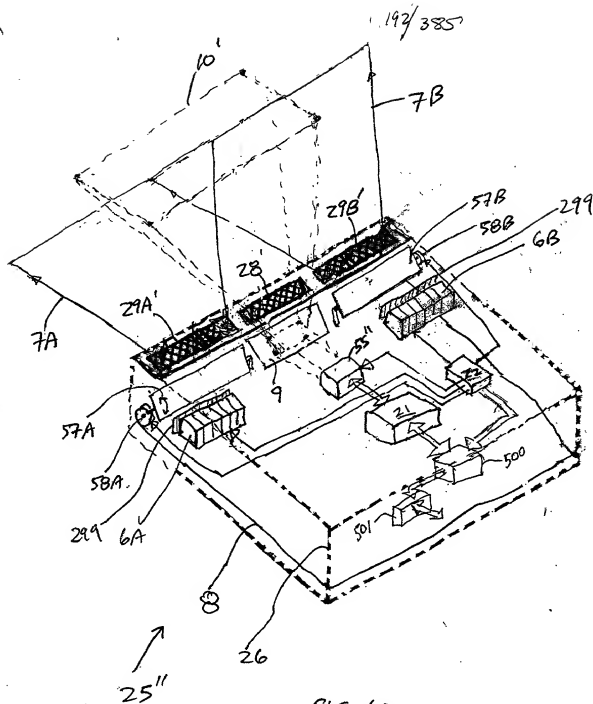
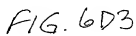


FIG. 6C5

00000000.112101





195/385

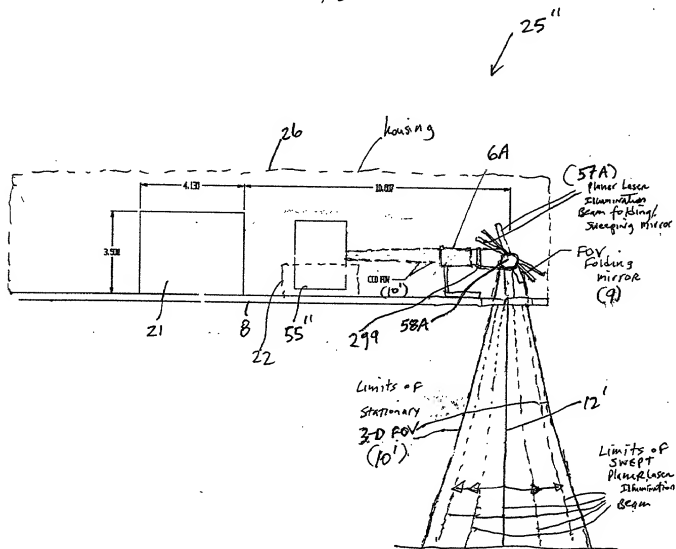
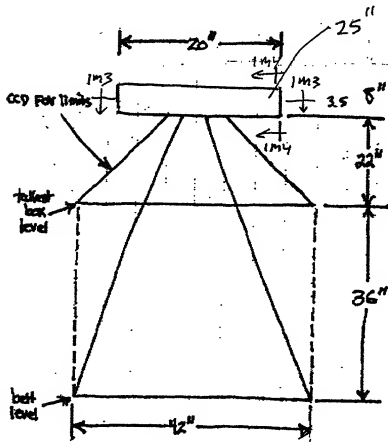


FIG. 6D4

WILEY

FIG. 6D5



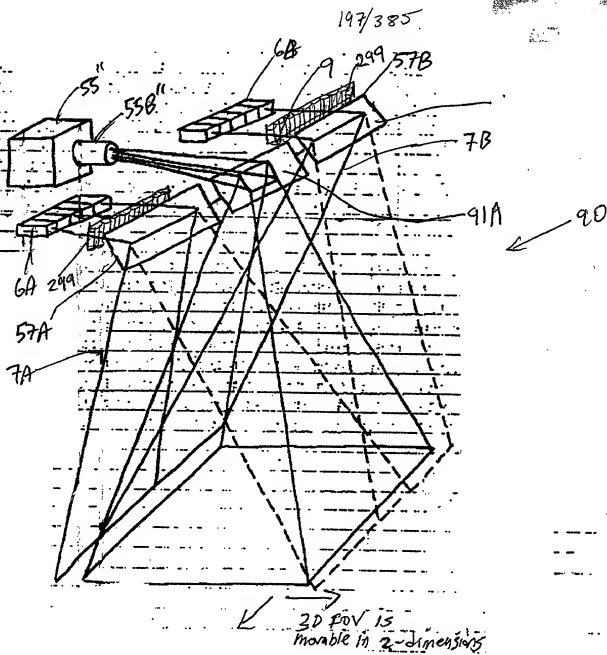


FIG. 6E1

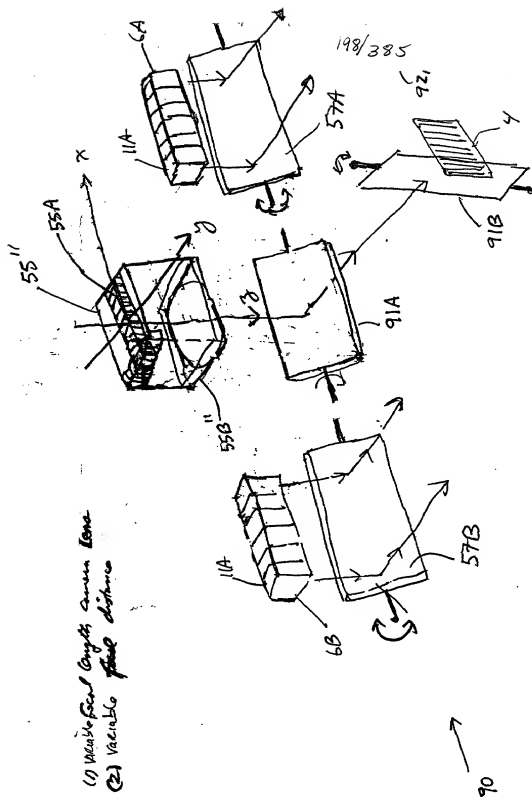


FIG. 6E2

(1) Vacuum tube
(2) Vacuum tube

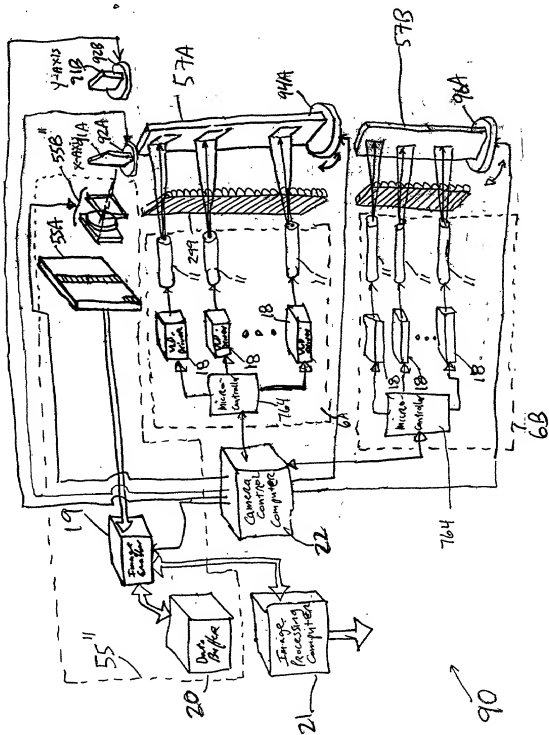


FIG. 6E3

200/385

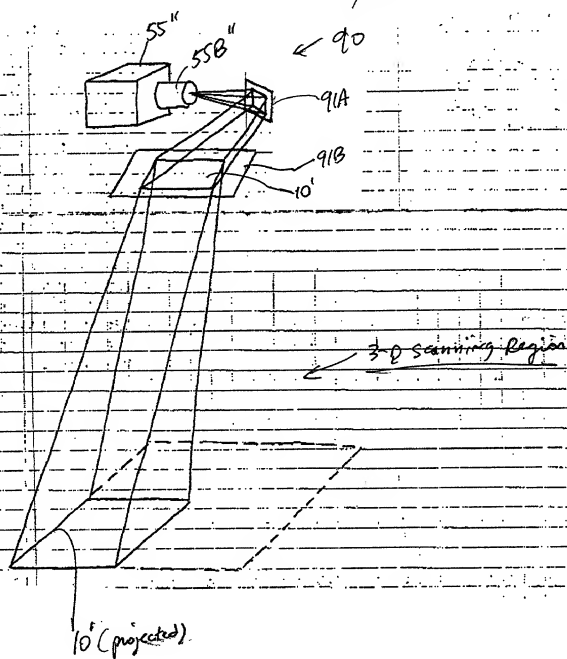


FIG. 6R4

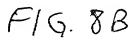
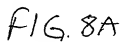


FIG. 9.

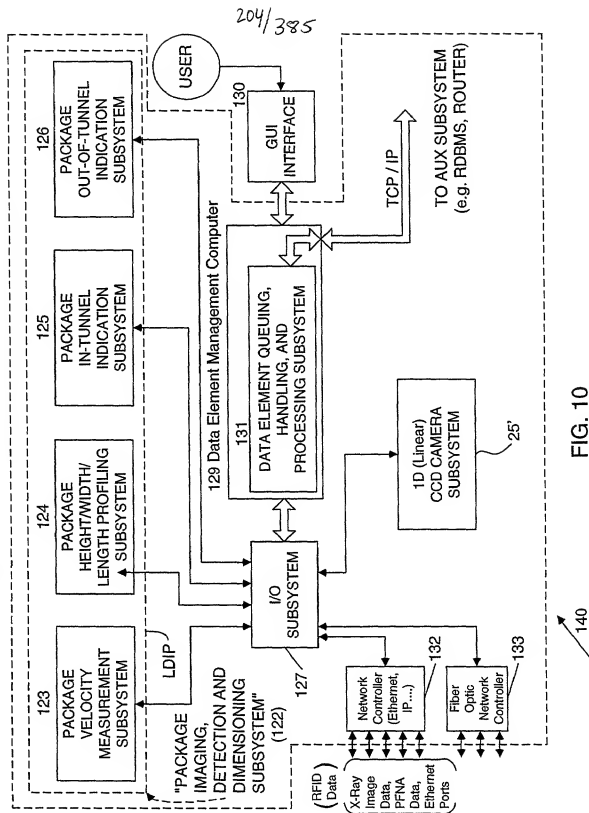


FIG. 10

Data Element Queuing, Handling, and Processing Subsystem (131)

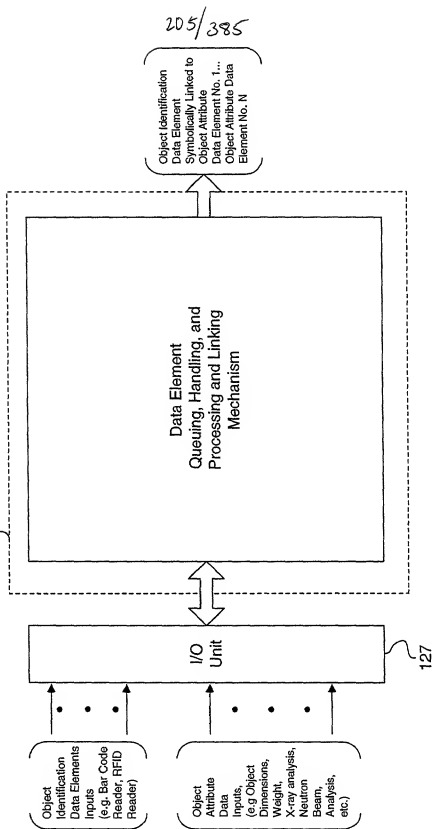


FIG. 10A

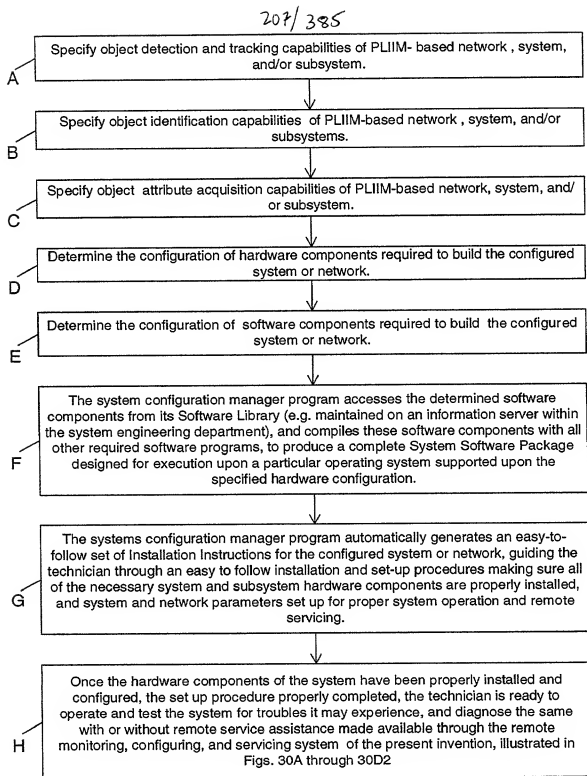


FIG. 10C

208/285

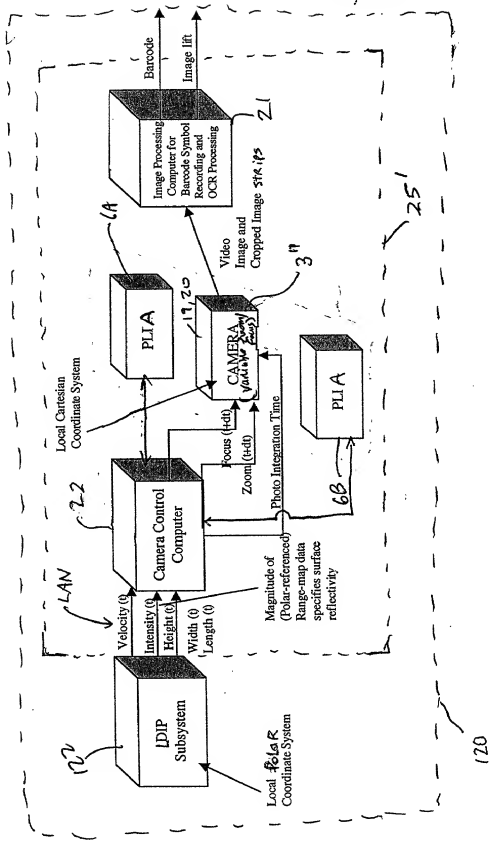


FIG. 11

209/385

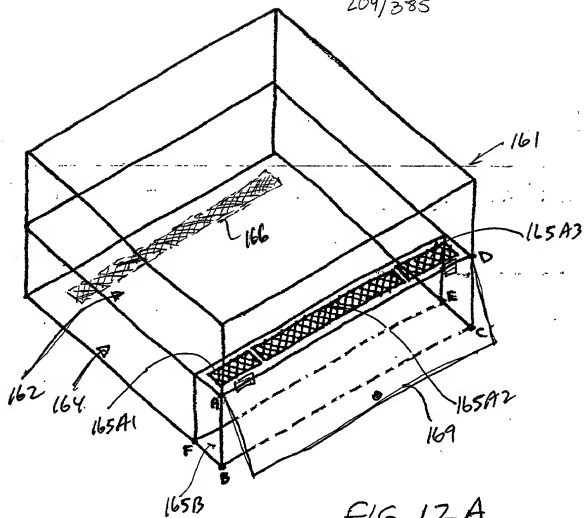


FIG. 12A

211/385

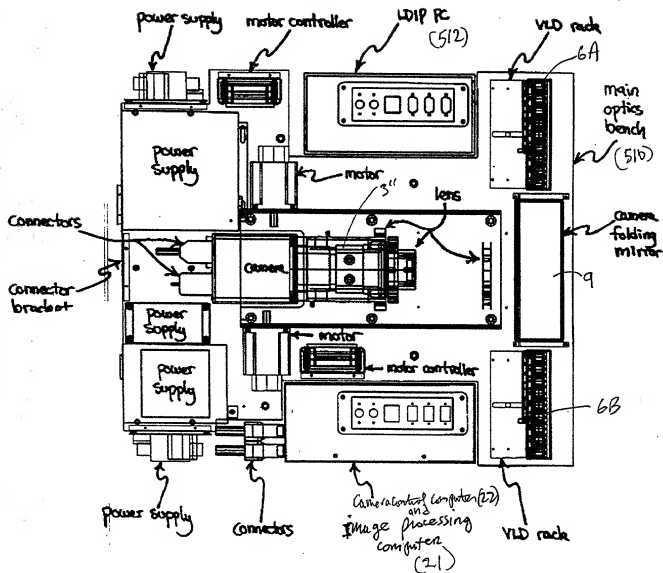


FIG. 12C

212/385

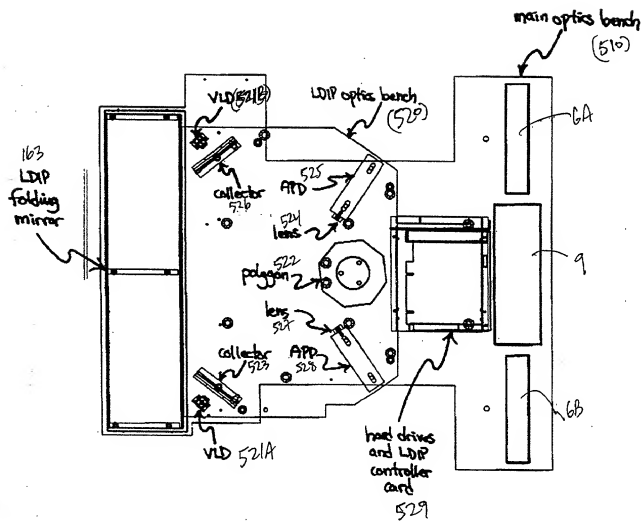
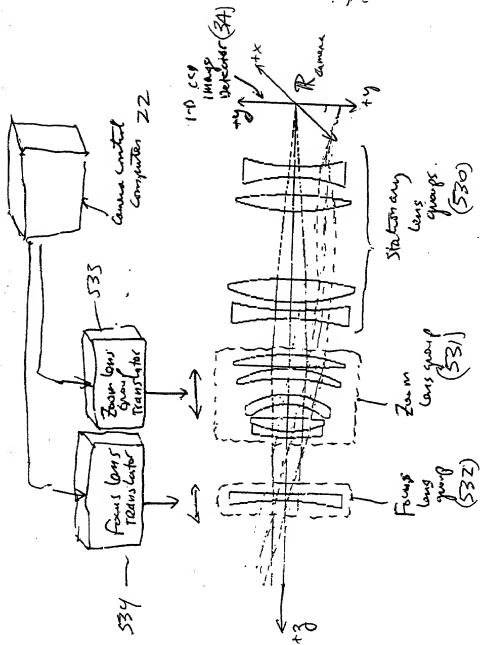


FIG. 12D

213/285



(main optics)
(Lens groups)

FIG. 12E

214/385

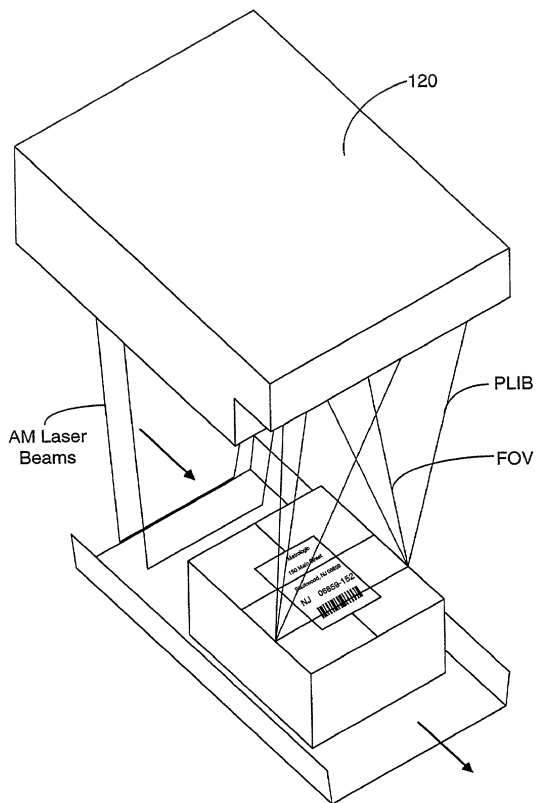


FIG. 13A

215/385

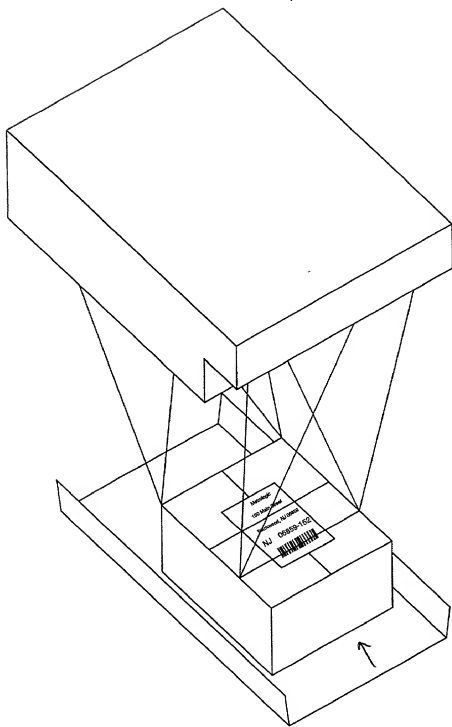


FIG. 13A

216/385

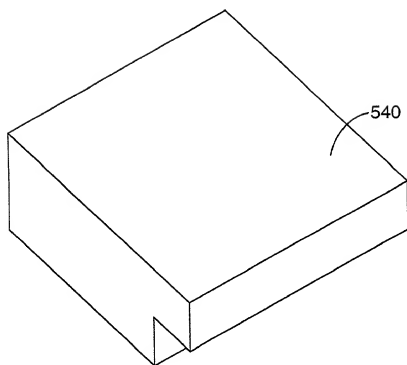


FIG. 13B

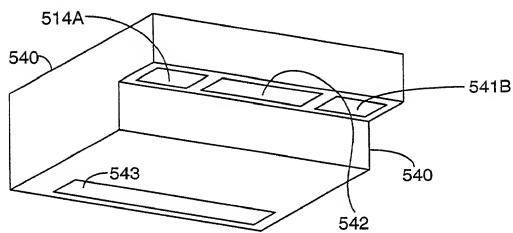


FIG. 13C

27/ 385
 PLLIM-BASED PACKAGE IDENTIFICATION AND
 DIMENSIONING (PID) SYSTEM

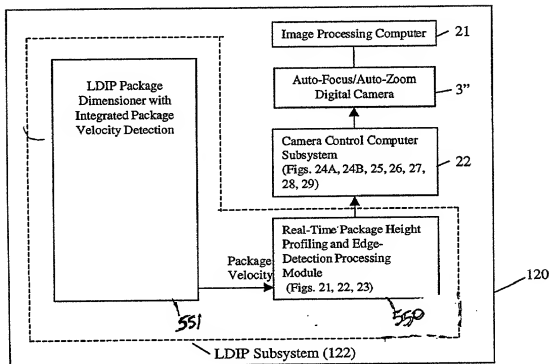


FIG. 14

218/395

LDIP REAL-TIME PACKAGE HEIGHT PROFILE AND EDGE DETECTION METHOD

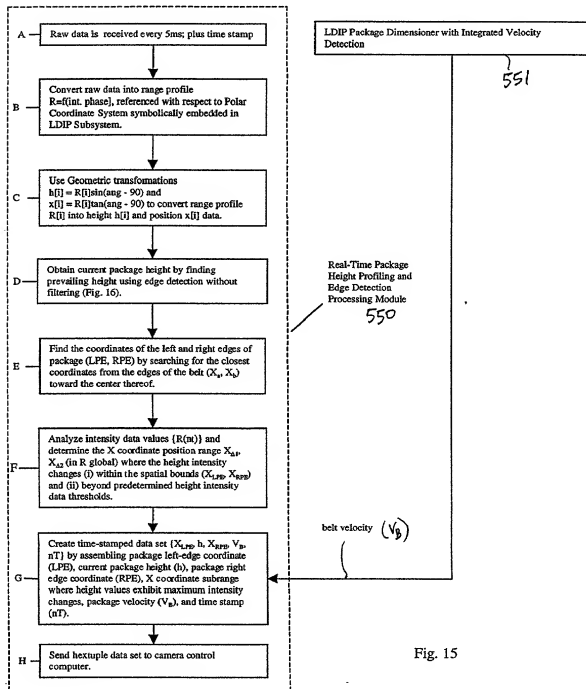


Fig. 15

219/385

LDIP Real Time Package Edge Detection

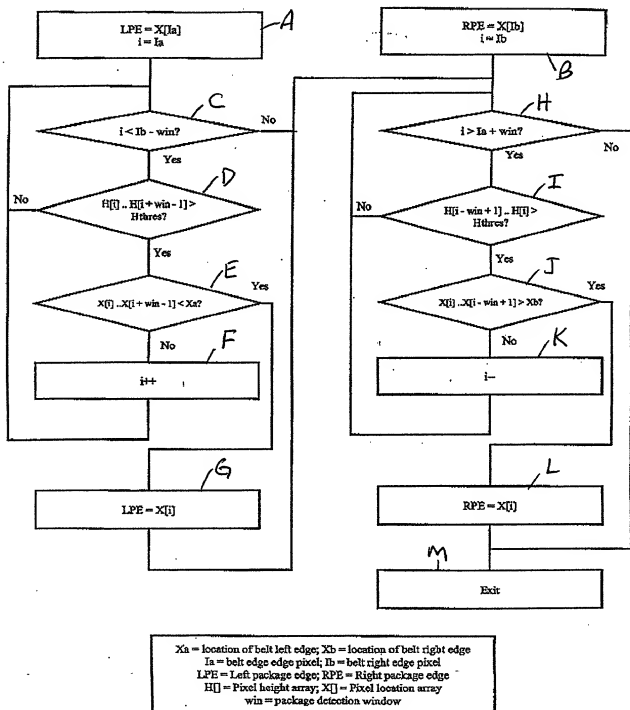


FIG. 16

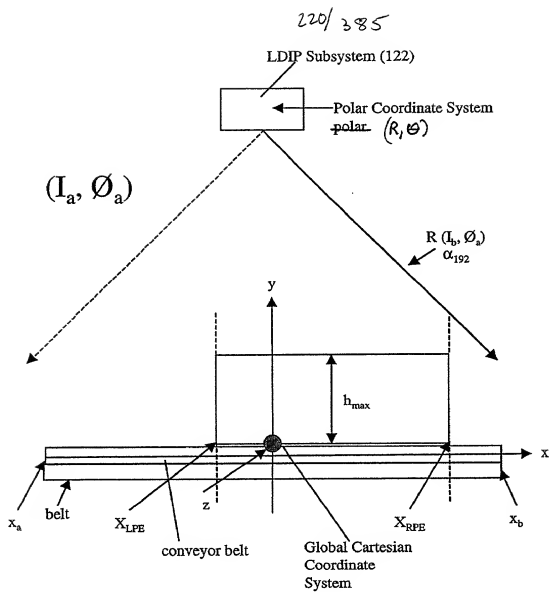


Fig. 17

24/385
INFORMATION MEASURED AT SCAN ANGLES BEFORE
COORDINATE TRANSFORMS

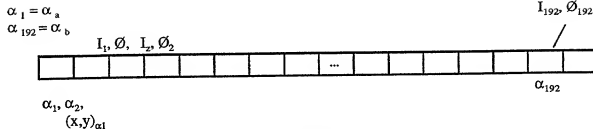


Fig. 17A

RANGE AND POLAR ANGLE MEASURES TAKEN AT SCAN
ANGLE α BEFORE COORDINATE TRANSFORMS

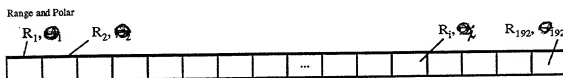


Fig. 17B

MEASURED PACKAGE HEIGHT AND POSITION VALUES
AFTER COORDINATE TRANSFORMS

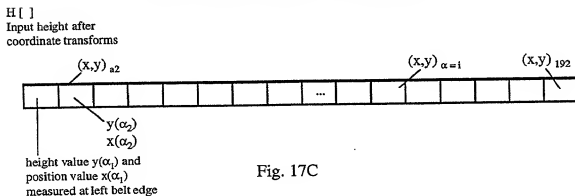


Fig. 17C

222/385

CAMERA CONTROL PROCESS CARRIED OUT WITHIN THE CAMERA CONTROL SUBSYSTEM OF EACH OBJECT IDENTIFICATION AND ATTRIBUTE ACQUISITION SYSTEM OF PRESENT INVENTION

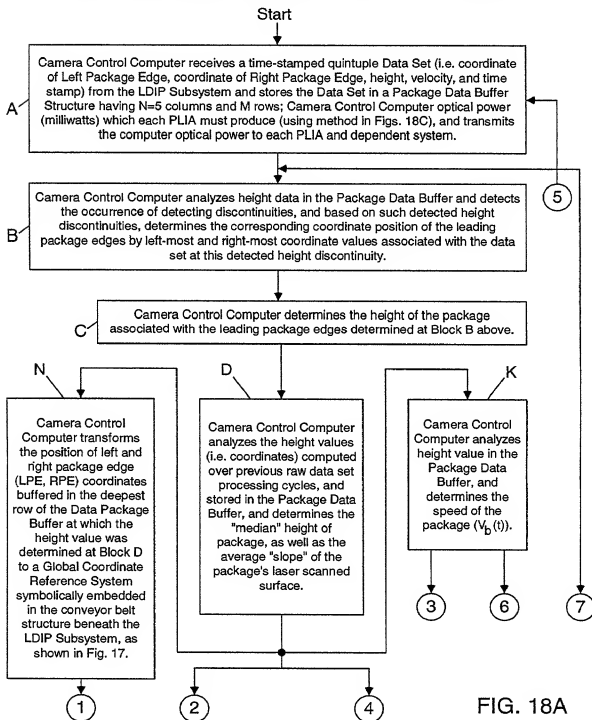


FIG. 18A

223/385

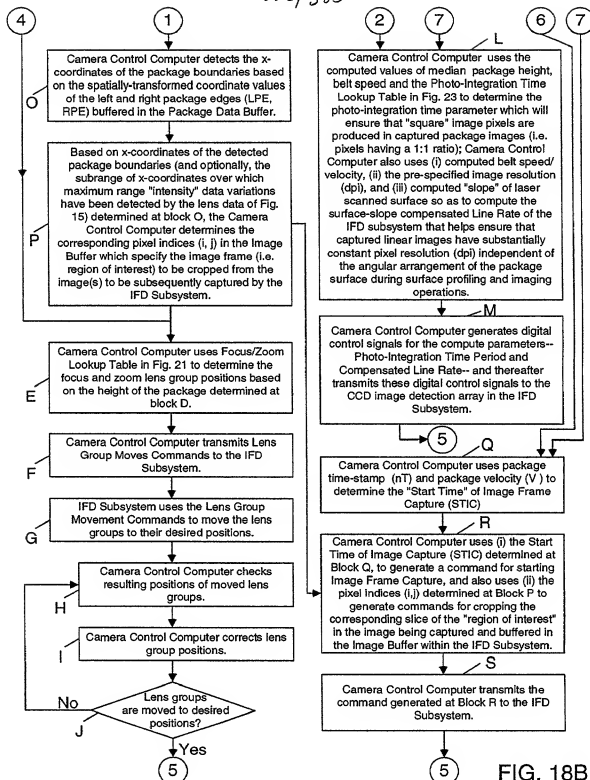


FIG. 18B

224/385

METHOD OF COMPUTING OPTICAL OUTPUT POWER FROM CASE
DIODES IN PLANAR LASER ILLUMINATION ARRAY (PLIA) FOR
CONTROLLING CONSTANT WHITE LEVEL IN IMAGE PIXELS CAPTURED
BY PLIIM-BASED LINEAR IMAGER

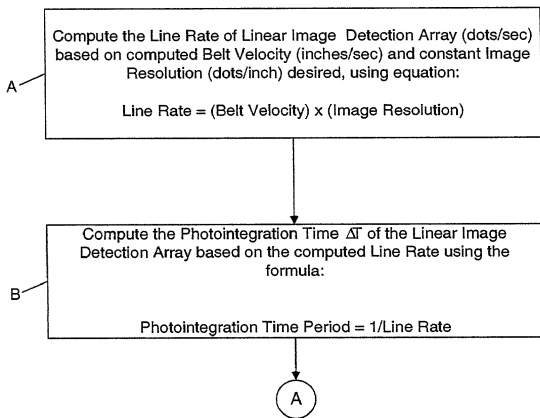


FIG. 18C1

225/385

A



Compute the Optical Power (milliwatts) of each PLIA based on computed Photointegration Time Period (ΔT) using the following formula:

$$\text{Optical Power of VLD (milliwatts)} = \frac{\text{constant}}{\text{Photointegration Time Period } \Delta T}$$

FIG. 18C2

226/325

METHOD OF COMPUTING COMPENSATED LINE RATE FOR CORRECTING
VIEWING-ANGLE DISTORTION OCCURRING IN IMAGES OF OBJECT
SURFACES CAPTURED AS OBJECT SURFACES MOVE PAST PLIIM-
BASED LINEAR IMAGER AT NON-ZERO SKEWED ANGLE

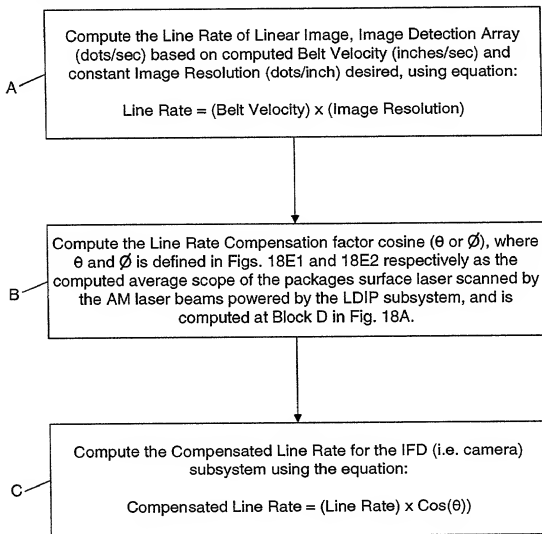


FIG. 18D

227/385

CASE 1:
Top Down Imaging

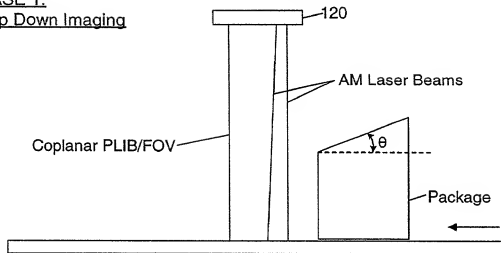


FIG. 18E1

CASE 2:
Side Imaging

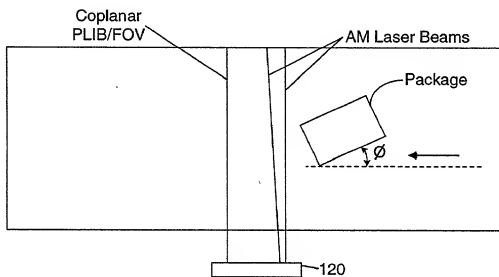


FIG. 18E2

228/385

X coordinate subrange where
maximum range "intensity"
variations have been detected

Left Package Edge (LDE)	Package Height (h)	Right Package Edge (RPE)	Package Velocity	Time-stamp (nT)	
					Row 1
					Row 2
					Row 3
					Row 4
					Row 5
					Row M

Package Data Buffer (FIFO)

Fig. 19

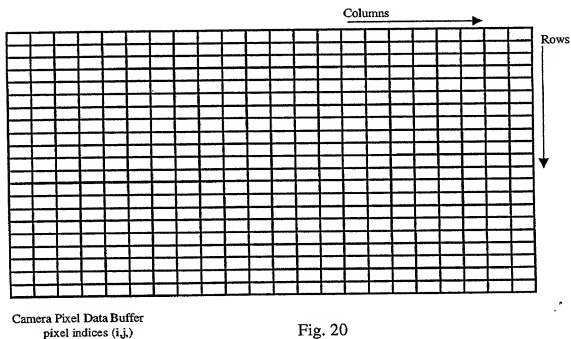


Fig. 20

229/385

Zoom and Focus Lens Group position
Looking Table

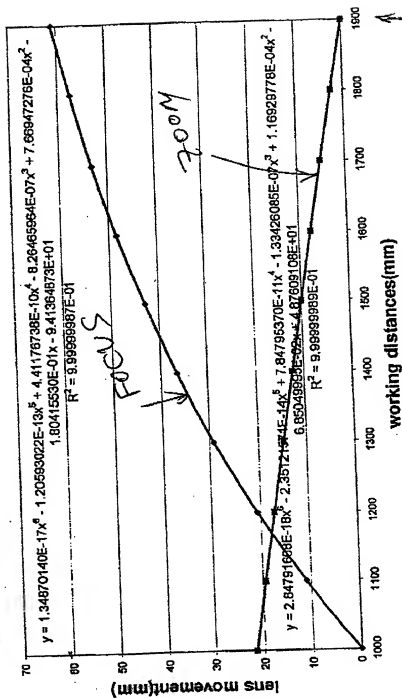
Distance from Camera H (mm)	Zoom group distance (mm) Y (Zoom)	Focus group distance (mm) Y (Focus)
1000	21.57489228	2.47E-05
1100	19.38089696	10.90009783
1200	17.10673434	20.65783177
1300	14.77137314	29.10917002
1400	12.39153565	36.47312595
1500	9.979114358	42.87845436
1600	7.540638114	48.44003358
1700	5.078794775	53.25495831
1800	2.595989366	57.40834303
1900	0.099872739	60.98883615

(Use
interpolation
techniques
for walking
distances
between listed
points in
table)

AG. 21.

* Note: on feed distance & zoom (eff. feed length) to camera lens are coupled (interdependent) in this camera has a fixed aperture F5.6

Focus and Zoom lens movement vs. working distances



zoom 1 zoom 2 Poly. (zoom 1) Poly. (zoom 2)

working distances (mm)

↑ (inches)

30 above conveyor belt

← Package height above conveyor

conveyor-belt surface

FIG. 22A

230/385

231/385

Photo-Integration Time Look-Up Table

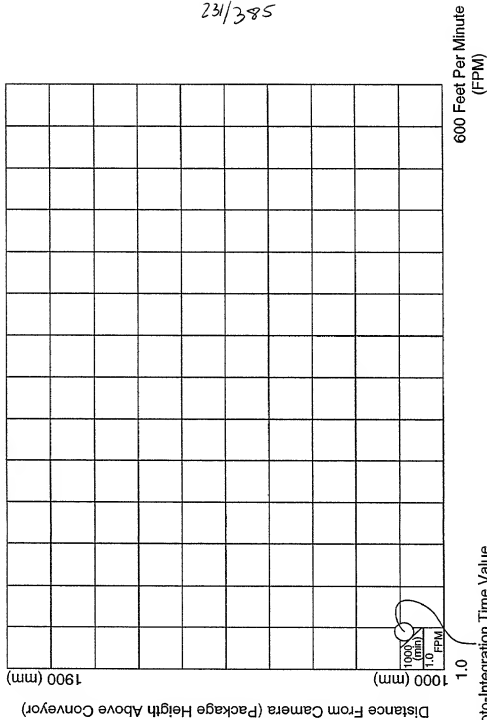


FIG. 22B

232/385

3D Surface Profile And High Resolution

Linear Image Data Capture At PLIIM-Based Profiling And Imaging System

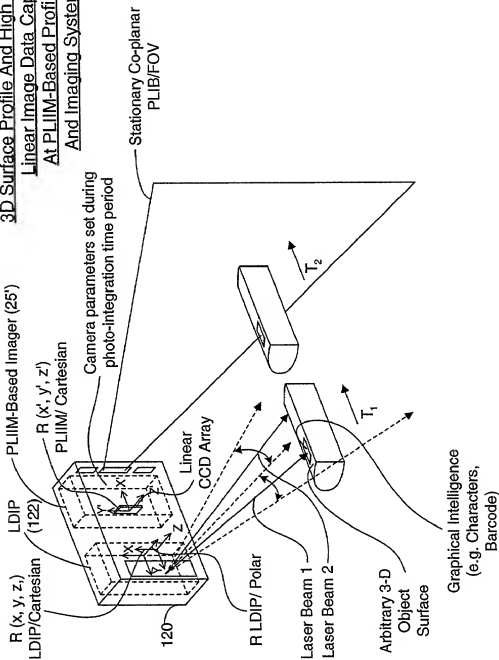


FIG. 23A

Geometrical Modelling Of Arbitrary 3-D Object Surface At Image Processing Computer

PLIIM-Based Imager 25'

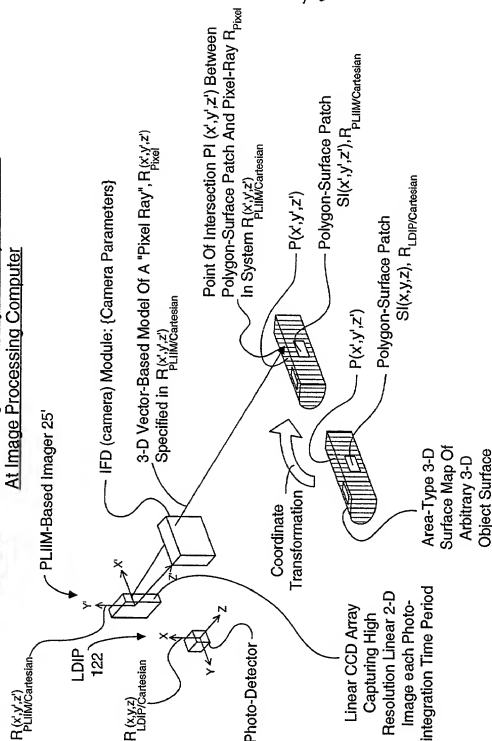


FIG. 23B

233/385

234/385

METHOD OF AND APPARATUS FOR PERFORMING AUTOMATIC
RECOGNITION OF GRAPHICAL INTELLIGENCE CONTAINED IN 2-D
IMAGES CAPTURED FROM ARBITRARY 3-D OBJECT SURFACES

STEP 1: At the unitary PLIIM-based object imaging and profiling system, use the laser doppler imaging and profiling (LDIP) subsystem employed therein to (i) consecutively capture a series of linear 3-D surface profile maps on a targeted arbitrary (e.g. non-planar or planar) 3-D object surface bearing forms of graphical intelligence and (ii) measure the velocity of the arbitrary 3-D object surface, wherein the polar coordinates of each point in the captured linear 3-D surface profile map are specified in a local polar coordinate system $R_{LDIP/polar}$, symbolically embedded within the LDIP subsystem.

A

STEP 2: At the unitary PLIIM-based object imaging and profiling system, use coordinate transforms to automatically convert the polar coordinates of each point $p(\alpha, R)$ in the captured linear 3-D surface profile map into x, y, z Cartesian coordinates specified as $p(x, y, z)$ in a local Cartesian coordinate system $R_{LDIP/Cartesian}$, symbolically embedded within the LDIP subsystem.

B

STEP 3: At the unitary PLIIM-based object imaging and profiling system, use the PLIIM-based imager employed therein to consecutively capture high-resolution linear 2-D images of the arbitrary 3-D object surface bearing forms of graphical intelligence (e.g. symbol character strings), wherein (i) the x', y' coordinates of each pixel in each said captured high-resolution linear 2-D image is specified in local Cartesian coordinate system $R_{PLIIM/Cartesian}$ symbolically embedded within the PLIIM-based imager, and (ii) the intensity value of the pixel $I(x', y')$ is associated with the x', y' Cartesian coordinates of the image detection element in the linear image detection array at which the pixel is detected, and (iii) wherein also the planar laser illumination beam (PLIB) of the PLIIM-based imager is spaced from the amplitude modulated (AM) laser scanning beam of the LDIP subsystem is about D centimeters.

C

A

FIG. 23C1

235/385
A

STEP 4: At the unitary PLIIM-based object imaging and profiling system, capture and buffer the camera (IFD) parameters used to form and detect each linear high-resolution 2-D image captured during the corresponding photo-integration time period ΔT_K , by the PLIIM-based imager.

D

STEP 5: At the end of each photo-integration time period ΔT_K , use the unitary PLIIM-based object imaging and profiling system to transmit the following information elements to the Image Processing Computer for data storage and subsequent information processing:

(1) the converted coordinates x, y, z , of each point in the linear 3-D surface profile map of the arbitrary 3-D object surface captured during photo-integration time period ΔT_K ;

(2) the measured velocity(ies) of the arbitrary 3-D object surface during photo-integration time period ΔT_K ;

(3) the x', y' coordinates and intensity value $I(x', y')$ of each pixel in each high-resolution linear 2-D image captured during photo-integration time period ΔT_K and specified in the local Cartesian coordinate system $R_{PLIIM/Carthesian}$; and

(4) the captured camera (IFD) parameters used to form and detect each linear high-resolution 2-D image captured during the photo-integration time period ΔT_K

E

STEP 6: At the Image Processing Computer, receive the data elements transmitted from the PLIIM-based profiling and imaging system during Step 5, buffer data elements (1) and (2) in a first FIFO buffer memory structure, and data elements (3) and (4) in a second FIFO buffer memory structure.

F

B

FIG. 23C2

236/385
(B)

STEP 7: At the Image Processing Computer, use the x, y, z coordinates associated with a consecutively captured series of linear 3-D surface profile maps (i.e. stored in first FIFO memory storage structure) in order to construct a 3-D polygon-mesh surface representation of said arbitrary 3-D object surface, represented by $S_{LDIP}(x, y, z)$ and having (i) vertices specified by x, y, z in local coordinate reference system $R_{PLIIM/Carthesian}$, and (ii) planar polygon surface patches $s_i(x, y, z)$ and being defined by a set of said vertices.

G

STEP 8: At the Image Processing Computer, convert the x', y', z' coordinates of each vertex in the 3-D polygon-mesh surface representation into the local Cartesian coordinate reference system $R_{PLIIM/Carthesian}$ symbolically embedded within the PLIIM-based imager.

H

STEP 9: At the Image Processing Computer, specify the x', y', z' coordinates of each i -th planar polygon surface patch $s(x, y, z)$ represented in the local Cartesian coordinate reference system $R_{PLIIM/Carthesian}$, so as to produce a set of corresponding polygon surface patch $\{s_i(x', y', z')\}$ represented in system $R_{PLIIM/Carthesian}$

I

STEP 10: At the Image Processing Computer, for a selected linear high-resolution 2-D image captured at photo-integration time period ΔT_K , and spatially corresponding to one of the linear 3-D surface profile maps employed at Step 7, use the camera (IFD) parameters used and recorded (i.e. captured) during the corresponding photo-integration time period in order to construct a 3-D vector-based "pixel ray" model specifying the optical formation of each pixel in the linear 2-D image, wherein a pixel ray reflected off a point on the arbitrary 3-D object surface is focused through the camera's image formation optics (i.e. configured by the camera parameters) and is detected at the pixel's detection element in the linear image detection array of the IFD (camera) subsystem.

J

(C)

FIG. 23C3

237/385
C

STEP 11: At the Image Processing Computer, for each laser beam ray (producing one of the pixels in said selected linear 2-D image), (i) determine which polygon surface patch $s_i(x, y, z)$ the pixel ray intersects, (ii) compute the x, y, z coordinates of the point of intersection (POI) between the pixel ray and the polygon surface patch represented in Cartesian coordinate reference system $R_{PLIIM/Cartesian}$, and (iii) designate the computed set of points of intersection as $\{p_i(x, y, z)\}$.

K

STEP 12: At the Image Processing Computer, for each laser beam ray passing through a determined polygon surface patch $s_i(x', y', z')$ at a computed point of intersection $p_i(x, y, z)$, assign the intensity value $I(x', y')$ of the pixel ray to the x', y', z' coordinates of the point of intersection, thereby producing a linear high-resolution 3-D image comprising a 2-D array of pixels, each said pixel pixel having as its attributes (i) an Intensity value $I(x', y', z')$ and (ii) coordinates x', y', z' specified in the local Cartesian coordinate reference system $R_{PLIIM/Cartesian}$.

L

STEP 13: Put the computed linear high-resolution 3-D image in a third FIFO memory storage structure in the image processing computer.

M

STEP 14: Repeat Steps 1-6 to update the first and second FIFO data queues maintained in the image processing computer, and Steps 7-13 to update the consecutively computed linear high-resolution 3-D image stored in the third FIFO memory storage structure.

N

STEP 15: Assemble in an image buffer in the image processing computer, a set of consecutively computed linear high-resolution 3-D images retrieved from the third FIFO data storage device so as to construct an "area-type" high-resolution 3-D image of said arbitrary 3-D object surface.

O

D

FIG. 23C4

238/385
D

STEP 16: At the Image Processing Computer, map the intensity value $I(x', y', z')$ of each pixel in the computed area-type 3-D image onto the x', y', z' coordinates of the points on a uniformly-spaced apart "grid" positioned perpendicular to the optical axis of the camera subsystem (i.e. to model the 2-D planar substrate on which the forms of graphical intelligence was originally rendered), wherein said mapping process involves using an intensity weighing function based on the x', y', z' coordinate values of each pixel in the area-type high-resolution 3-D image, thereby producing an area-type high-resolution 2-D image of the 2-D planar substrate surface bearing said forms of graphical intelligence (e.g. symbol character strings).

P

STEP 17: At the Image Processing Computer, use said OCR algorithm to perform automated recognition of graphical intelligence contained in said area-type high-resolution 2-D image of said 2-D planar substrate surface so as to recognize said graphical intelligence and generate symbolic knowledge structures representative thereof.

Q

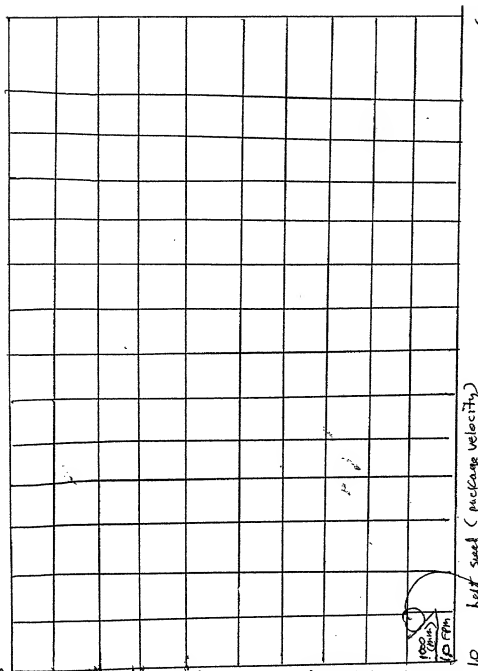
STEP 18: Repeat Steps 1-17 as often as required to recognize changes in graphical intelligence on the arbitrary moving 3-D object surface.

R

FIG. 23C5

Photo-Integration Time Look-up Table

1700 (in) Distance from camera (package height above conveyor)



239/385

600 feet per minute
(FPM)

10 feet speed (package velocity)

FIG. 22B

Photo-integration
Time value that
exceeds square image pixel
(1:1 aspect ratio)

TOTAL 58506600

240/395

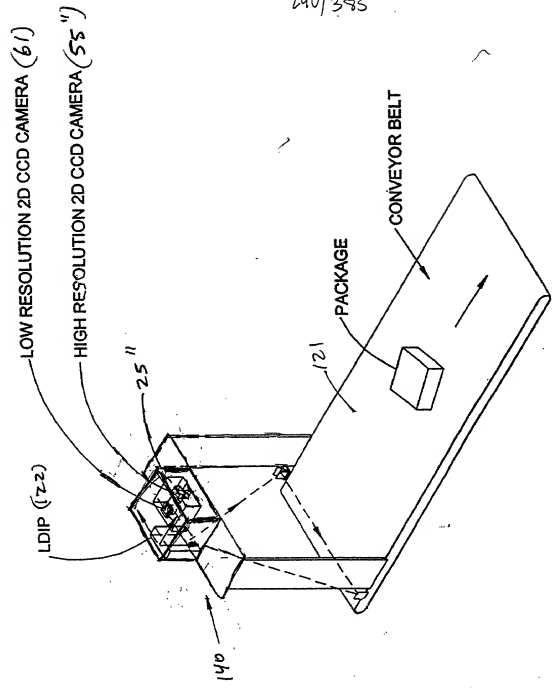


FIG 24

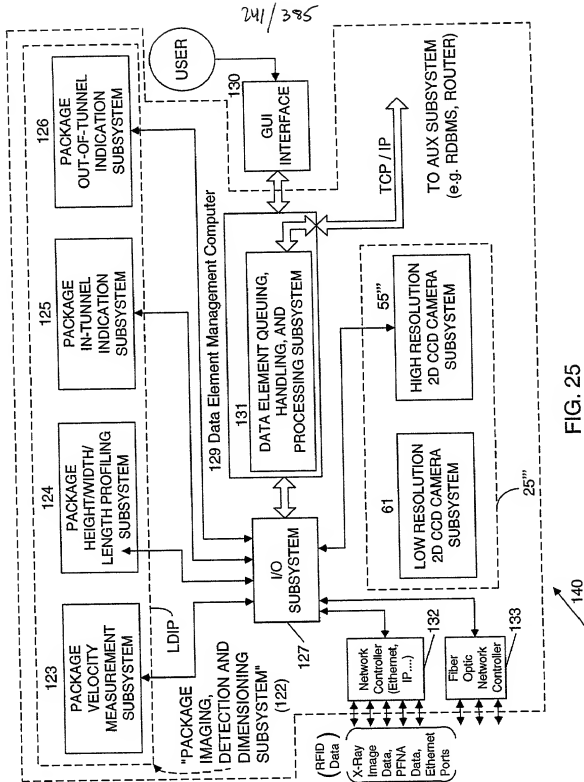


FIG. 25

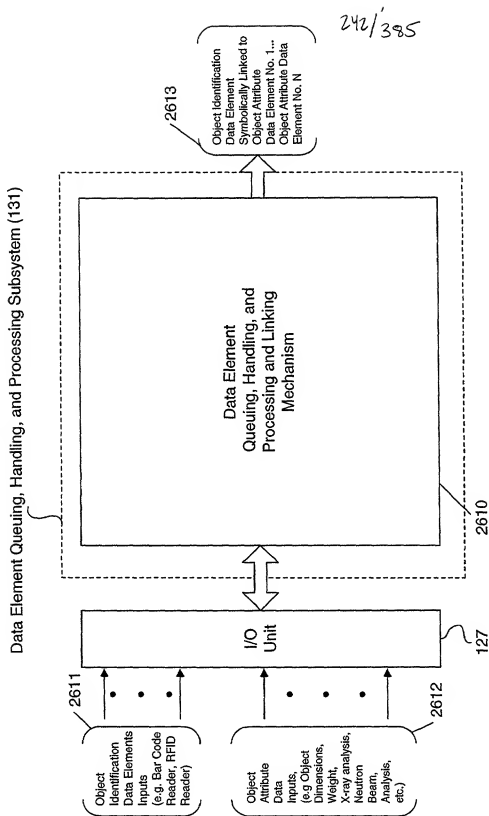


FIG. 25A

**Primary Network:
and/or System
Functions:**

A. Specification of Object
Detection and
Tracking Capability of
System

B. Specification of Object
Identification
Capability of System

C. Specification of
Object Attribute
Acquisition Capability
of System

**Specification of Object Detection, Tracking, and Identification and
Attribute-Acquisition Capabilities of a Configured System or Network.**

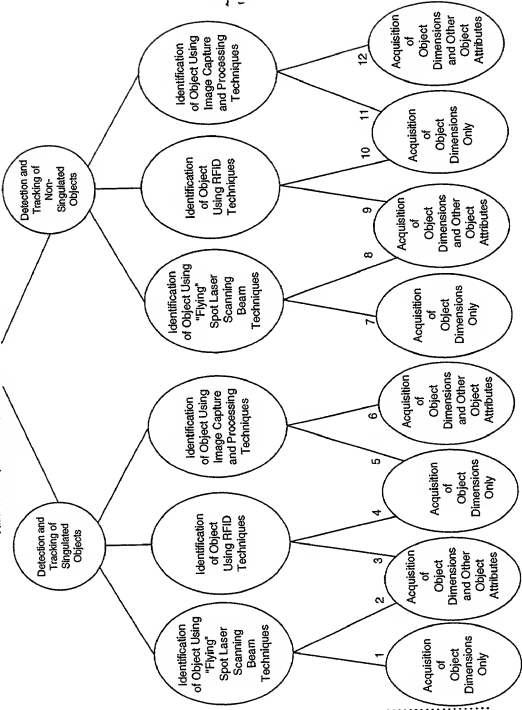


FIG. 25B

243/385

244/385

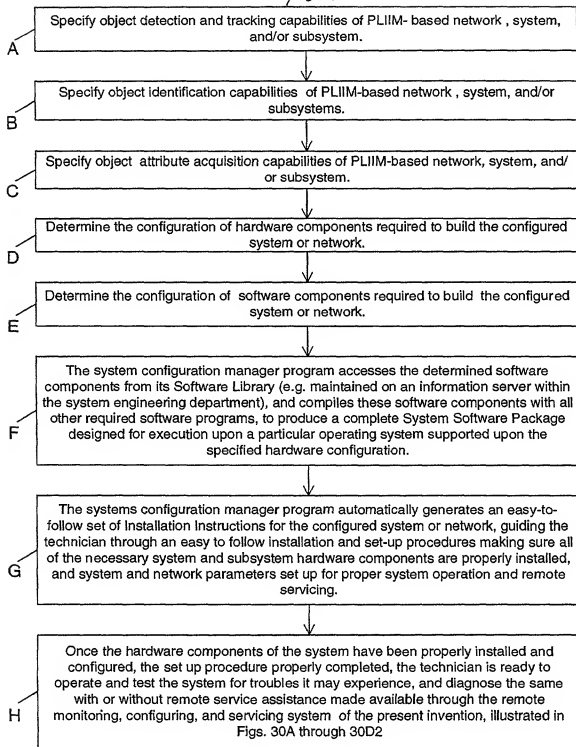


FIG. 25C

245/385

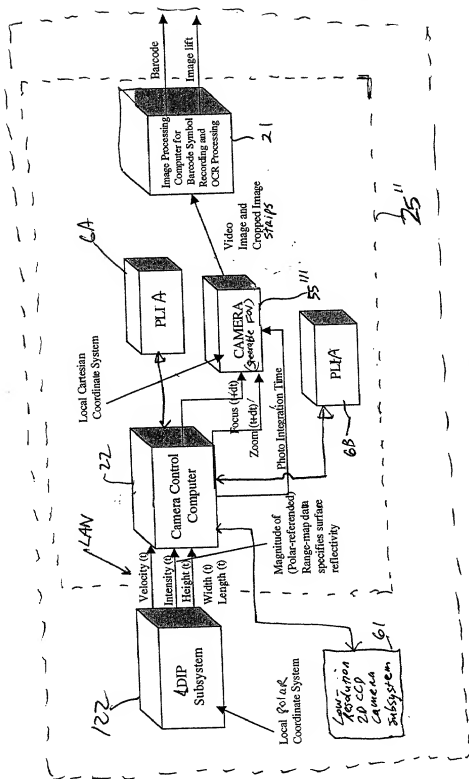


FIG. 26

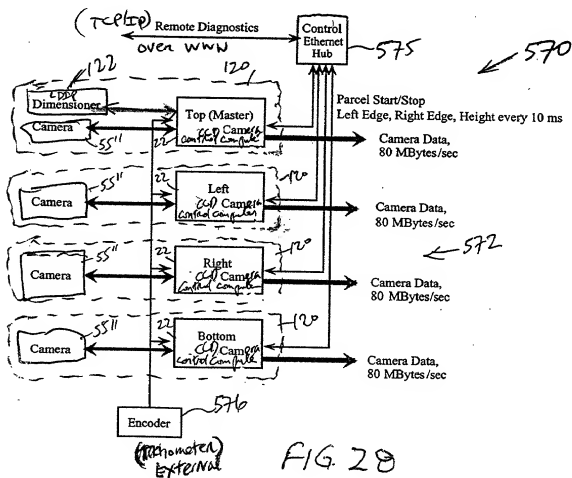
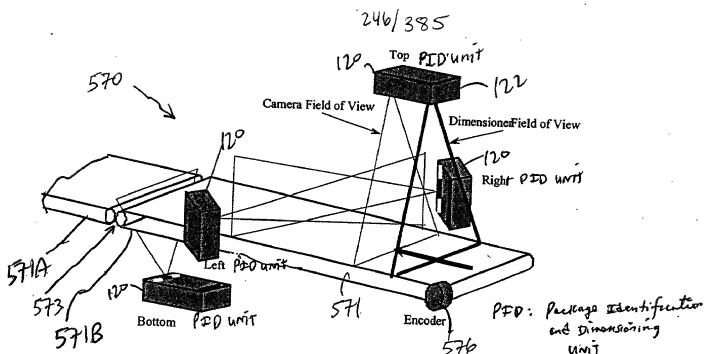


Figure 1 consists of 12 micrographs arranged in a vertical column, labeled 1 through 12. Each micrograph shows a different stage of embryonic development. The stages are: 1. Fertilized egg, 2. Two-cell stage, 3. Four-cell stage, 4. Morula stage, 5. Gastrula stage, 6. Early neurulation, 7. Late neurulation, 8. Early tail bud, 9. Late tail bud, 10. Hatching, 11. Hatching, 12. Hatching. The images show the progression from a single cell to a fully formed embryo with a visible tail and hatching process.

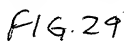
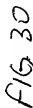


FIG. 29



249/385

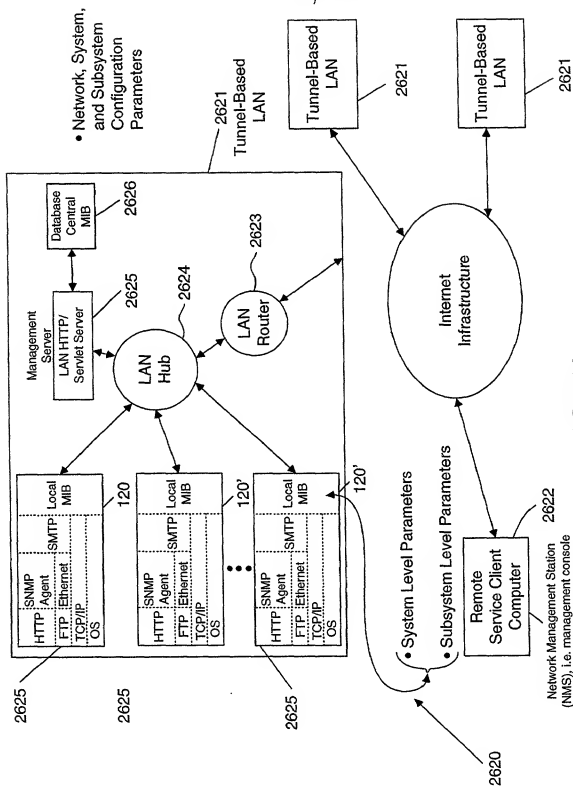


FIG. 30A

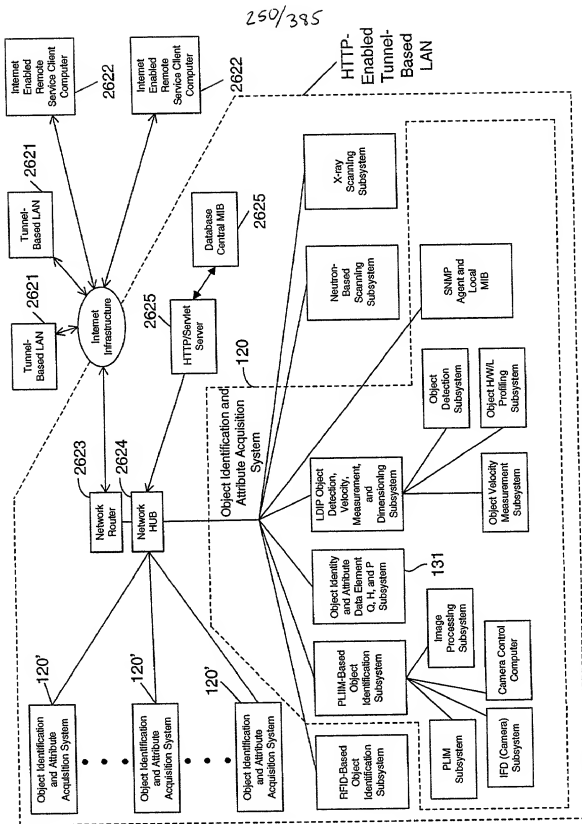


FIG. 30B

Network Configuration Parameters:

[Router IP address; no. of nodes (i.e. systems) in LAN; passwords; LAN location; name of customer facility; technical contact; phone no.; domain name; object identity codes; object attribute acquisition codes;....]

System Configuration Parameters:

[System IP Address; passwords; object identity codes; object attribute acquisition codes;....]

Monitorable and/or Configurable Parameters for Subsystems Within Each System:

- ☐ PLIM-based object identification subsystem: [object identity code; object attribute acquisition codes;....]
 - ☐ PLIM Subsystem: [VLD status; power VLD; TIM function; temp;....]
 - ☐ IFD (Camera) Subsystem: [sensor temp;]
 - ☐ Image Processing Subsystem (Computer): [processor load history; system up time; # of frames (ops); barcode read rate; current line rate;....]
 - ☐ Camera Contact Subsystem (Computer): [number of frames dropped; number of focused zoom commands; number and kinds of motor control errors;....]
- ☐ RFID-based object identification subsystem: [....]
- ☐ Object identity and attribute data element queuing, handling and processing subsystem: [....]
- ☐ LDIP object identification, velocity-measurement, and dimensioning subsystem: [....]
 - ☐ Object velocity measurement subsystem: [polygon RPM; polygon laser output X; channel X drift; channel X notes; trigger error events; instant lock reference drift; temperature]
 - ☐ Object HWVL profiling subsystem
 - ☐ Object detection subsystem: [non- singulation/ singulation code;....]
- ☐ X-ray scanning subsystem: [....]
- ☐ Neutron-beam scanning subsystem: [....]

These subsystems generate object identity parameters

This system links object attribute data element parameters (i.e. object identity parameters) to corresponding object identity parameters (i.e. object attribute data element)

These subsystems generate object attribute parameters

FIG. 30C

252/385

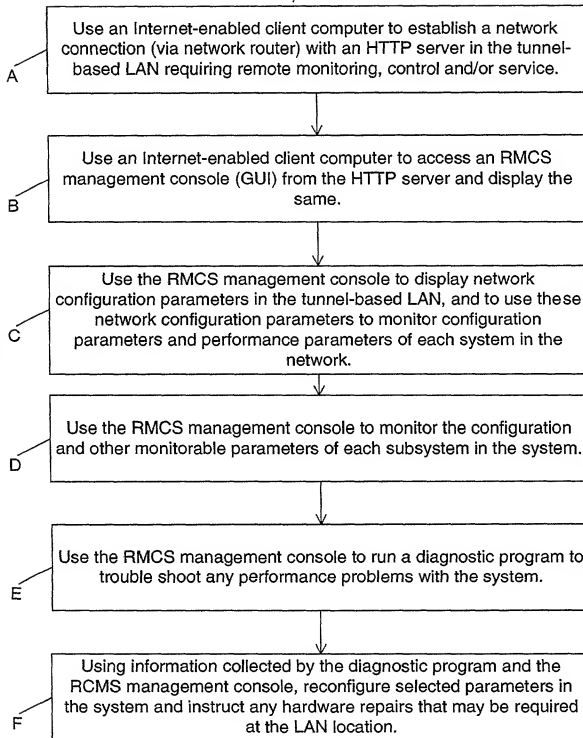


FIG. 30D1

253/385 (A)

G

Use the RMCS management console to rerun diagnostic programs on troubled systems and subsystems in the LAN after parameter reconfiguration and/or hardware repair at the LAN location, so as to test the performance of such systems and subsystems and the overall tunnel based LAN.

H

Use the RMCS management console to monitor parameters of the system and subsystems in the tunnel based LAN, from time to time, to determine whether or not the system and/or network tunnel is required.

I

Use the RMCS management console to record all monitored parameter records and result of diagnostic programs in a customer service database for future reference, and access during subsequent remote service calls over the Internet.

FIG. 30D2

255/385

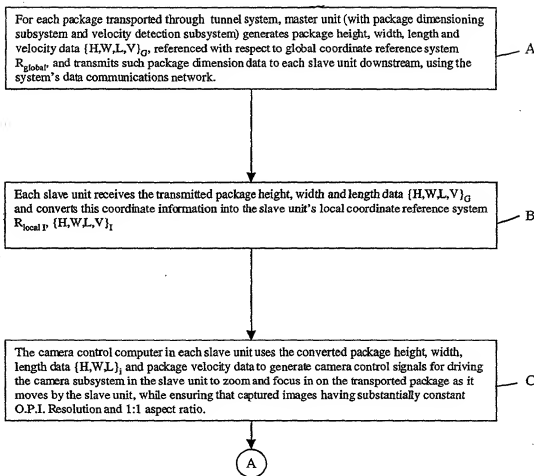


FIG. 32A



Each slave unit captures images acquired by its intelligently controlled camera subsystem, buffers the same, and processes the images to decode bar code symbol identifiers represented in said images, and/or to perform optical character recognition (OCR) thereupon.

D

The slave unit which decodes a bar code symbol in a processed image automatically transmits a package identification data element (containing symbol character data representative of the decoded bar code symbol) to the master unit (or other designated system control unit employing data element management functionalities) for package data element processing.

E

Master unit time-stamps received package identification data element, places said data element in a data queue, and processes package identification data elements and time-stamped package dimension data elements in said queue to link each package identification data element with one said corresponding package dimension data element.

F

FIG. 32B

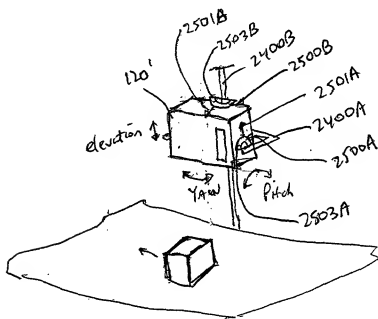
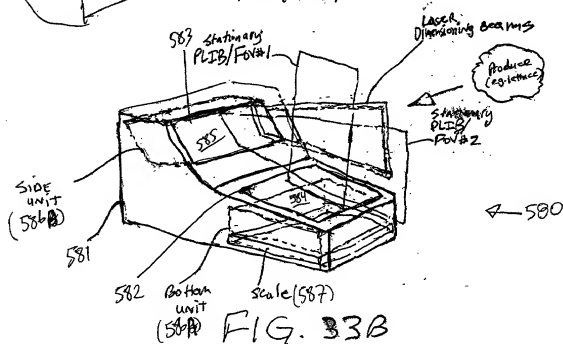
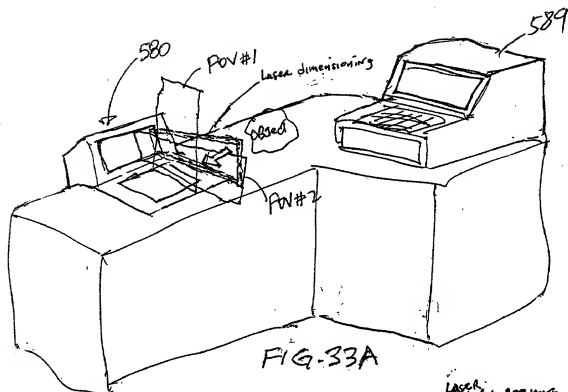
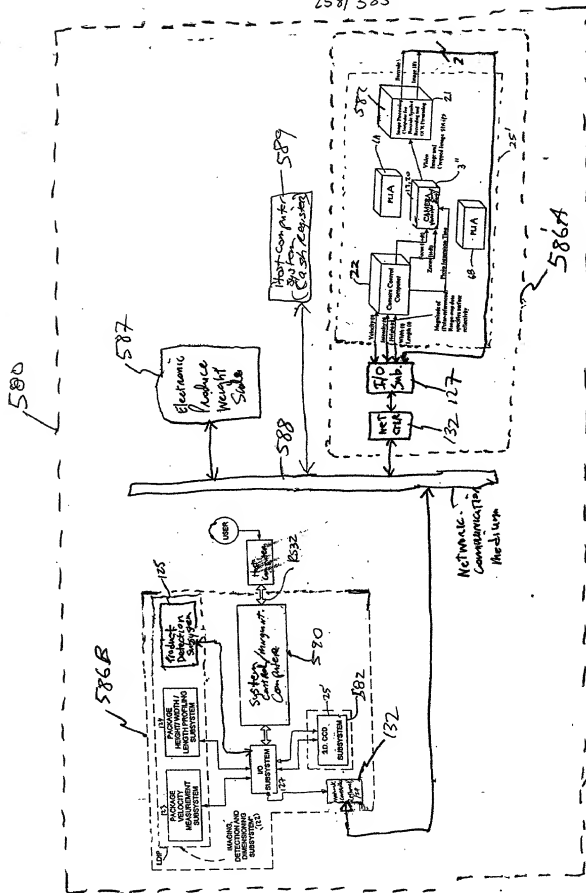


FIG. 31A

257/385



258/385



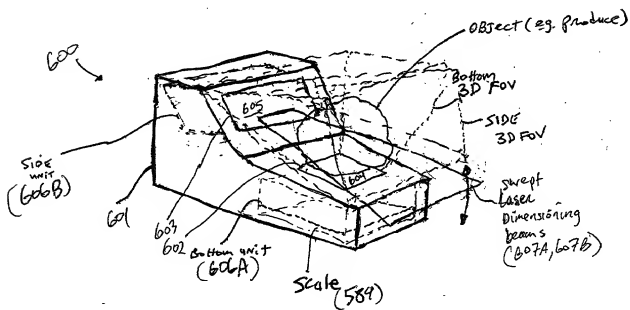
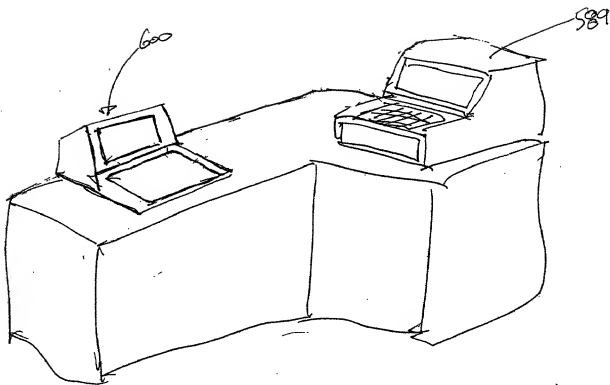
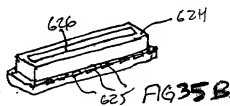
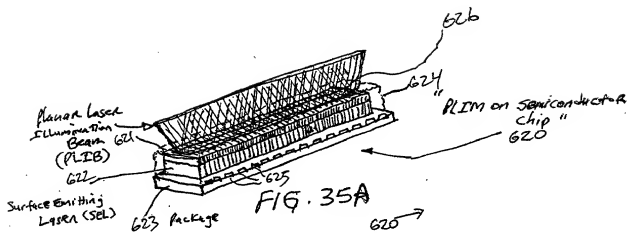
$$259 \overline{) 385}$$


FIG. 34B

261/385





263/3857

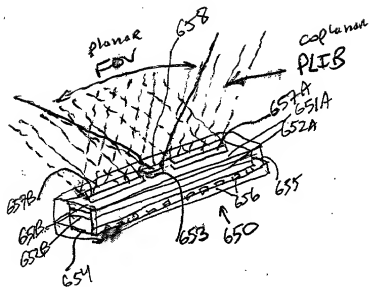


FIG. 37

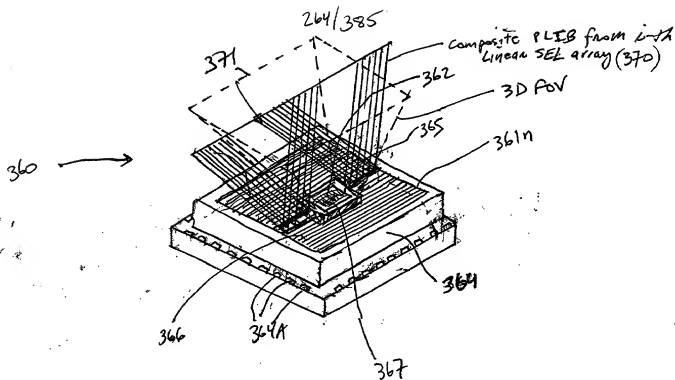


FIG. 38A

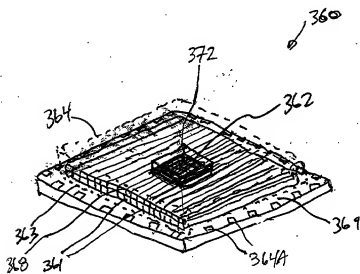


FIG. 38B

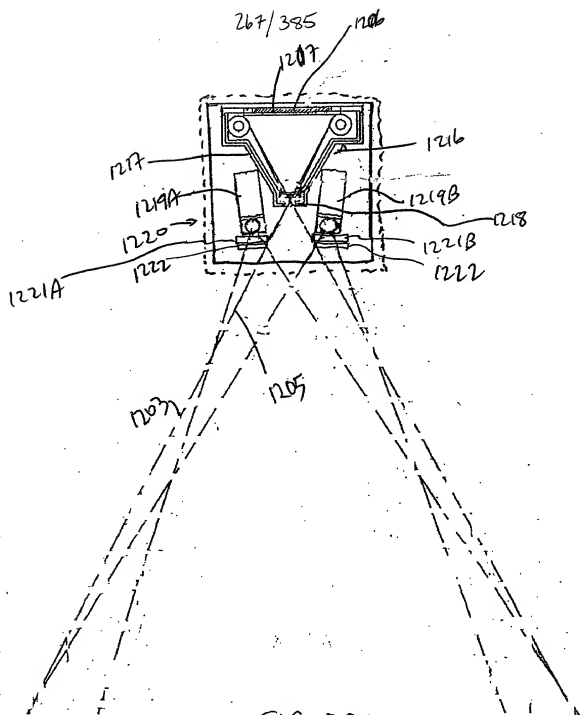


FIG. 39C

268/385

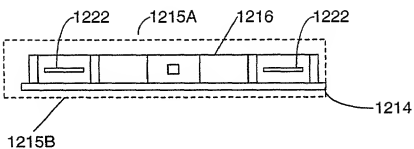


FIG. 39D

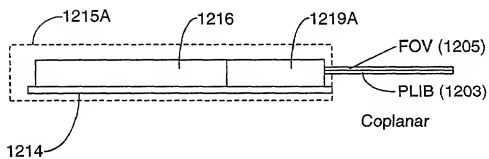


FIG. 39E

269/385

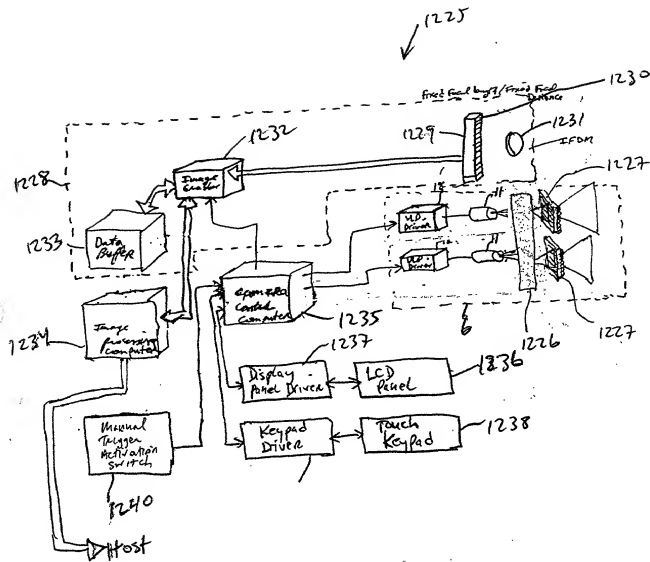
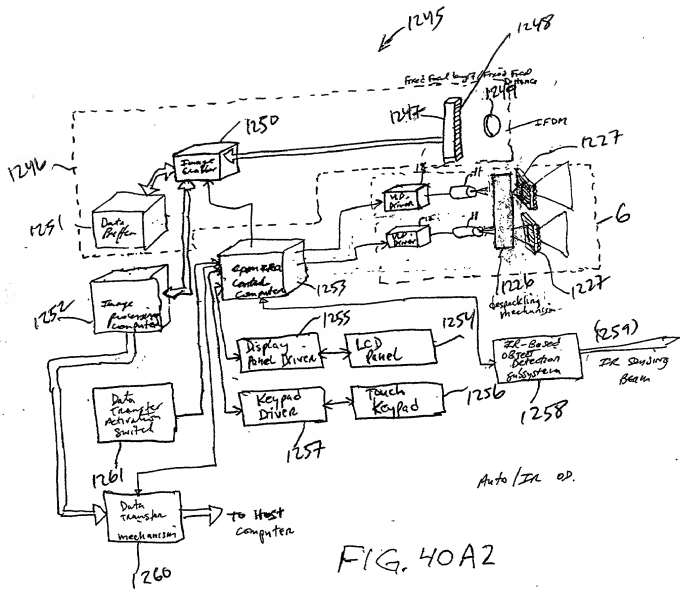
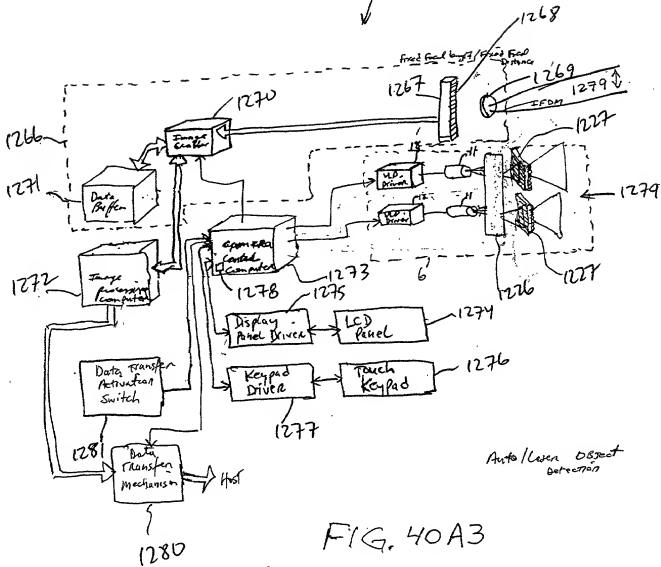


FIG. 40A1



271/385

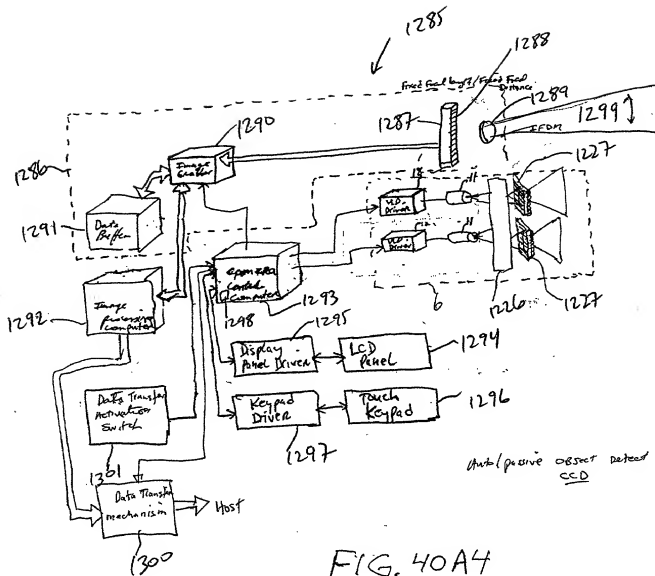
1265



Auto/Laser Object
Detection

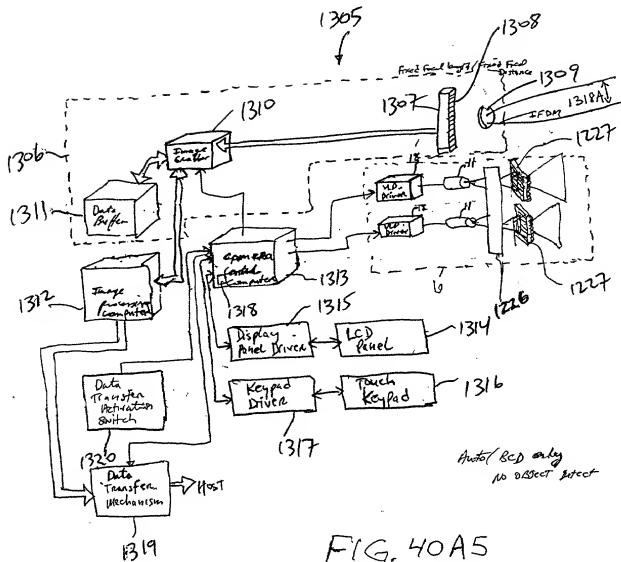
FIG. 40A3

272/385



Auto/passive OBSnet Datafeed
CCD

273/385



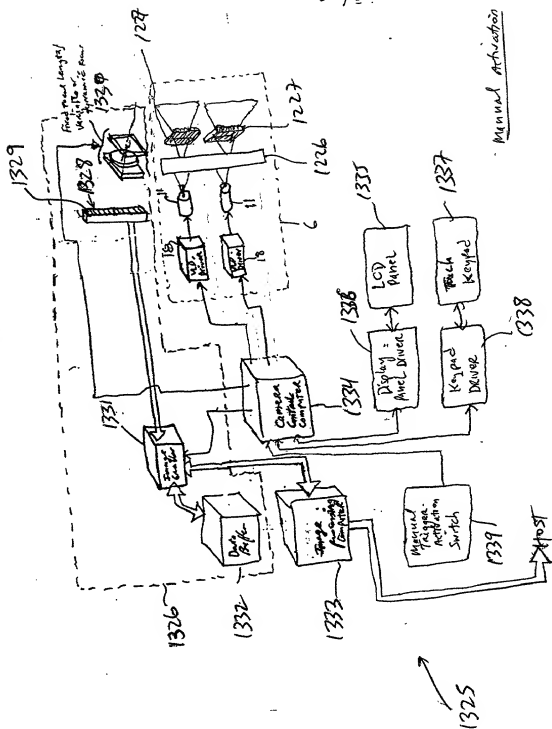


FIG. 40B1

275/385

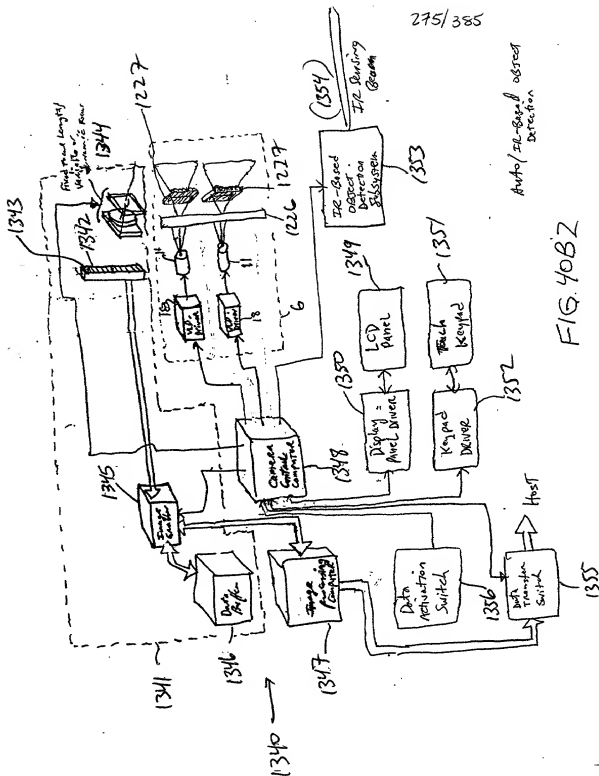


FIG. 40BZ

276/285

Antenna (Learn Object Detect)

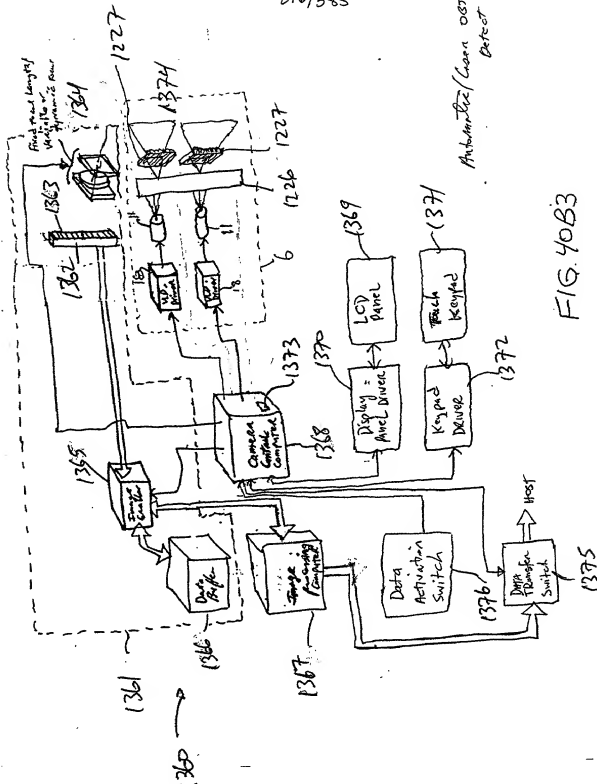


FIG. 40B3

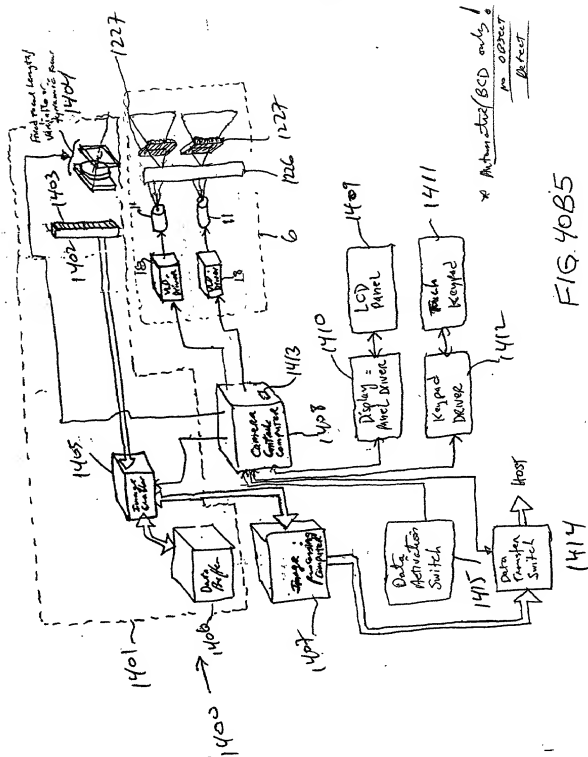
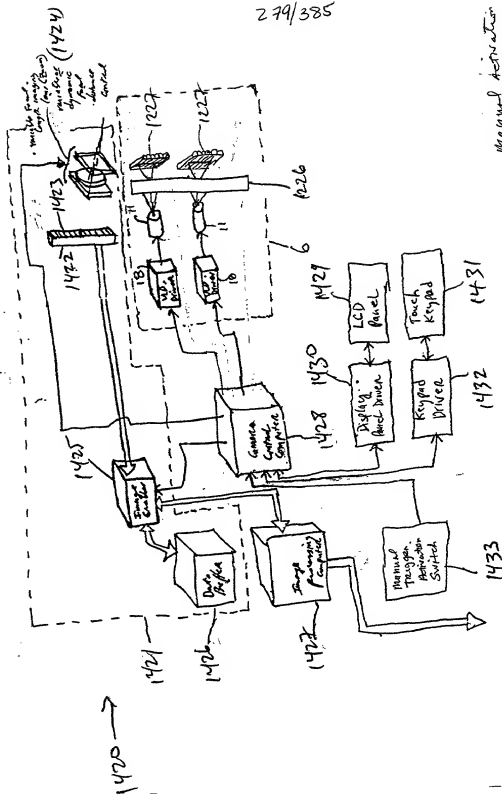


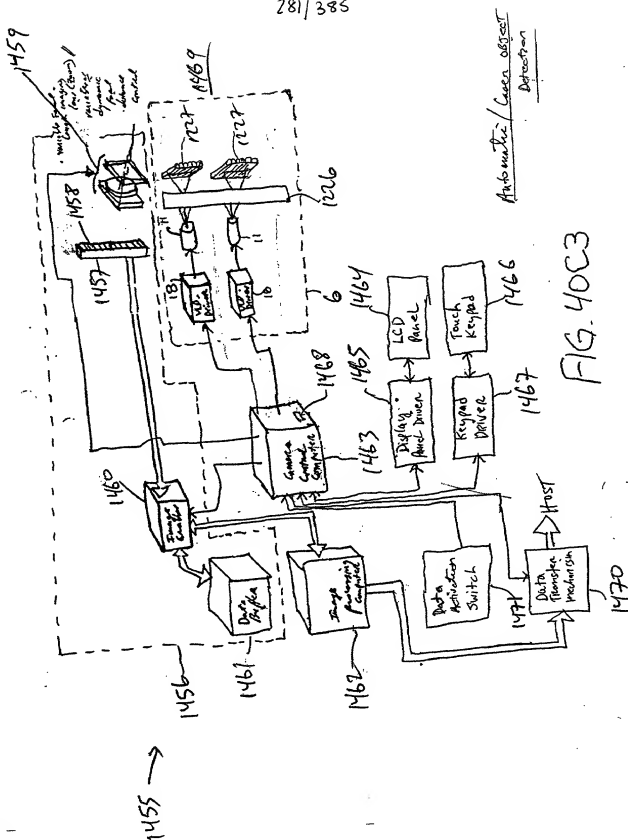
FIG. 40B5

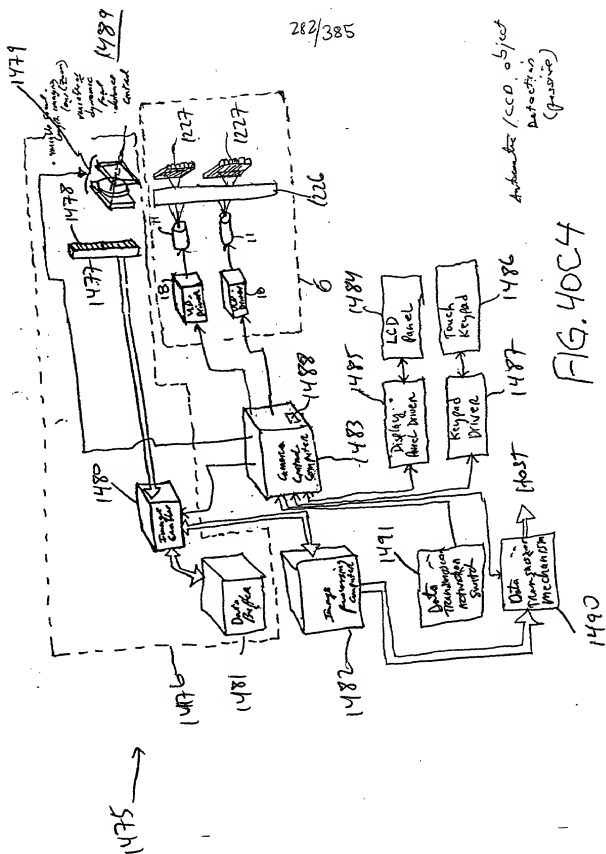
279/385



Manual Navigation

FIG. 40C1





283/385

1499

1509

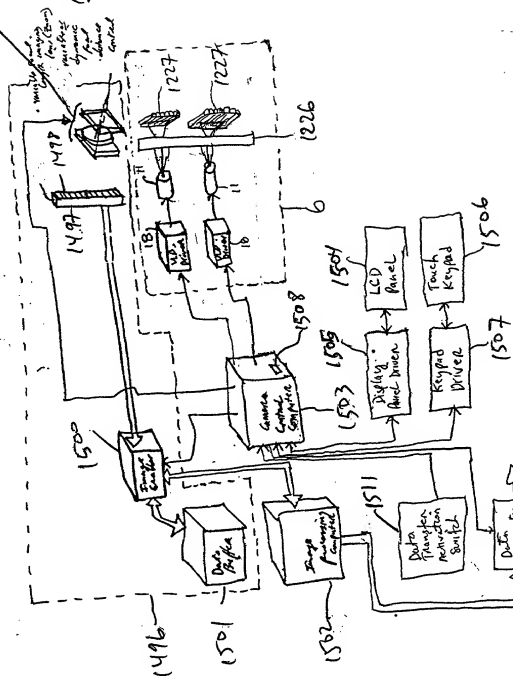
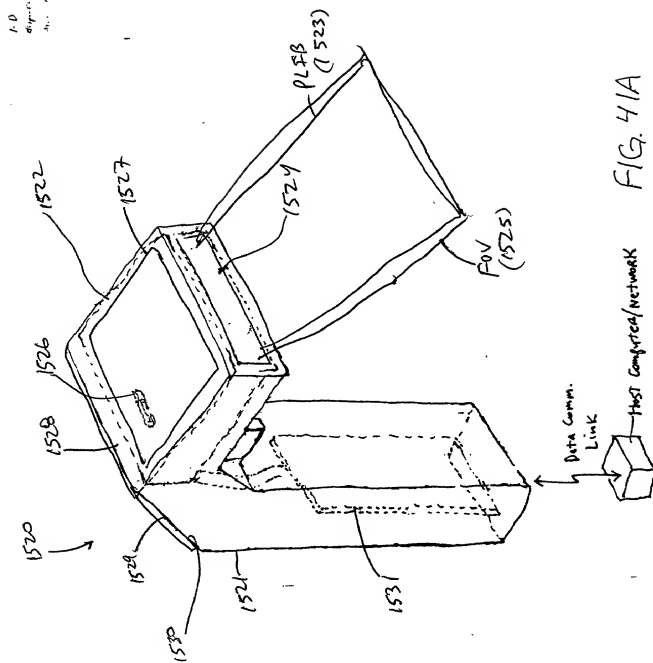


FIG. 40C5

Automatic/PCD only
-no split-test

1510



285/385

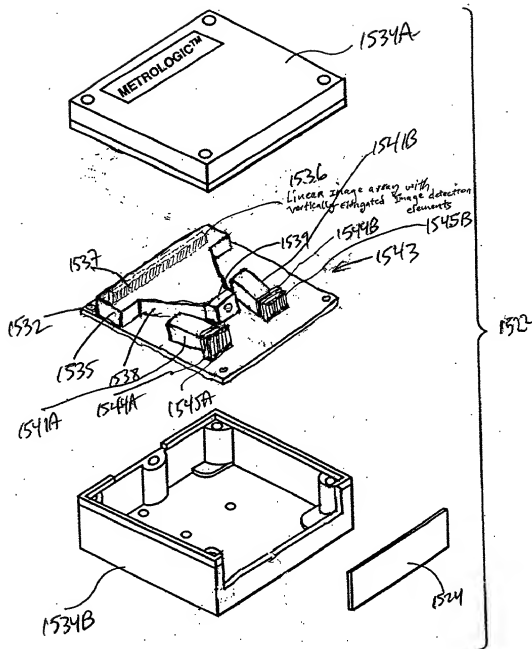


FIG. 41B

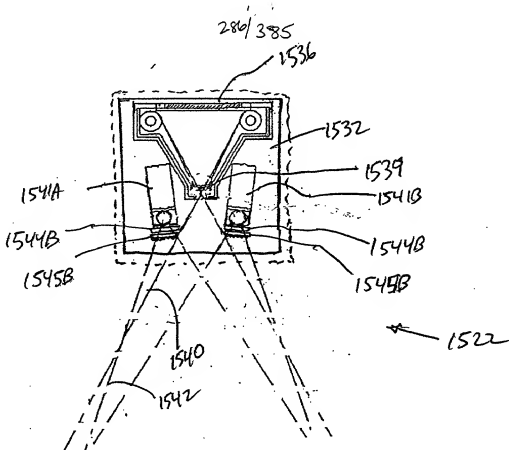


FIG. 41C

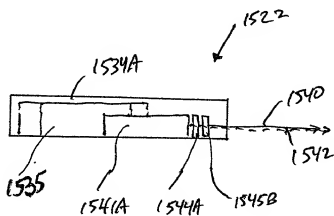
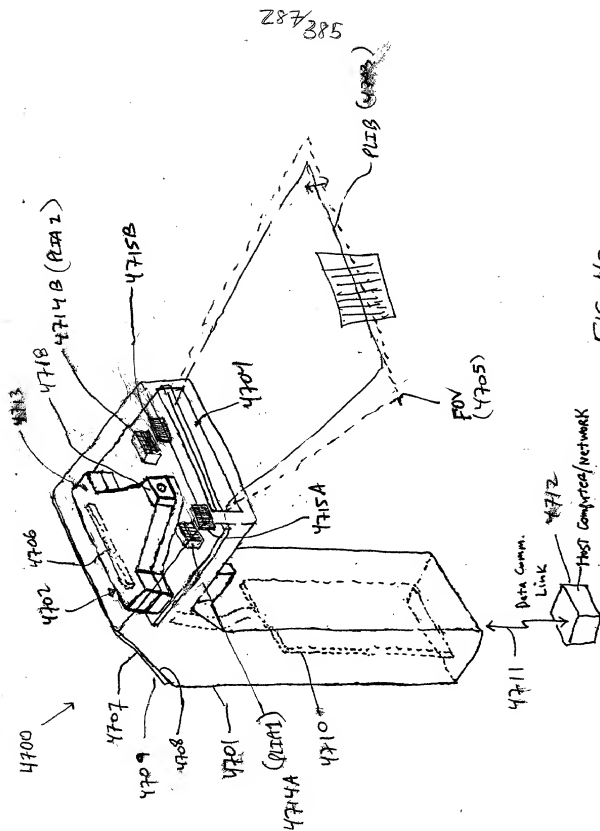


FIG. 41D



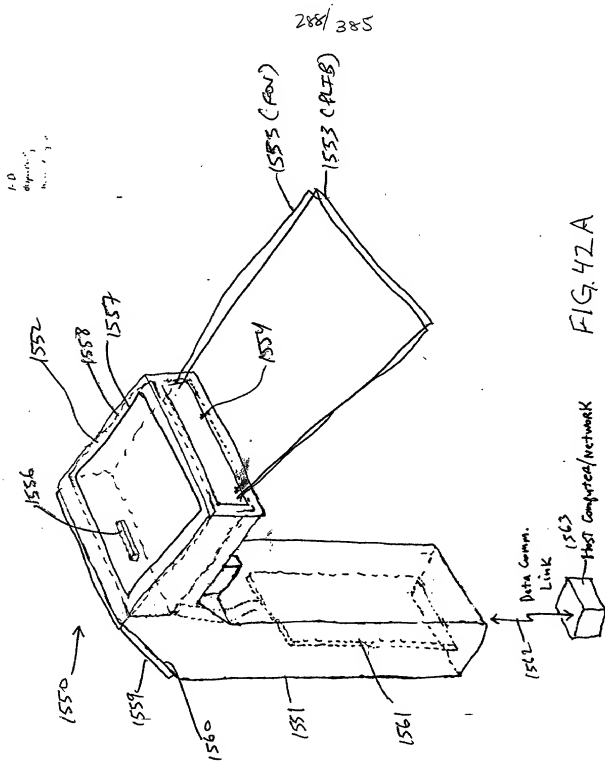


FIG. 42A

289/385

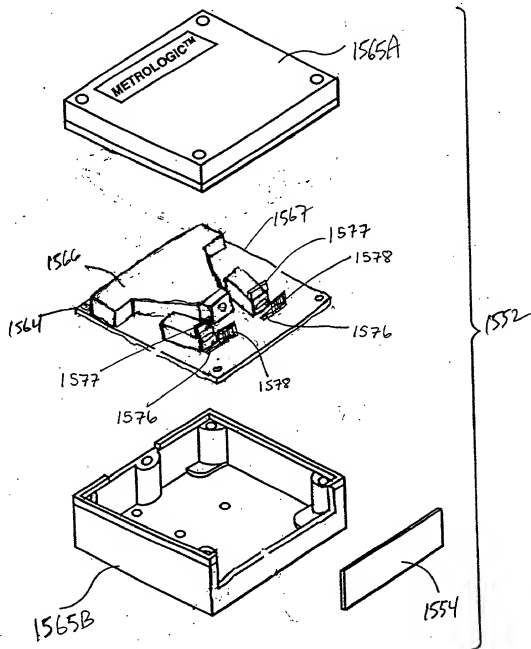


FIG. 42B

240/385

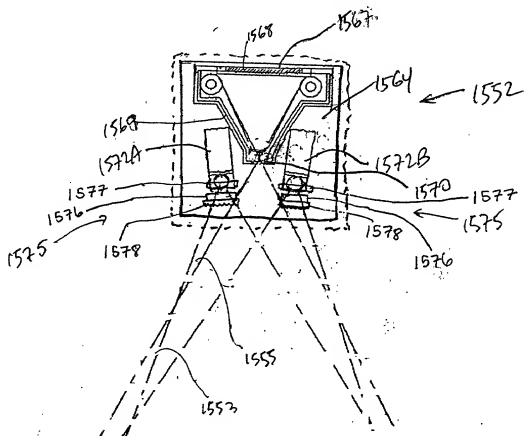


FIG. 42C

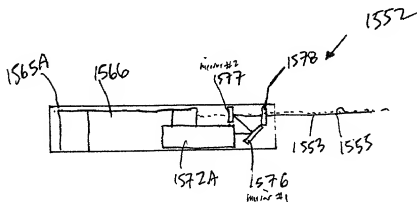


FIG. 42D

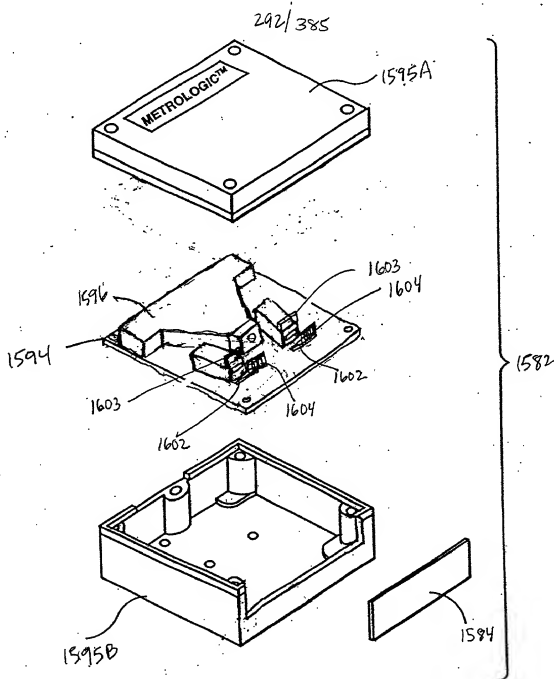


FIG. 43B

293/385

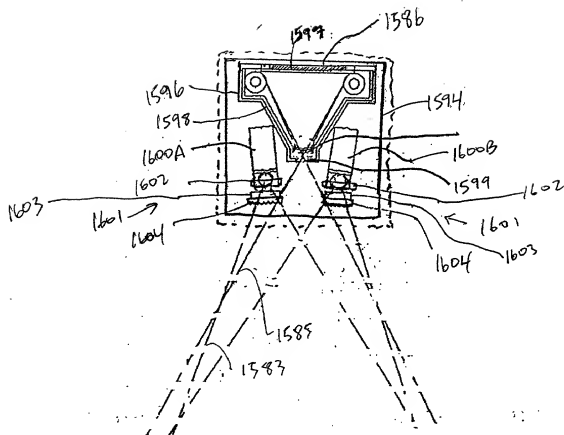


FIG. 43C

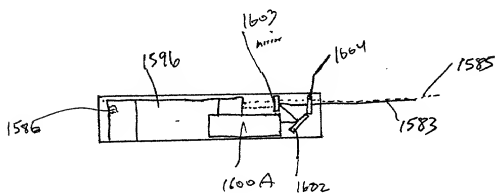


FIG. 43D

294/385

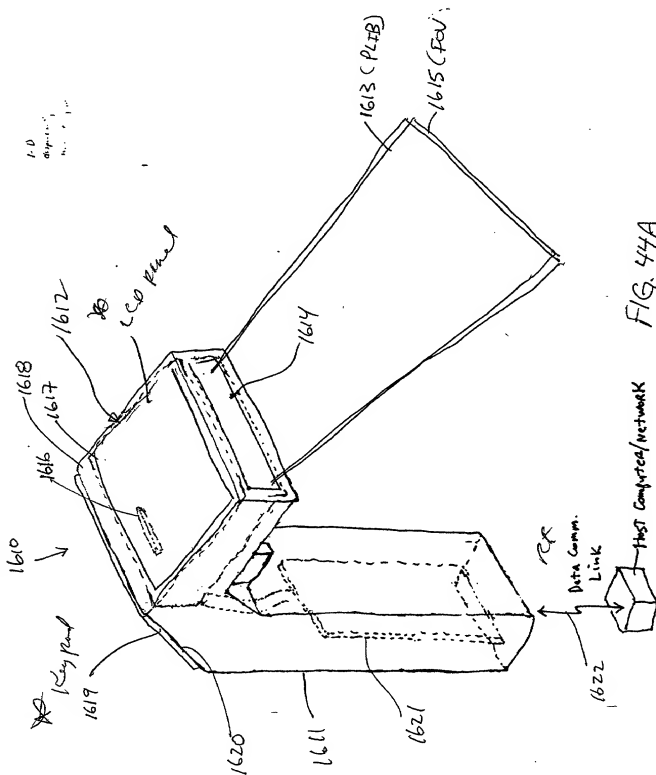


FIG. 44A

Host Computer/Network

Data Comm. Link

TX

RX

295/385

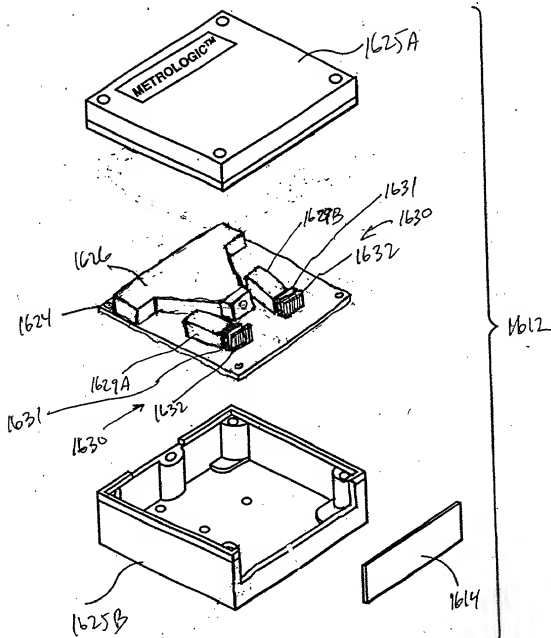
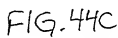


FIG. 44B



298/385

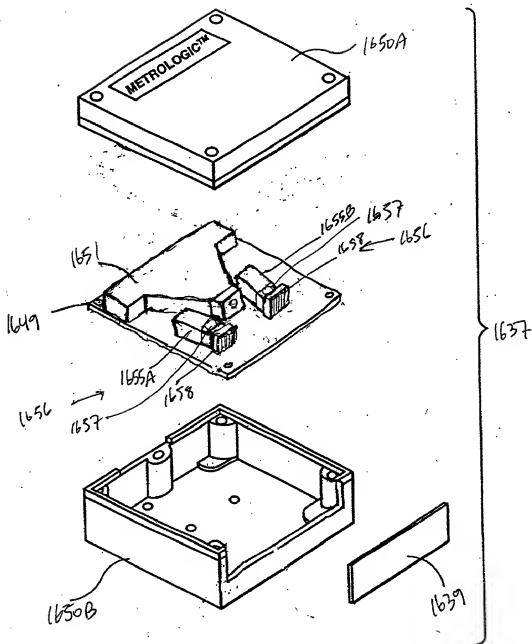


FIG. 45B

0000585.112101

FIG. 46A

301/385

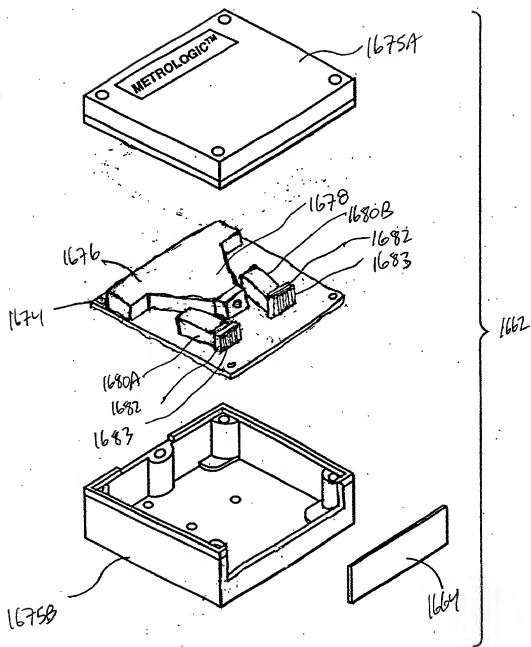
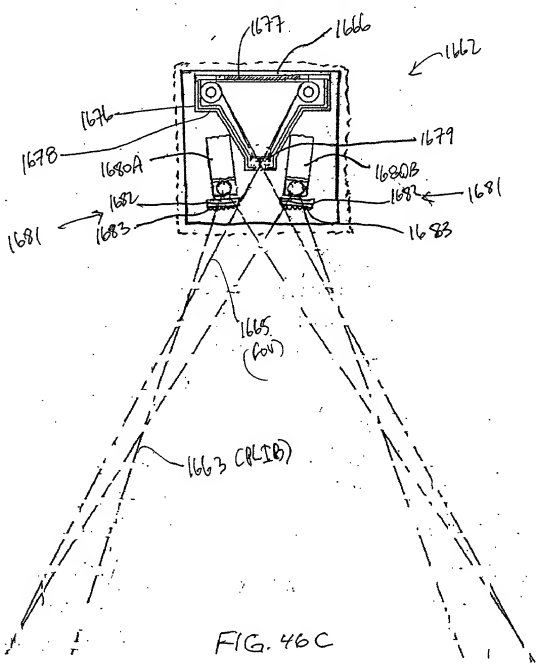


FIG. 46B

00000285-1A101

302/385



304/385

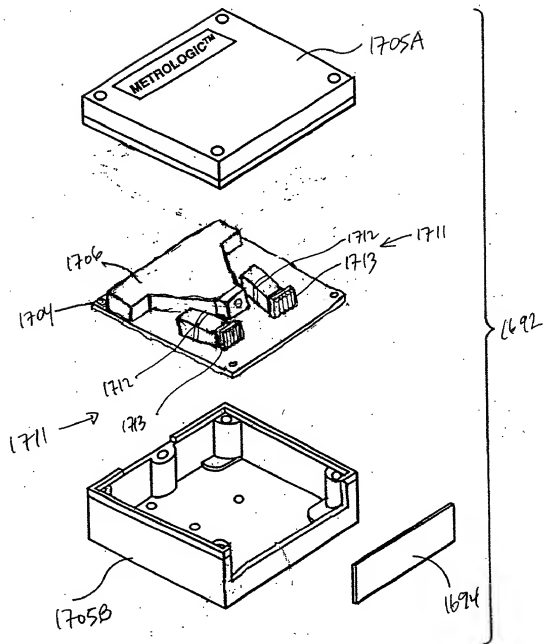
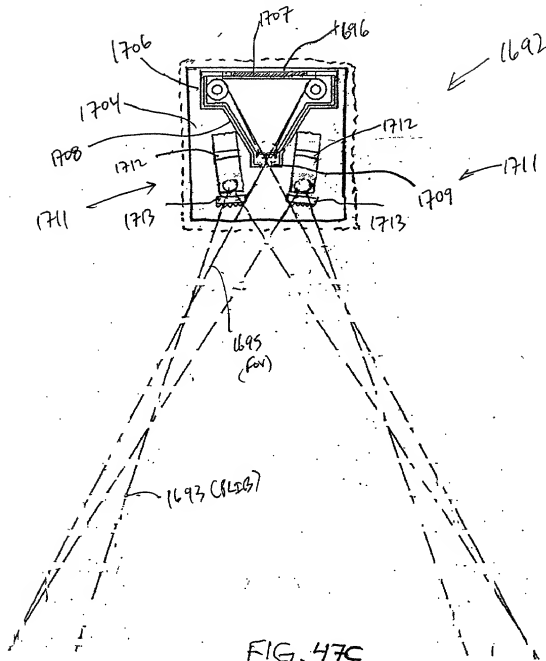


FIG. 47B

305/385



306/385

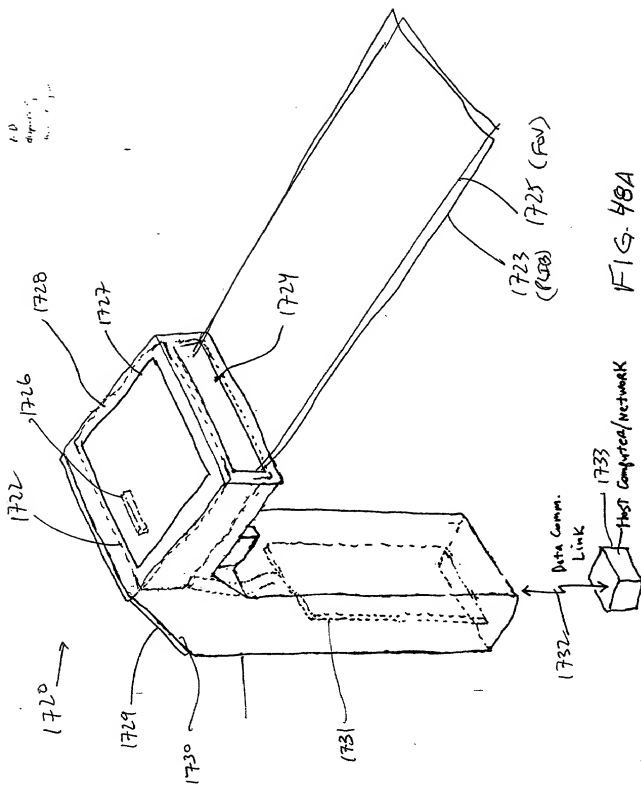


FIG. 48A

307/385

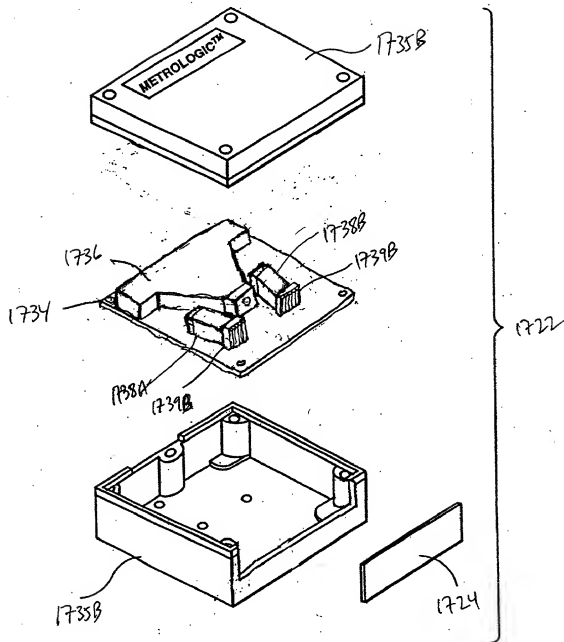
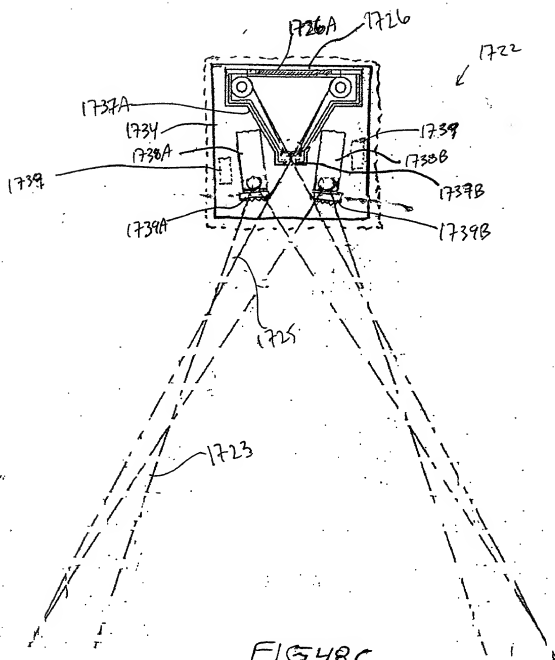


FIG. 48B

$$308/385$$


310/385

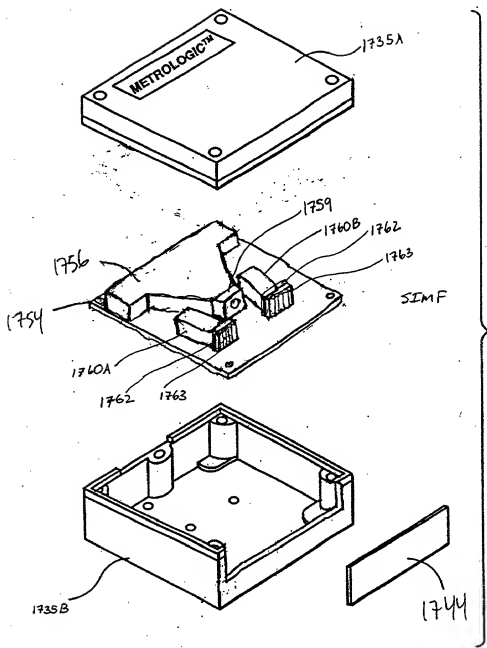
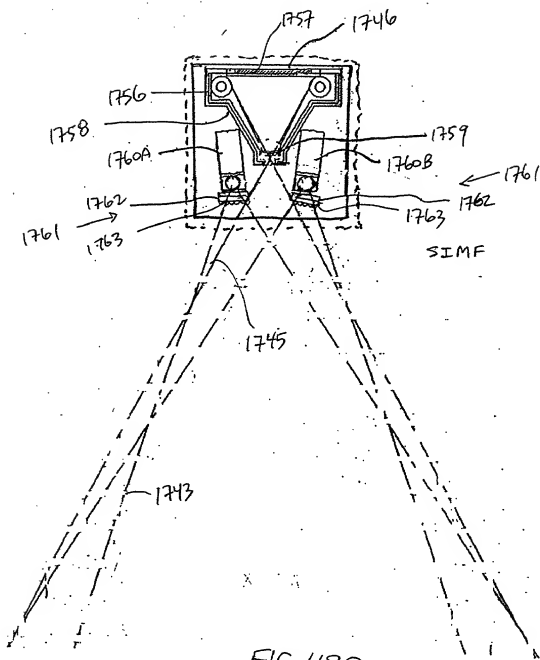


FIG. 49B

(311/385)



312/385

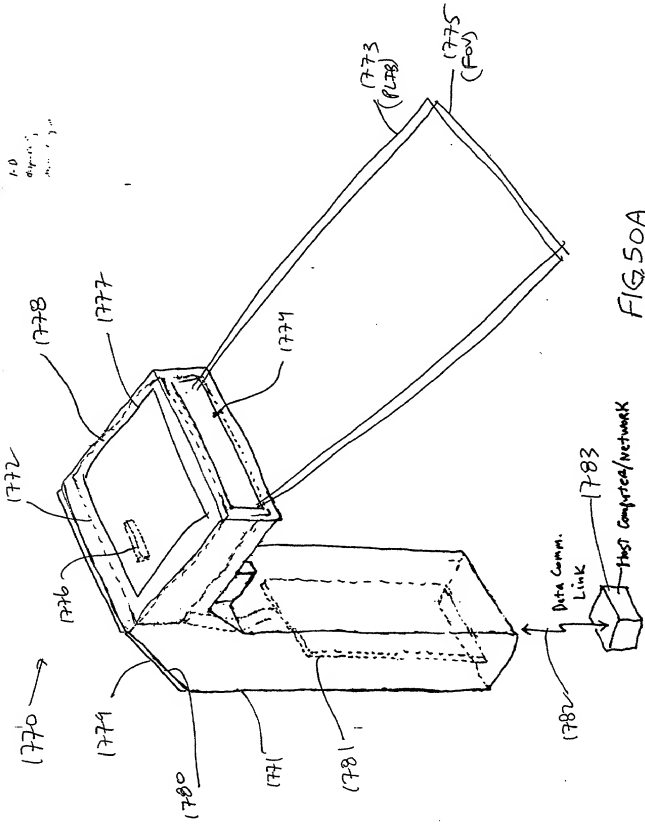


FIG 50A

313/385

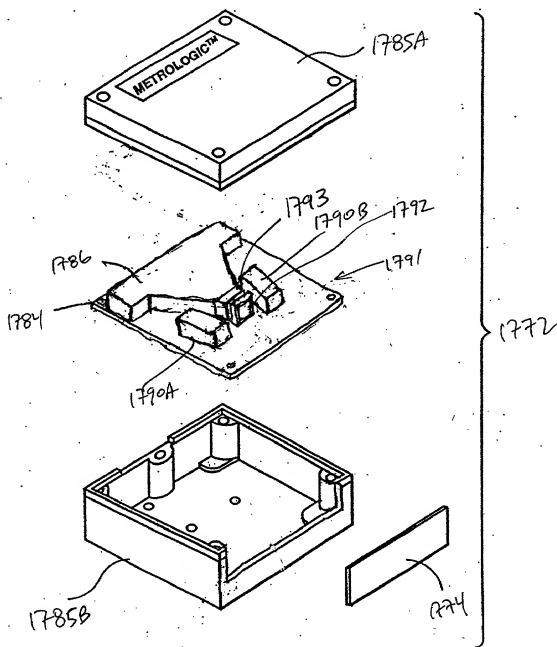


FIG. 50B

314/385

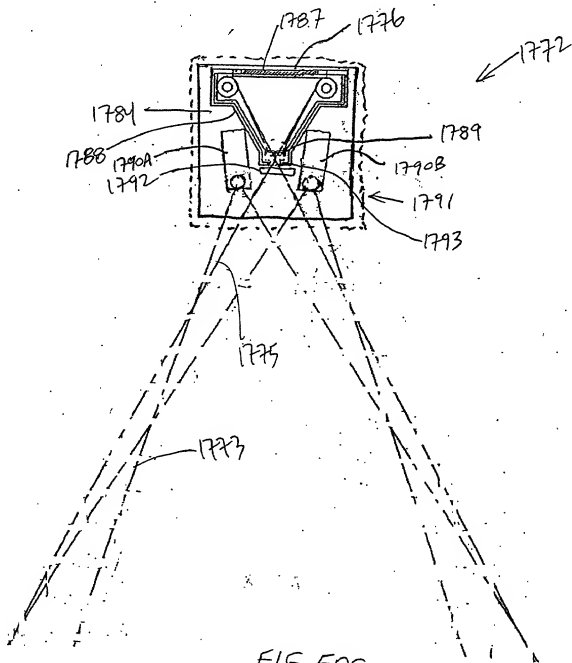
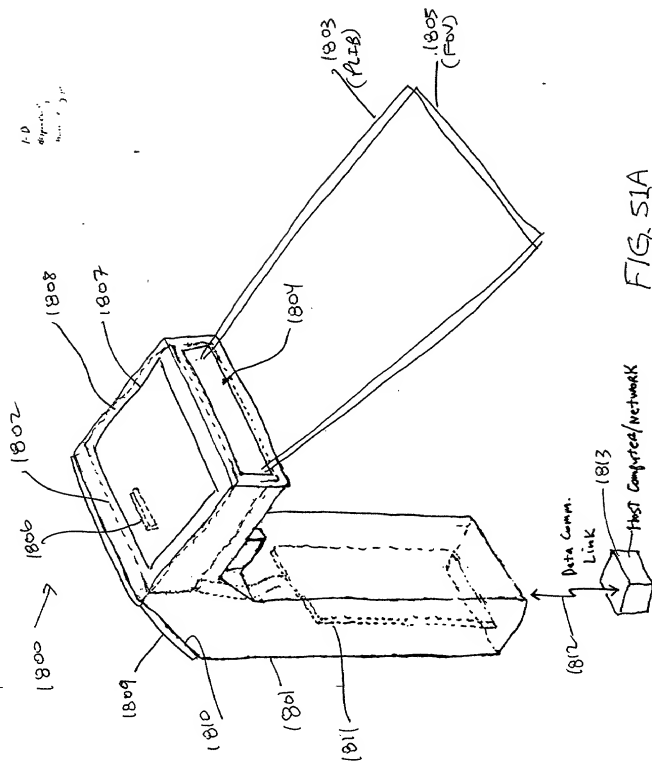


FIG. 50C



1-D
Displacement,
Time, s

36/385

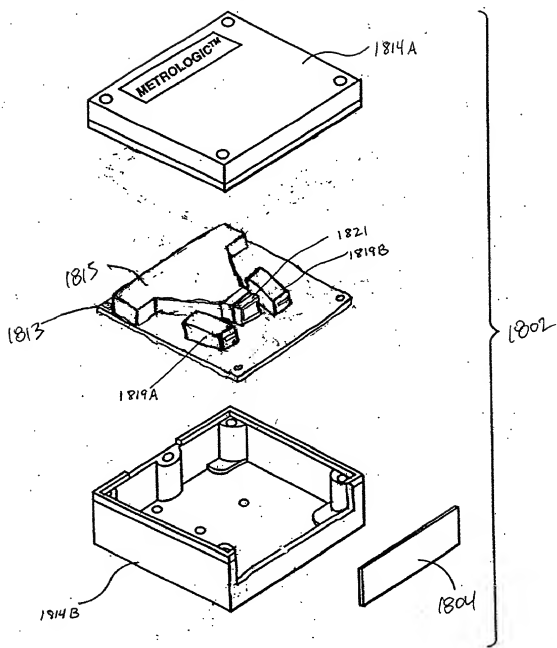
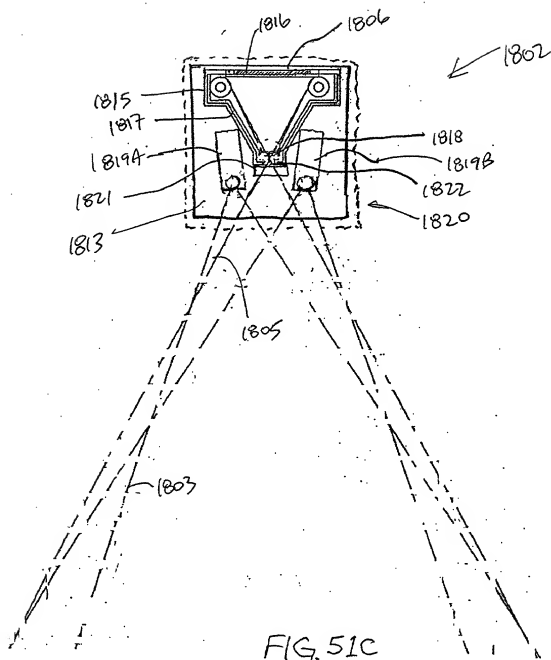


FIG. 51B

317/385



318/385

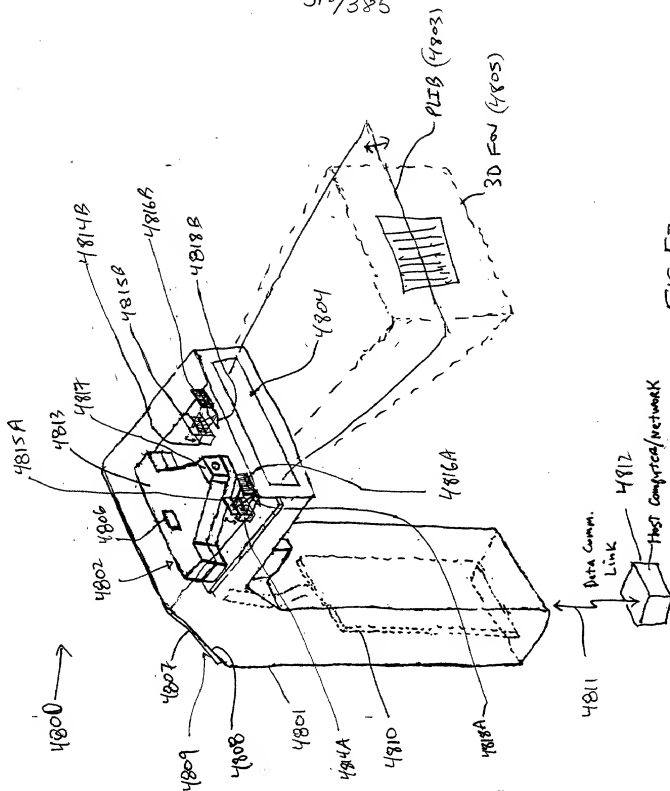


FIG. 52

320/385

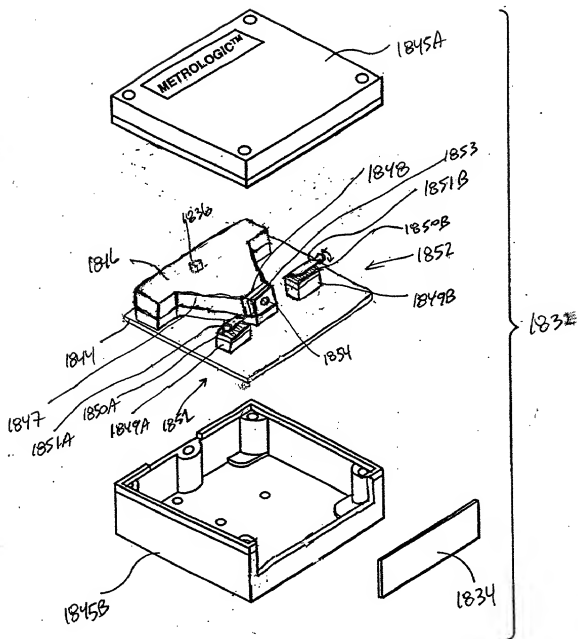
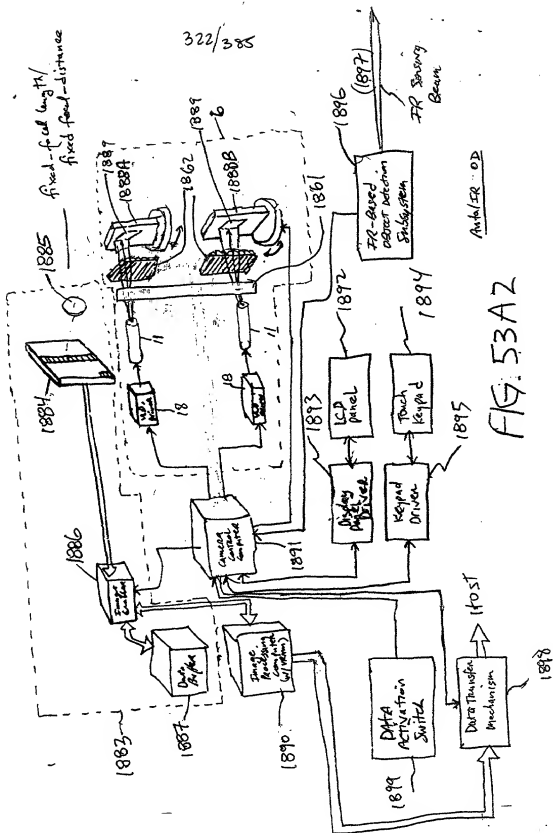
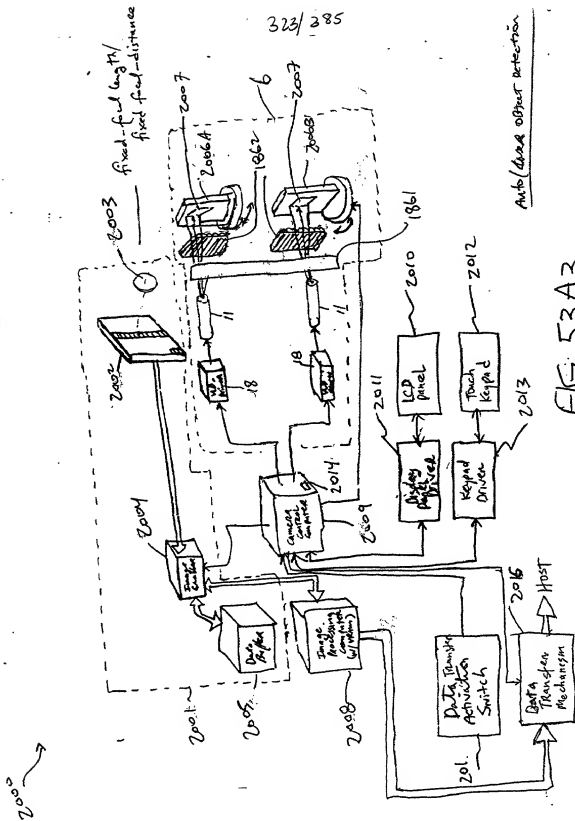


FIG. 52B

Fig. 1I34-3B

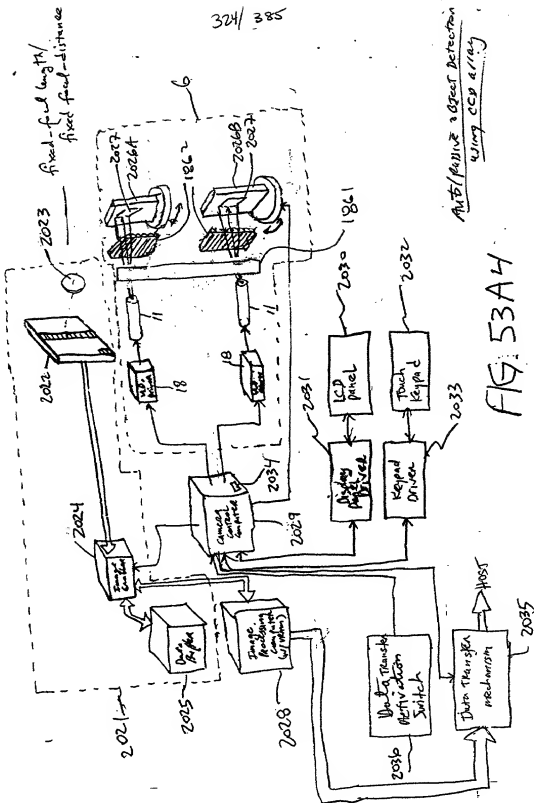
1880





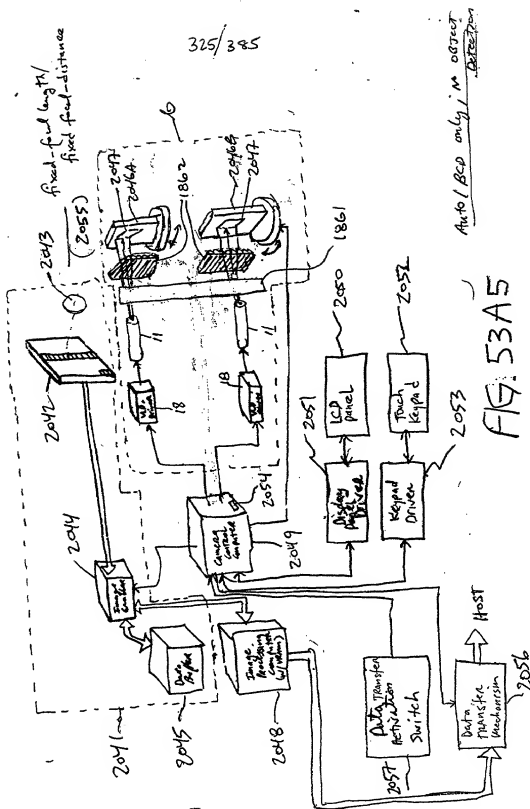
Auto/dance object detection

2020 →



325/385

2040



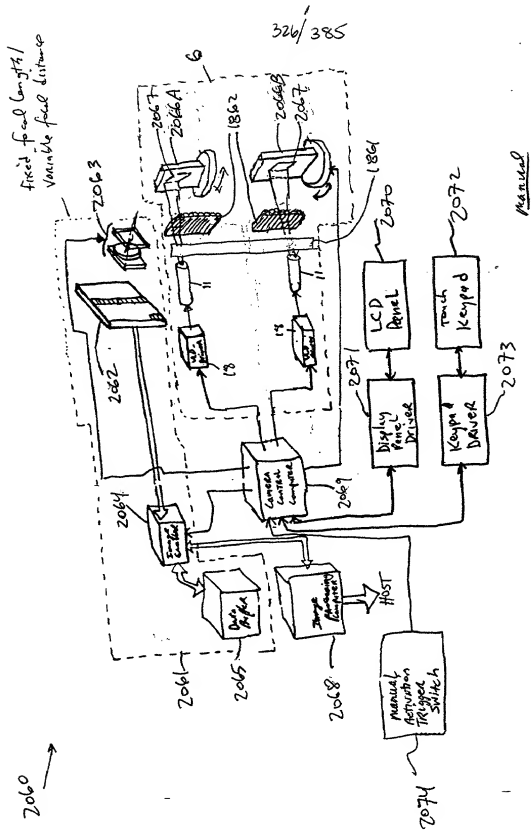
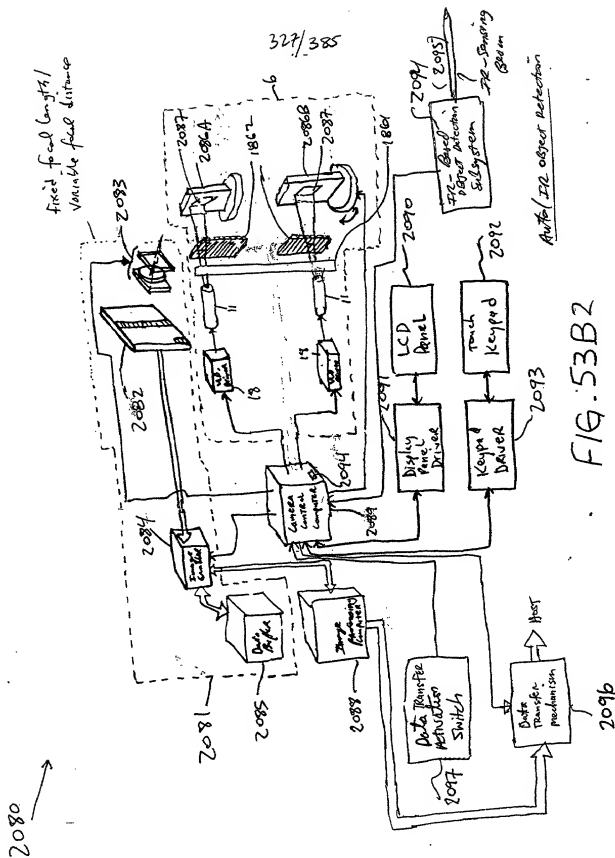
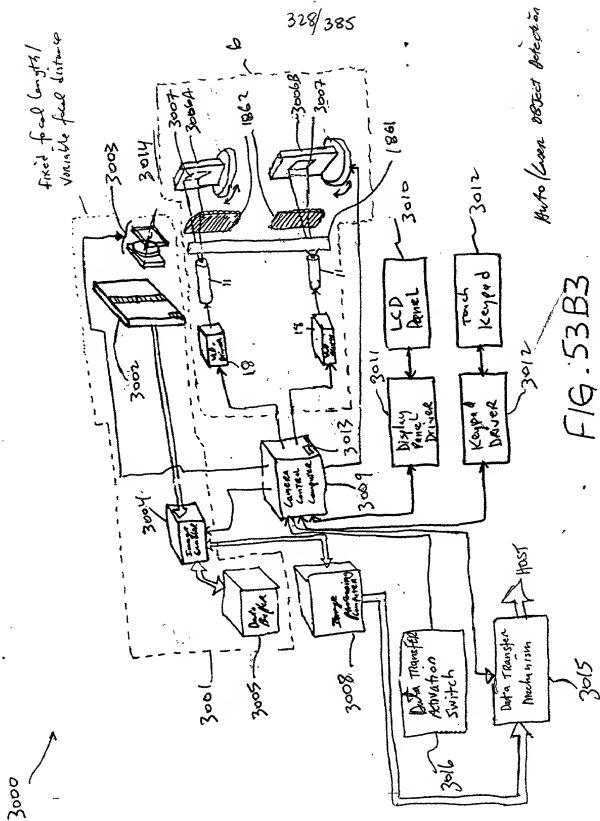


FIG. 53B1





fixed focal length/
variable focal distance

330/385

3040 →

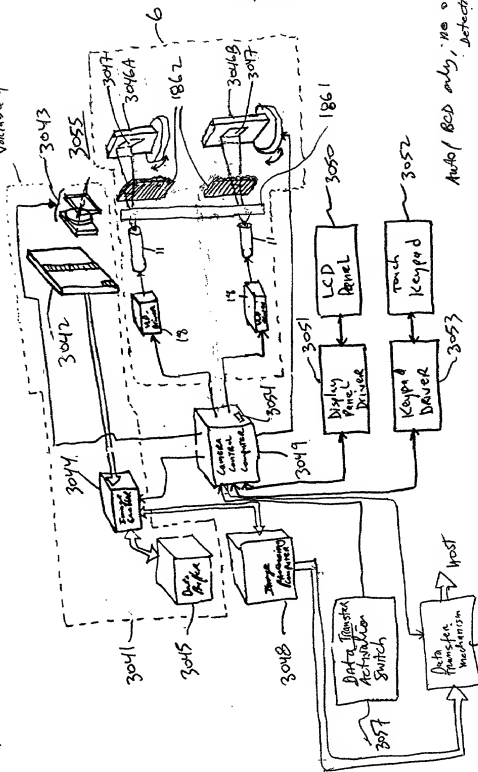


FIG. 53B5

Auto/Boo only, no object detection

321/385

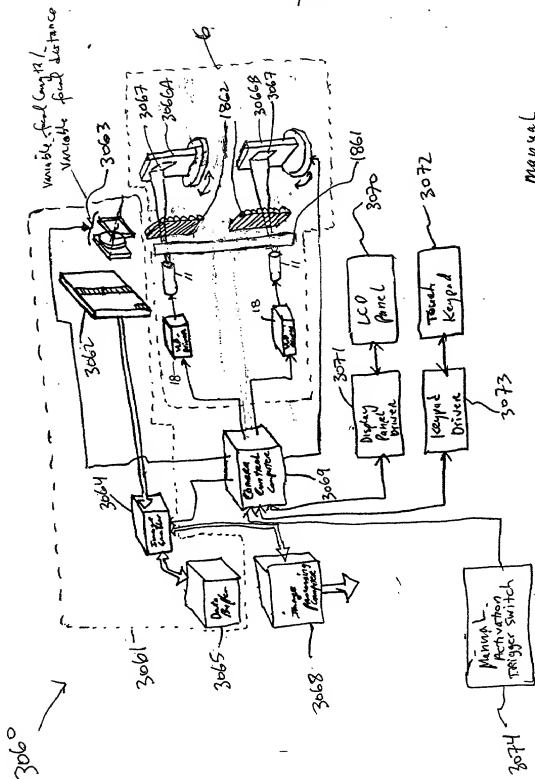
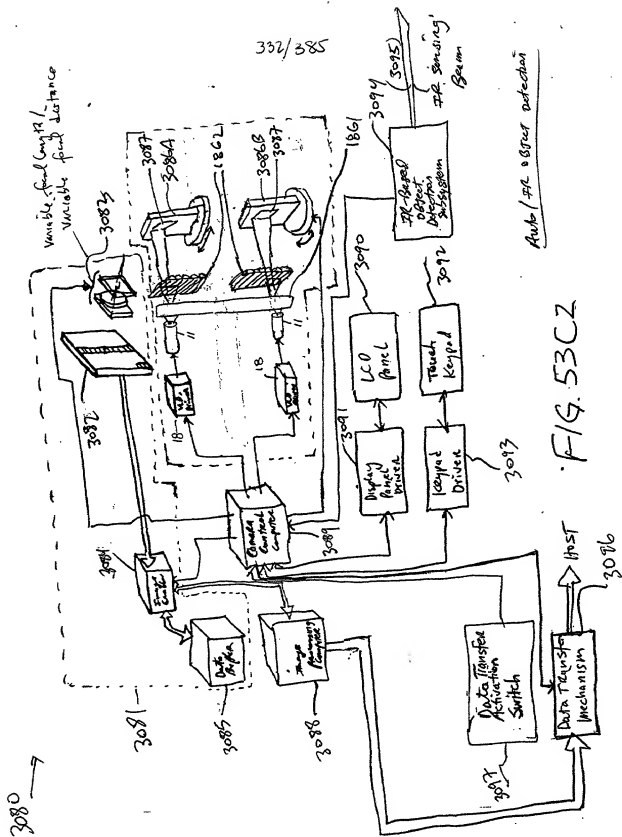


FIG. 53C1



334/385

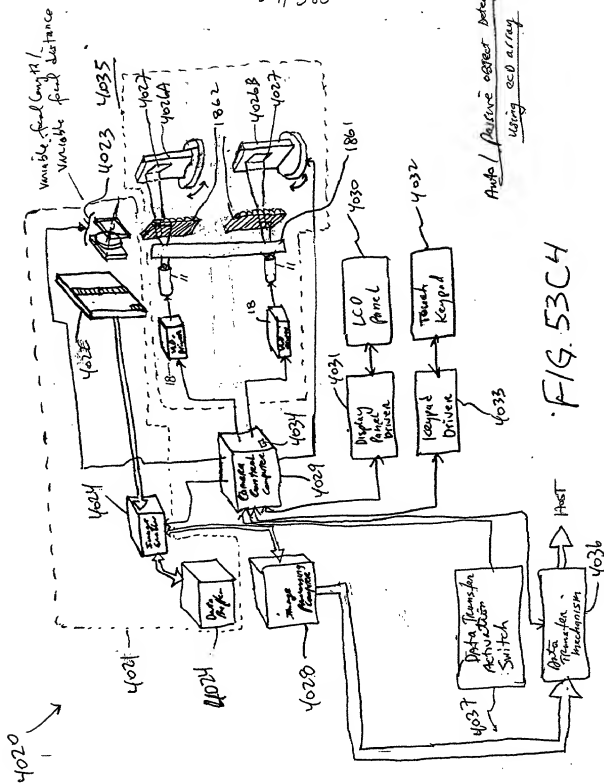


FIG. 534

337/385

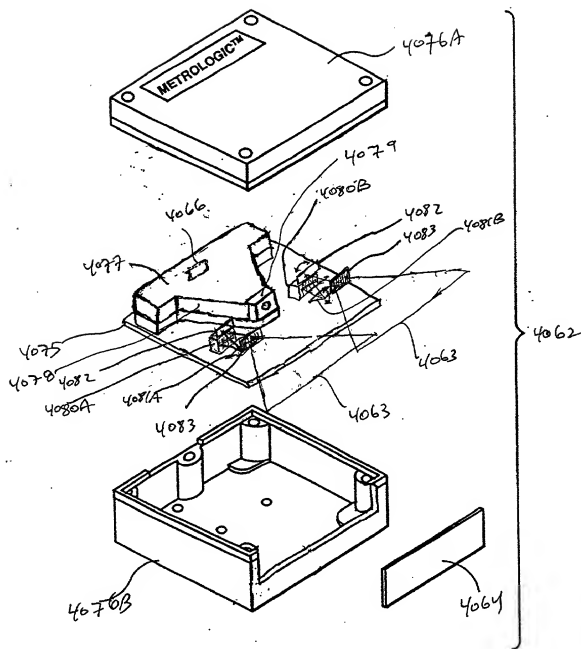


FIG. 54B

(break micro)
Fig. 125A-SP1

338/385

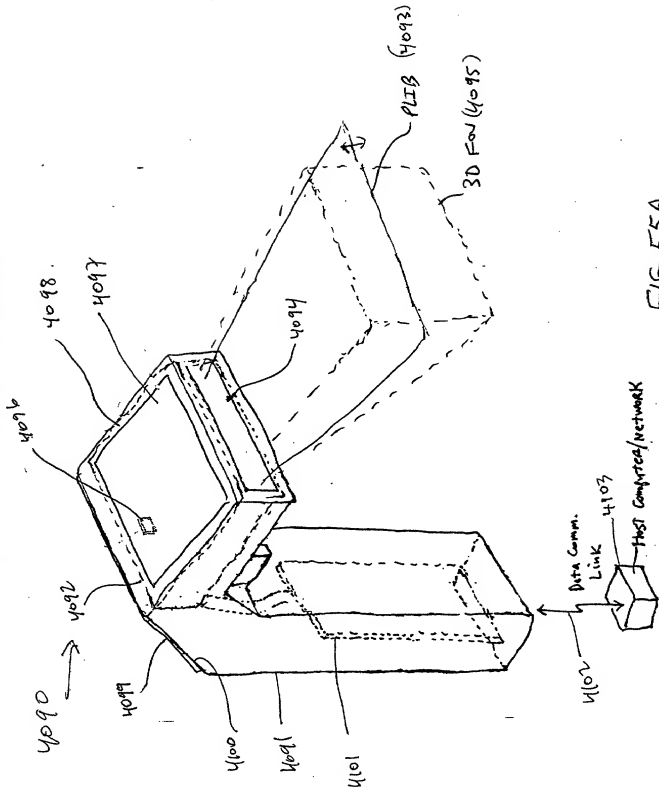


FIG. 55A

334/385

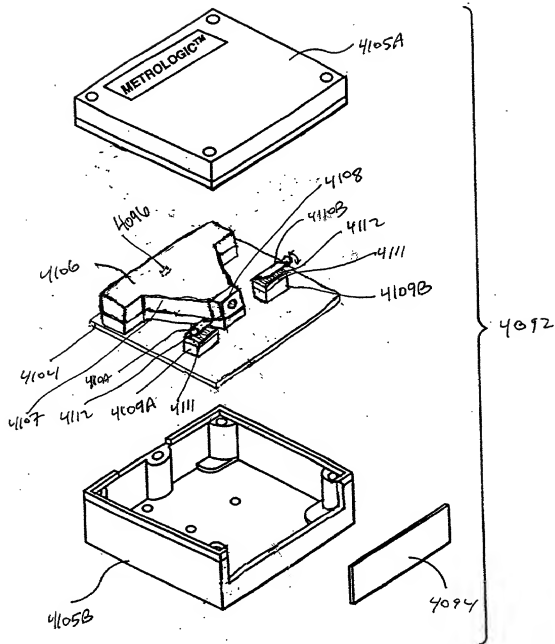


FIG. 55B

Briggs cell
Fig. 126A-6B

340/385

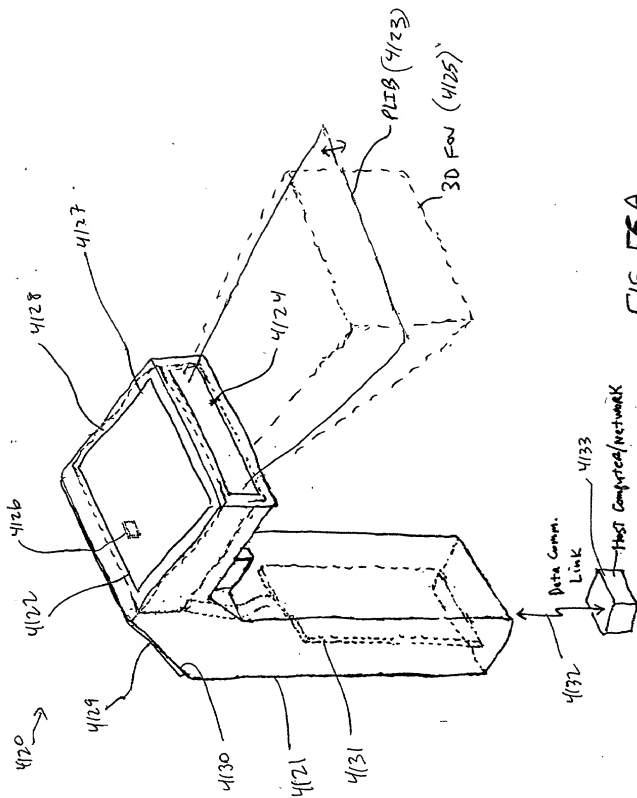


FIG. 56A

341/385

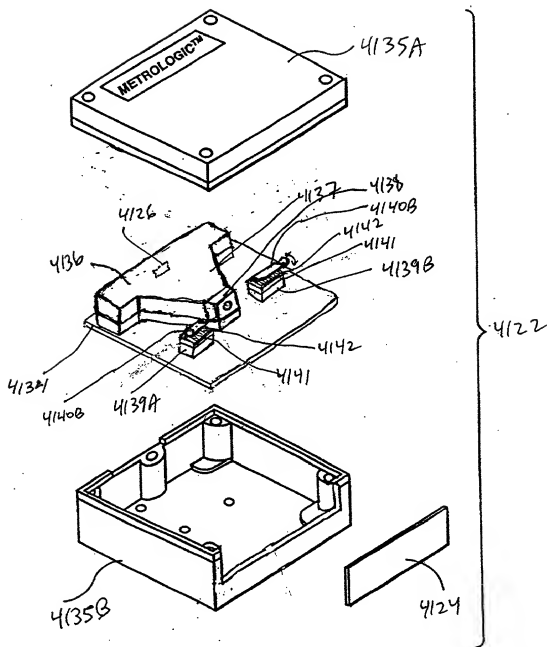


FIG. 56B

DM
Fig. 1I 7A-7C

342/385

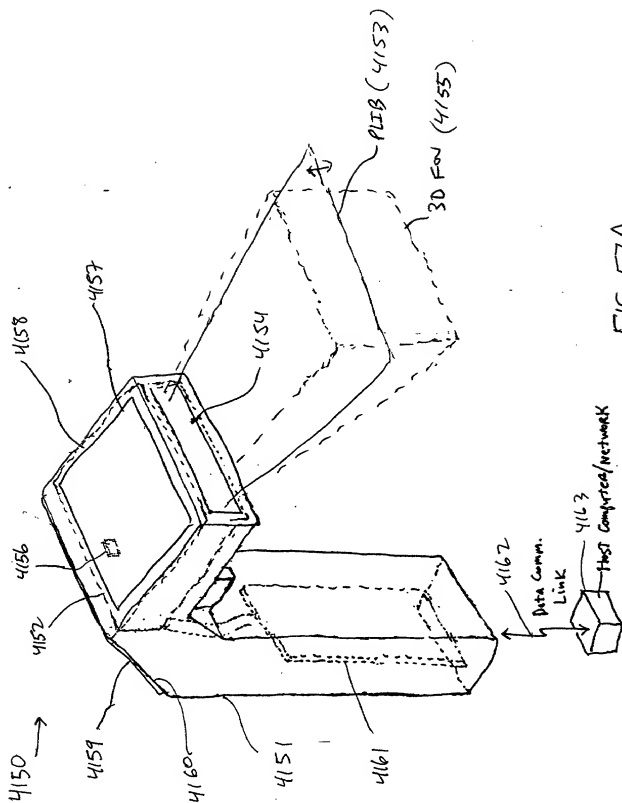


FIG. 57A

343/385

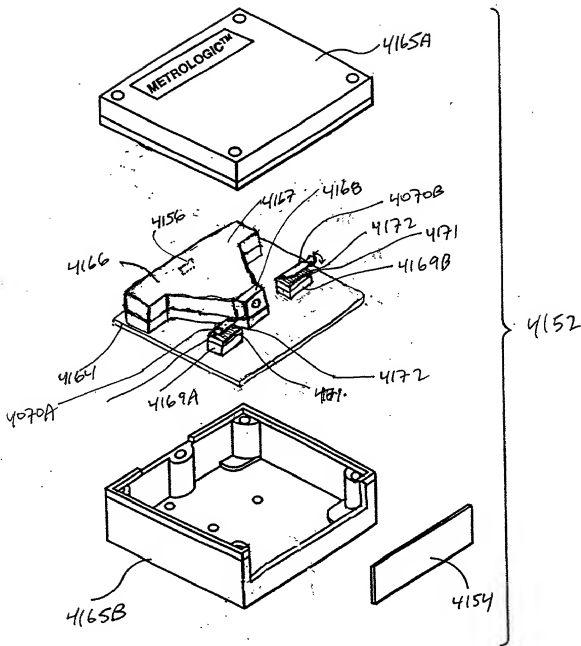


FIG. 57B

Pluses only Lcs
on panel

Figs 178F-8G

345/385

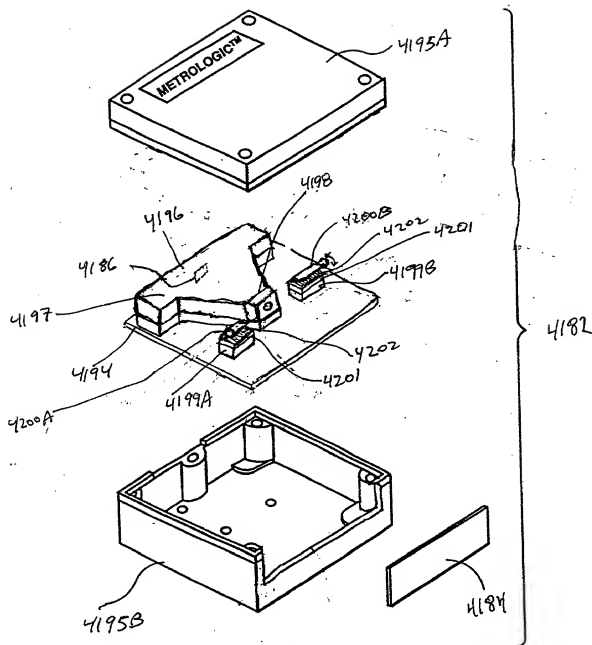


FIG. 58B

115 optical sensor
Fig. 17 14A-14B

346/385

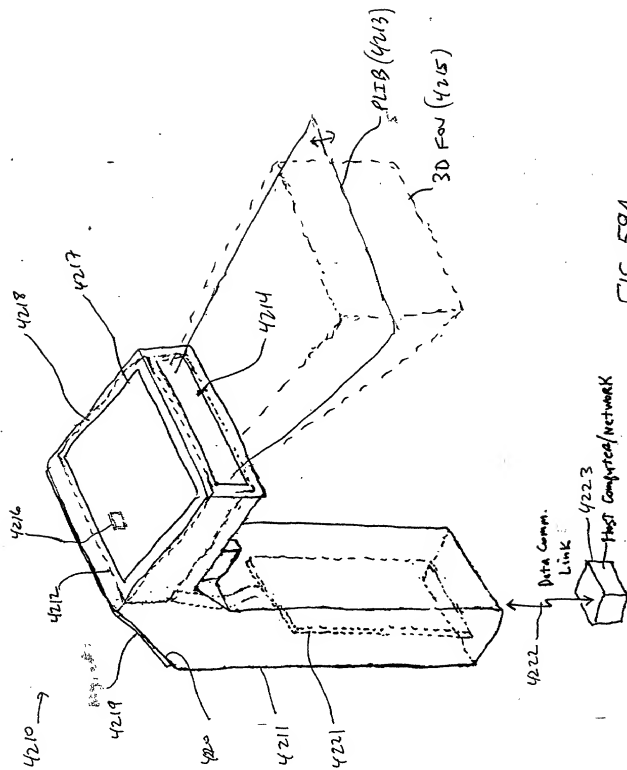


FIG. 59A

347/385

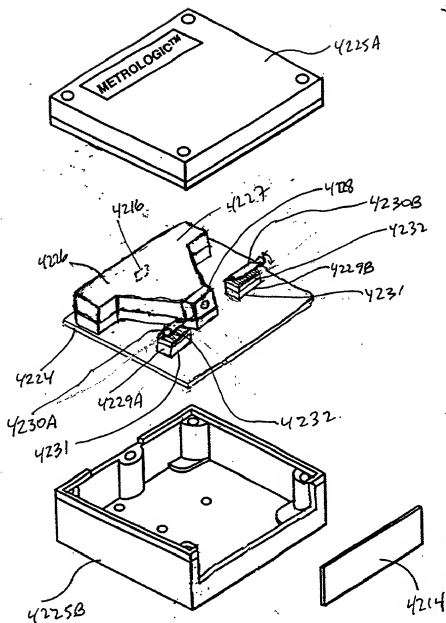


FIG. 59B

W. L. L. D.
Fig. 1515A-158

349/385

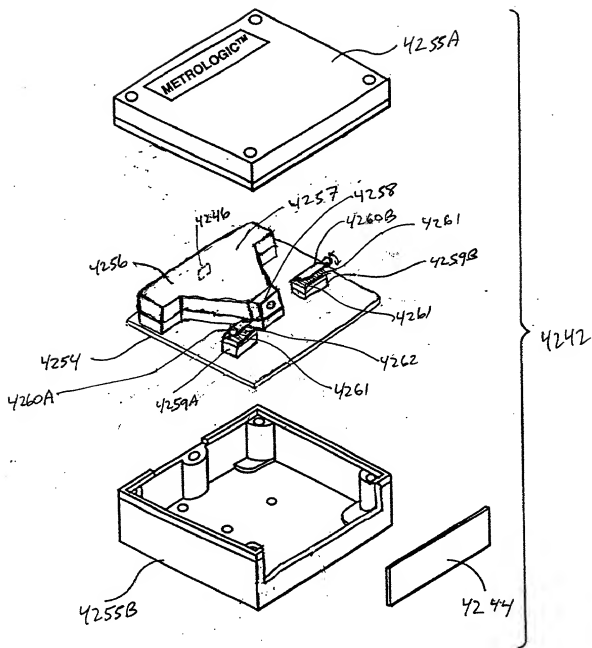
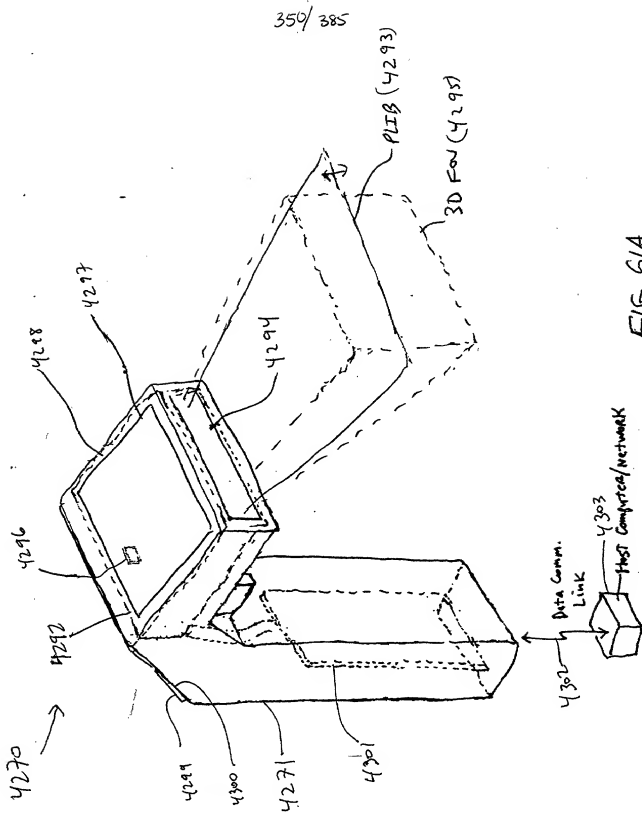


FIG. 60B

(Tong. phase
mod.)
Bthalon
Fig. 1 I 17A-17B



351/385

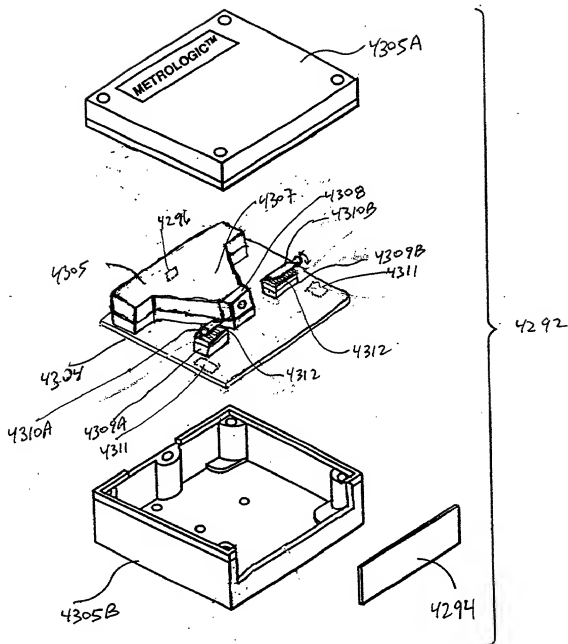


FIG. 61B

mod. hopping

Fig. 1194-19B

353/385

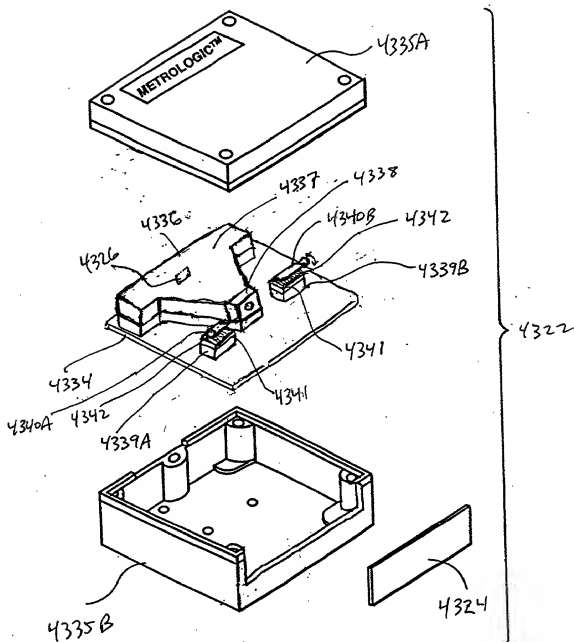


FIG. 62B

Micro-oscillator
Spatial intensity
Mod. panel

Fig. 1F21A-21D

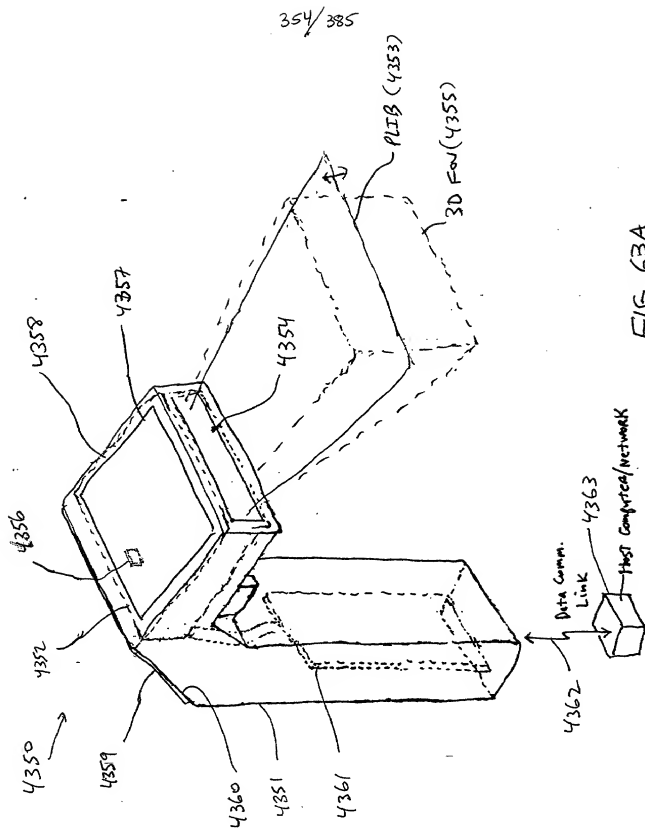


FIG. 63A

355/385

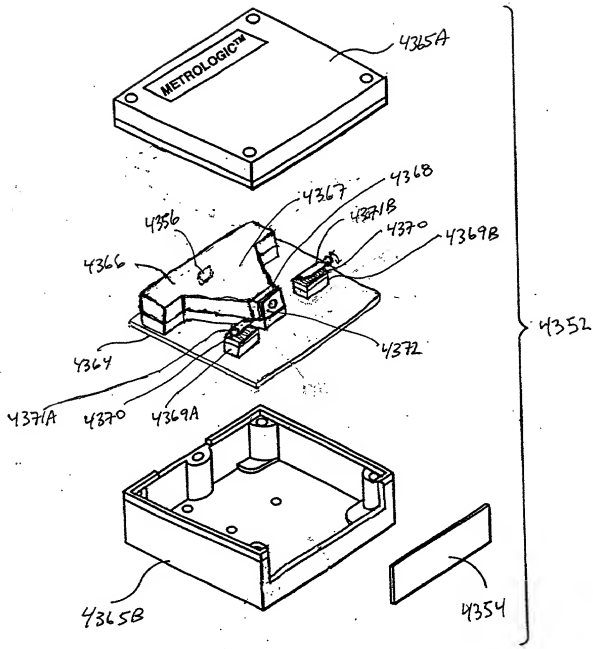


FIG. 63B

ED or.
mechanical fastening
Fig. 1E
23A-23B

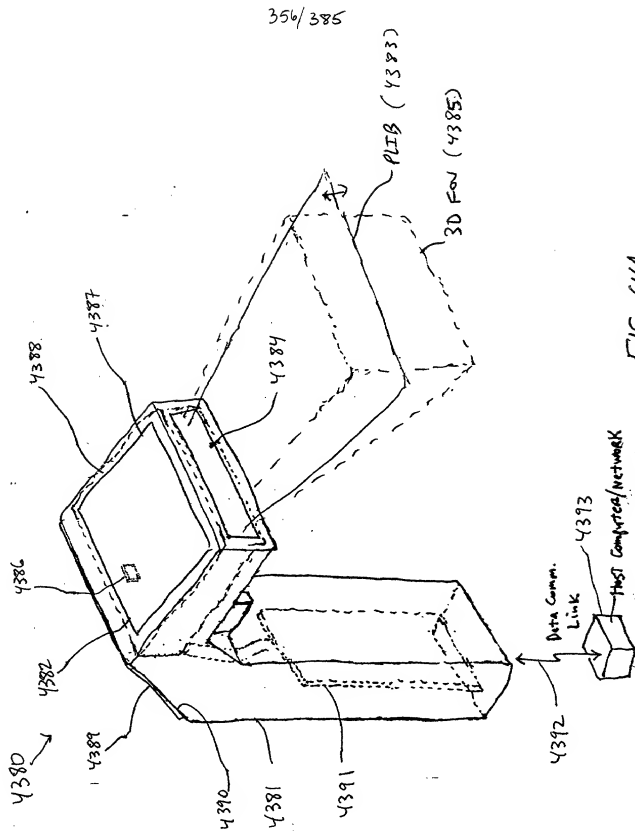


FIG. 64A

358/285

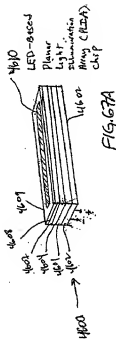


FIG. 67A

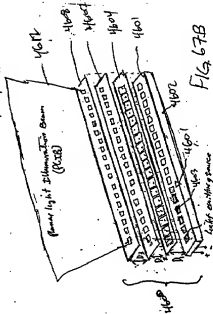


FIG. 67B

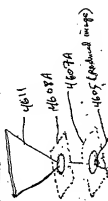


FIG. 67C

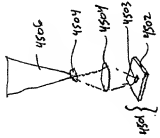


FIG. 65B

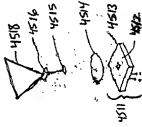


FIG. 66B

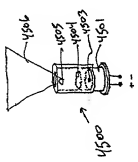


FIG. 65A

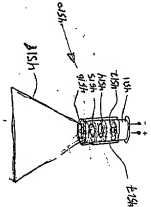


FIG. 66A

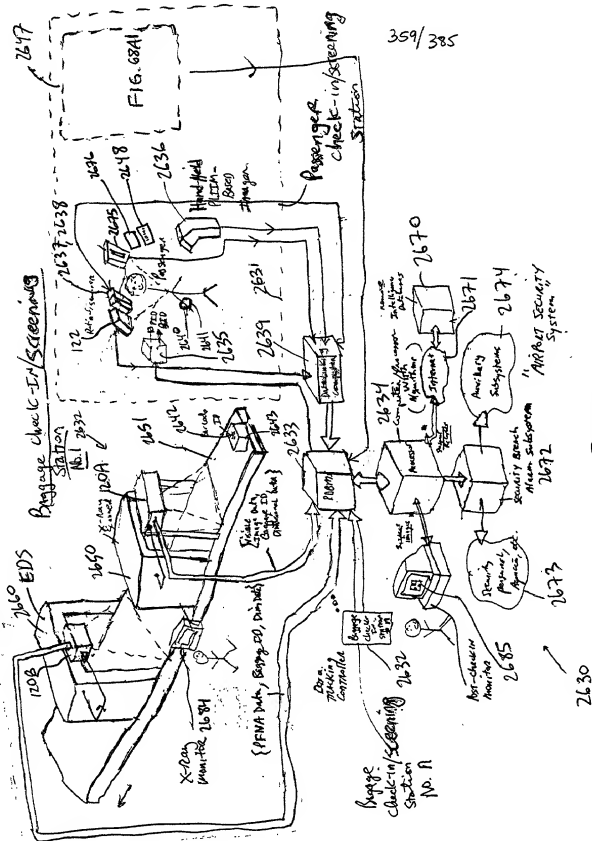


FIG. 68.

360/385

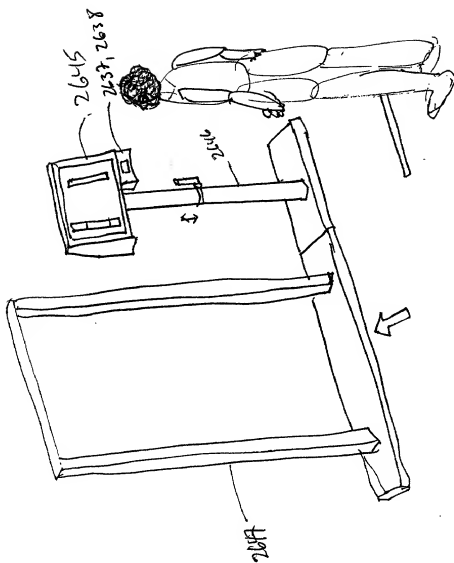


FIG. 68A

361/385

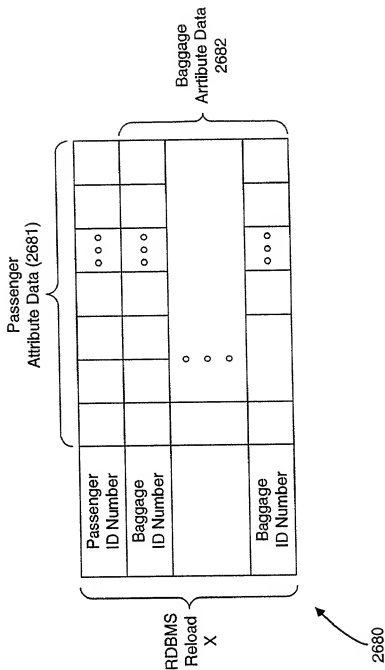


FIG. 68B

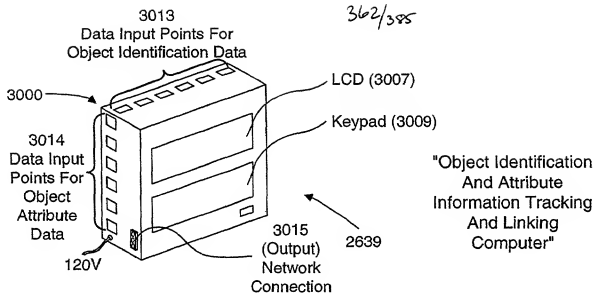


FIG. 68C1

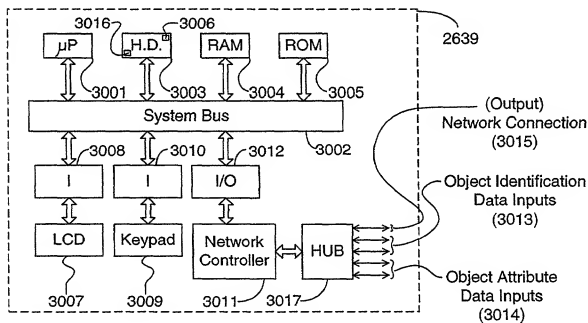


FIG. 68C2

Object Identification And Attribute Information Tracking And Linking Computer System.

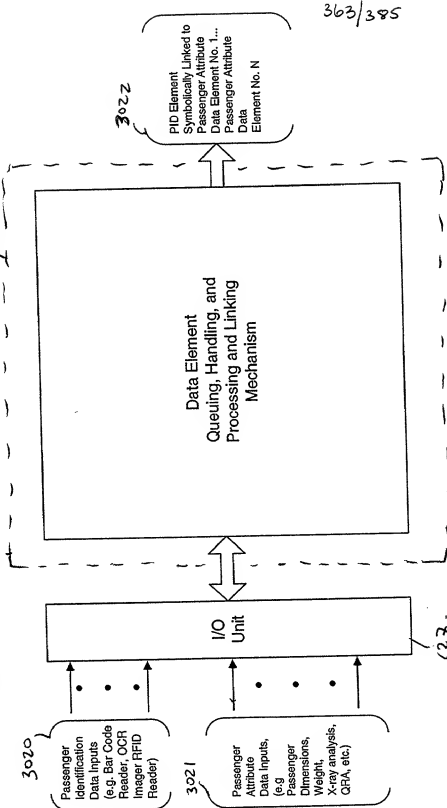


FIG. 68C3

Data Element Queuing, Handling, and Processing Subsystem Employed In The Object Identification And Attribute Acquisition System Of The Present Invention. (131)

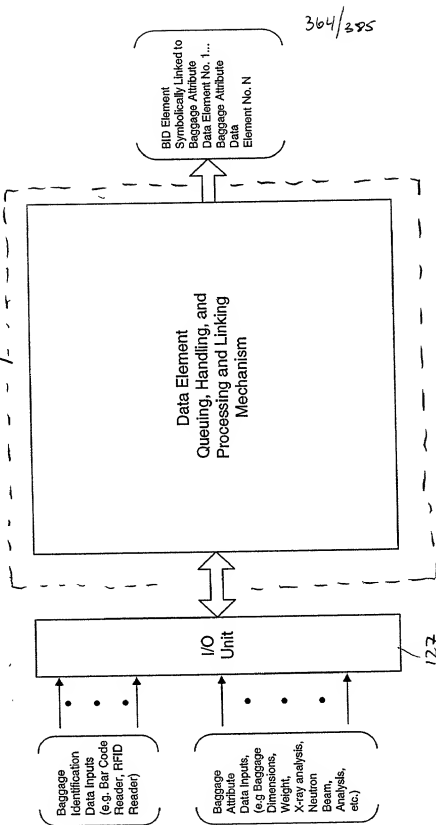


FIG. 68C4

365/385

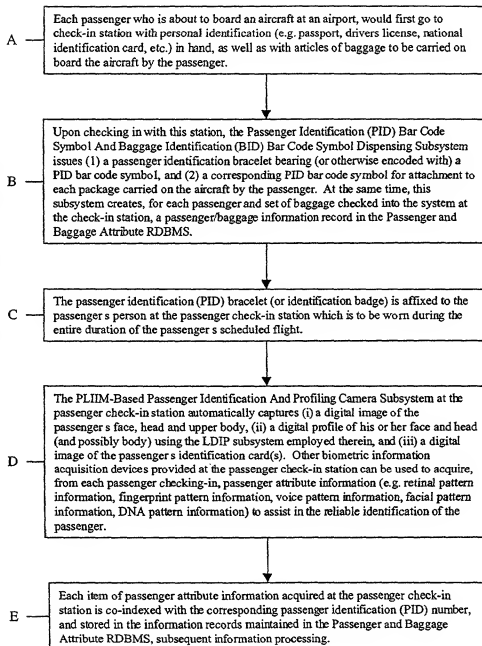


FIG. 68D1

366/385

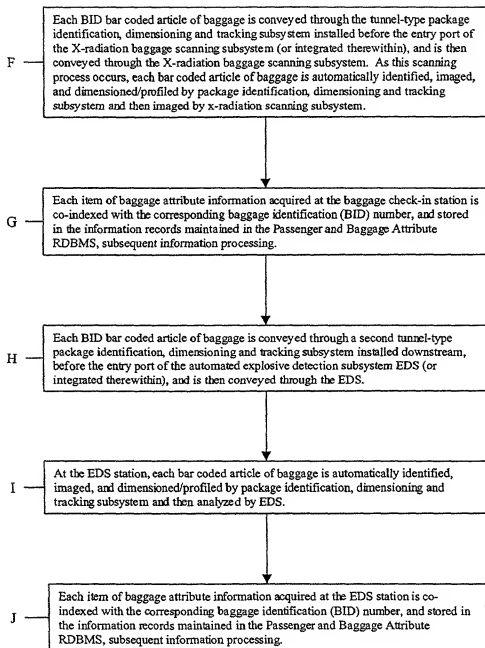


FIG. 68D2

367/385

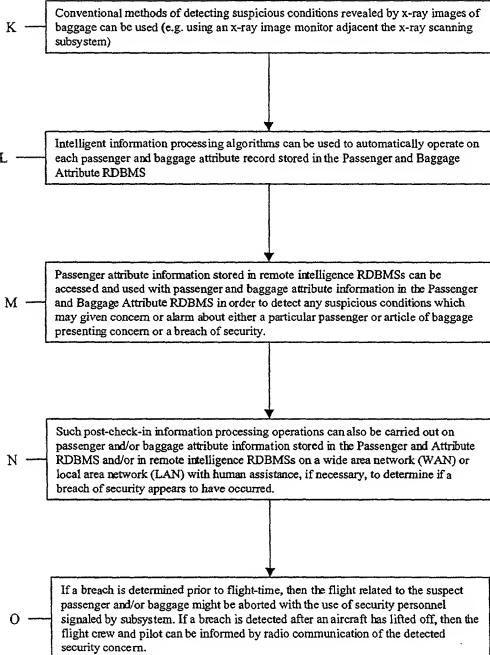


FIG. 68D3

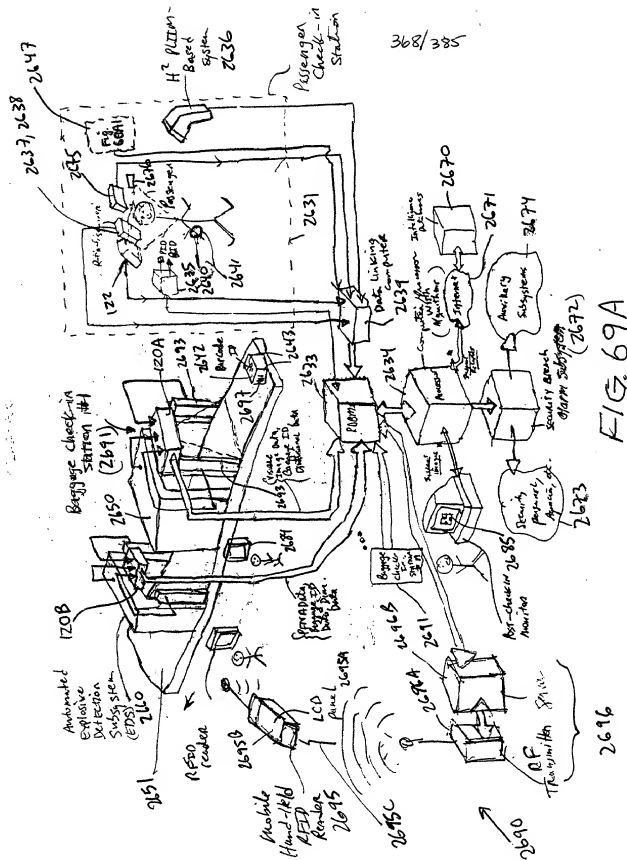


FIG. 69A

369/385

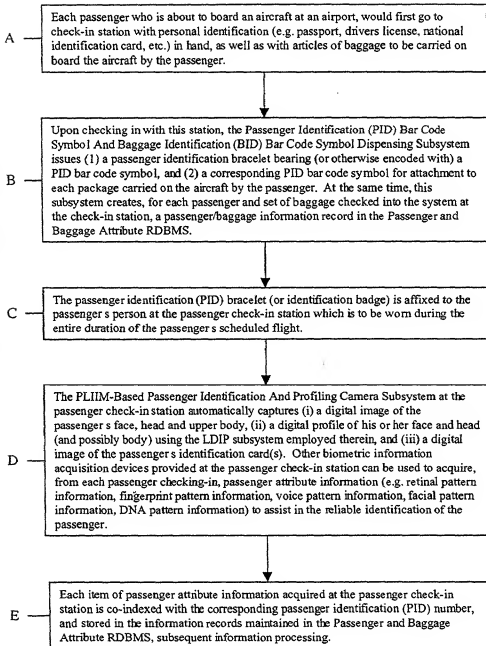


FIG. 69B1

370/395

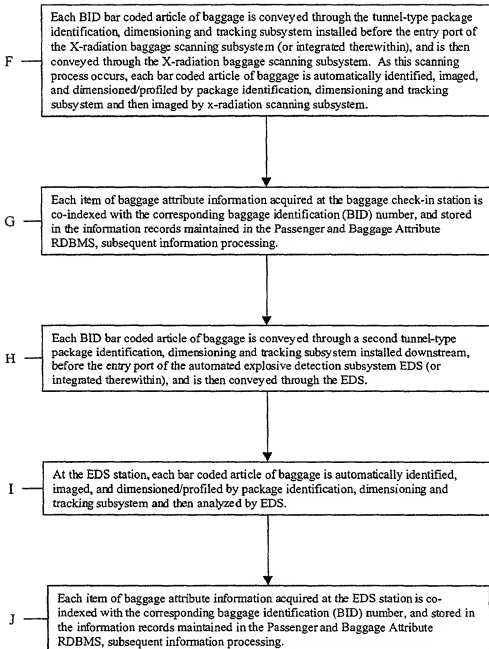


FIG. 69B2

371/385

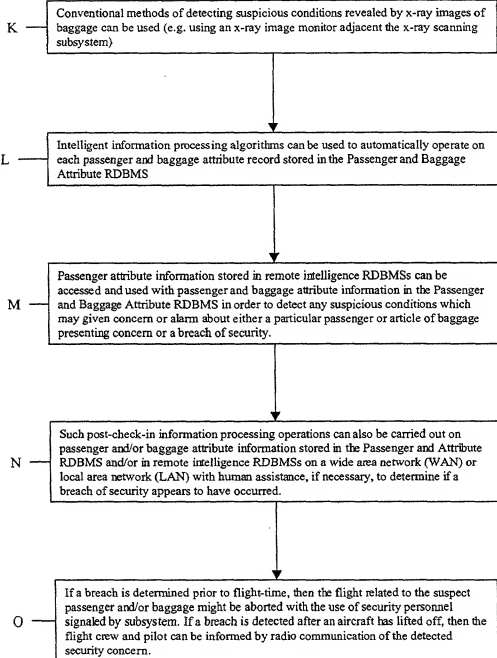


FIG. 69B3

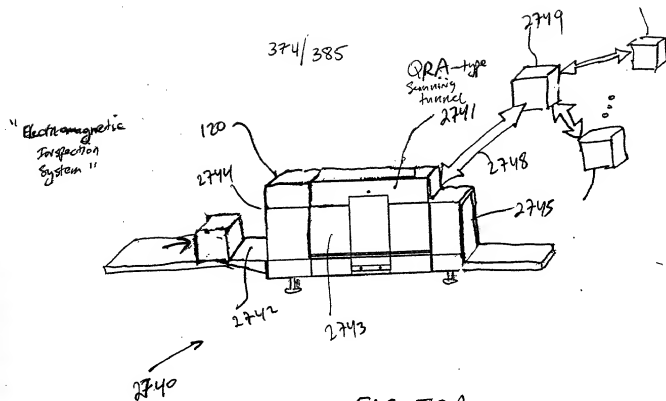


FIG 72A

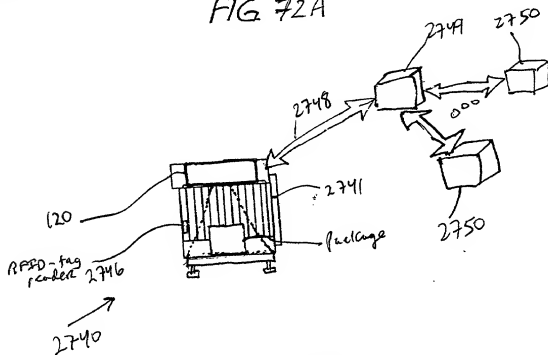
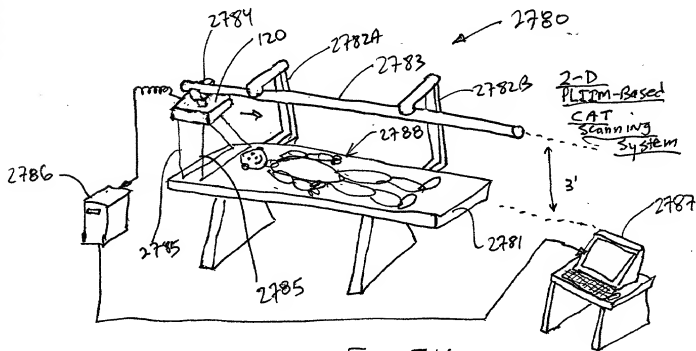
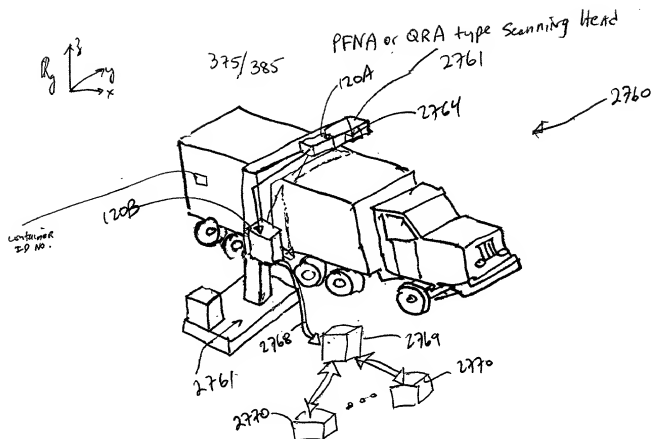
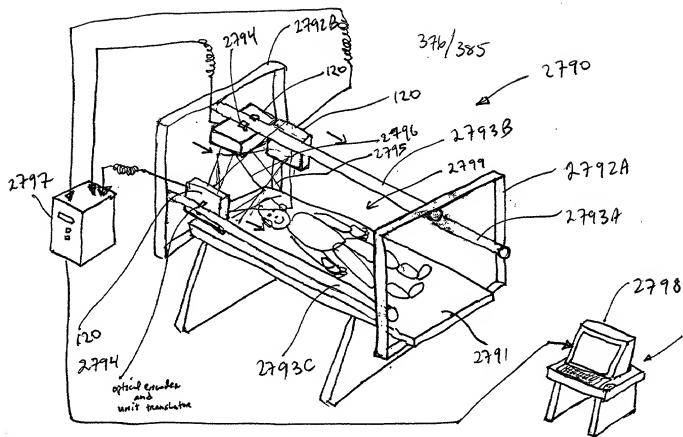


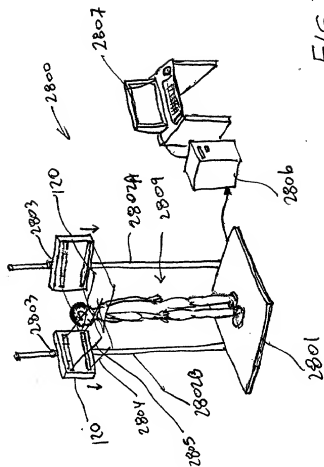
FIG 72B





3-D PLIM-Based
CAT Medical scanning
System

FIG. 75



377/385

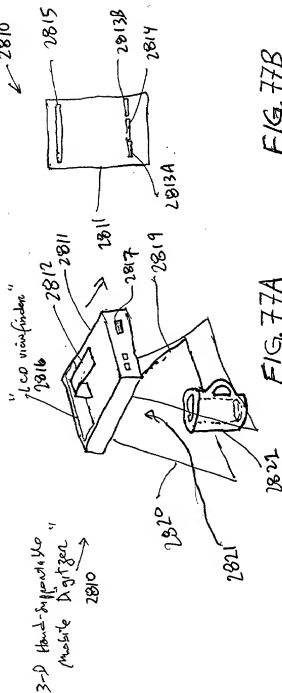


FIG. 77B

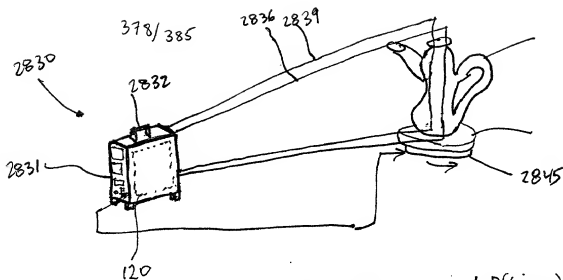


FIG. 78A

1-D (Linear) Sensor

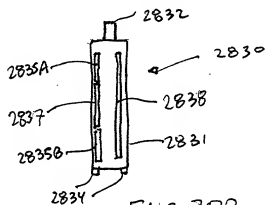


FIG. 78B

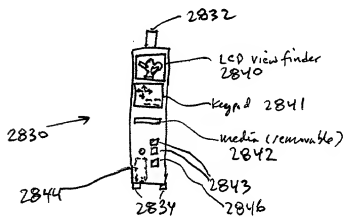
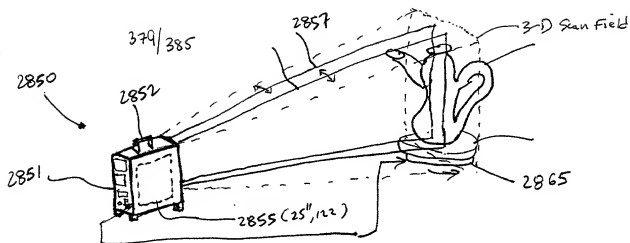
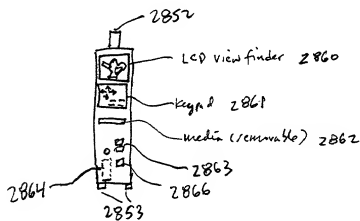
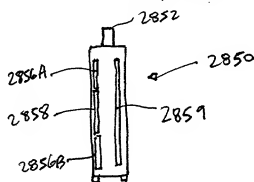


FIG. 78C



2-D (AREA) sensor



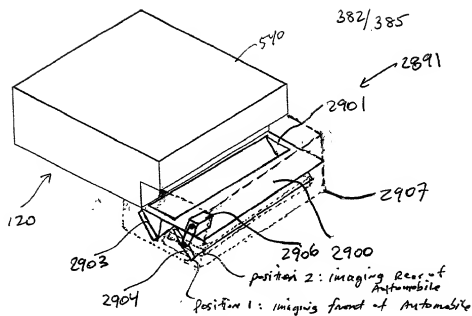


FIG. 81B

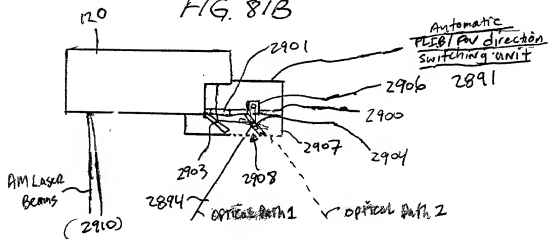
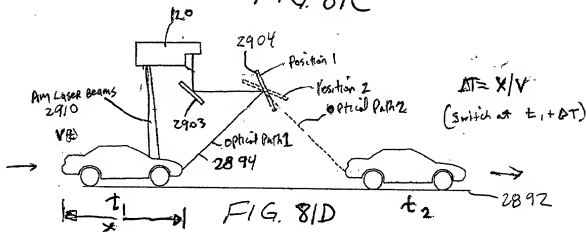
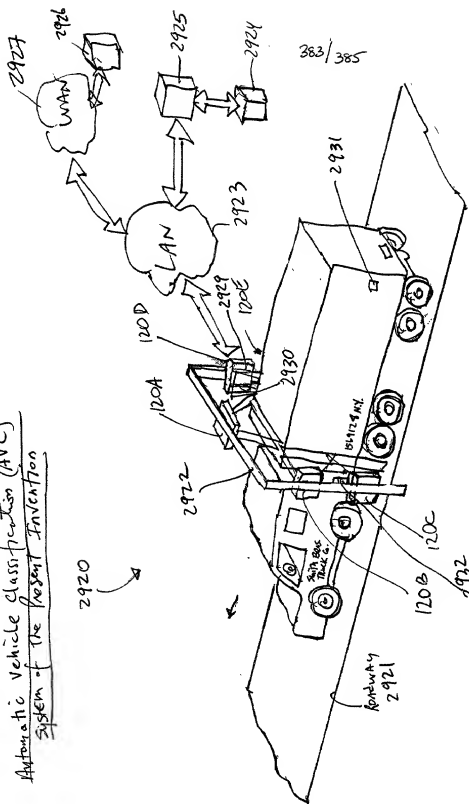


FIG. 81C



Automatic Vehicle Classification (AVC)
System of the Present Invention



Employing overhead and lateral
profiling and imaging
techniques

FIG. 82

Automatic Vehicle
Identification and
Classification (AVIC)
System of the
Present Invention

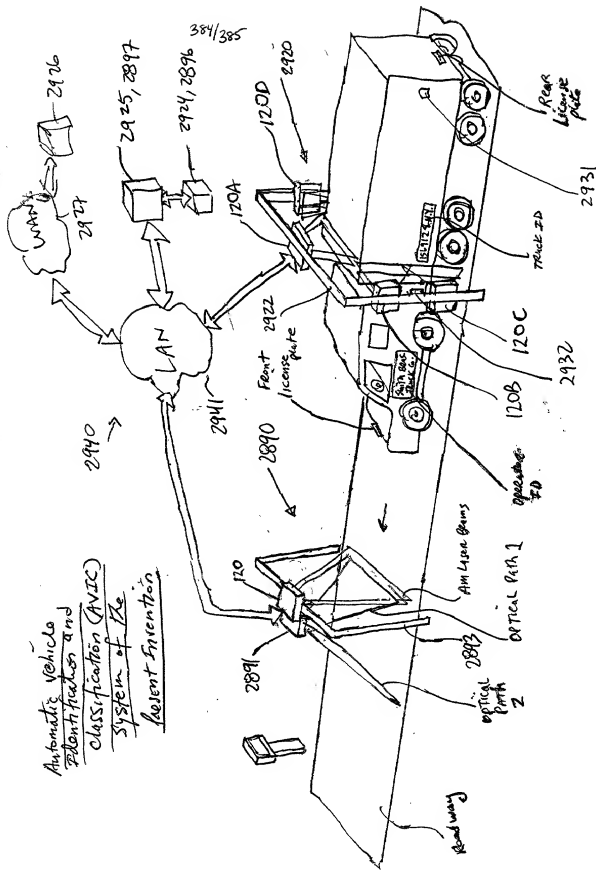


FIG. 83

385/385.

